Titre: Title:	Seismic Deformations of Taller Reinforced Concrete Shear Walls Located in Eastern Canada
Auteur: Author:	Armin Sadeghian
Date:	2018
Type:	Mémoire ou thèse / Dissertation or Thesis
Référence: Citation:	Sadeghian, A. (2018). Seismic Deformations of Taller Reinforced Concrete Shear Walls Located in Eastern Canada [Thèse de doctorat, École Polytechnique de Montréal]. PolyPublie. https://publications.polymtl.ca/3117/

UNIVERSITÉ DE MONTRÉAL

SEISMIC DEFORMATIONS OF TALLER REINFORCED CONCRETE SHEAR WALLS LOCATED IN EASTERN CANADA

ARMIN SADEGHIAN

DÉPARTEMENT DES GÉNIES CIVIL, GÉOLOGIQUE ET DES MINES

ÉCOLE POLYTECHNIQUE DE MONTRÉAL

THÈSE PRÉSENTÉE EN VUE DE L'OBTENTION

DU DIPLÔME DE PHILSOPIAE DOCTOR

(GÉNIE CIVIL)

AVRIL 2018

UNIVERSITÉ DE MONTRÉAL

ÉCOLE POLYTECHNIQUE DE MONTRÉAL

Cette thèse intitulée :

SEISMIC DEFORMATIONS OF TALLER REINFORCED CONCRETE SHEAR WALLS LOCATED IN EASTERN CANADA

présentée par: SADEGHIAN Armin

en vue de l'obtention du diplôme de : Philosophiae Doctor

a été dûment acceptée par le jury d'examen constitué de :

M. BOUAANANI Najib, Ph. D., président

Mme KOBOEVIC Sanda, Ph. D., membre et directrice de recherche

M. BEN FTIMA Mahdi, Ph. D., membre

M. PALERMO Dan, Ph. D., membre

DEDICATIONS

To my parents, Ali and Robab

And to Abtin, Maryam and Arash

And to anyone who thought me something

ACKNOWLEDGEMENTS

I would like to express my earnest gratitude to my supervisor, Dr. Sanda Koboevic, for her support and direction through the course of this research project. I would also like to thank my evaluation committee members Professors Najib Bouaanani and Mahdi Ben Ftima from Polytechnique de Montreal and Professor Dan Palermo from York University for accepting to read and evaluate this dissertation. I would like thank Professor Pierre Léger for his support and appreciate his cooperation for sharing the computer models of his previous researches. I would also like to acknowledge the financial support of the Canadian Seismic Research Network (CSRN).

My gratitude also goes to my friends and the kind personnel at Polytechnique Montreal and specially the staffs of Groupe de Recherche en génie des Structures (GRS) who helped me throughout the period of my project. During the course of this project I had the precious chance to meet wonderful people, some became my lasting friends. I would like to thank all of them for their friendship and support. Special thanks to Poulad Daneshvar, Ali Imanpour, Yassaman Balazadeh, Morteza Dehghani, Sylvain Renaud, Joanie Smith and Fabien Lagier.

Last but not least, I would like to thank my lovely family for their love and support during this part of life journey. My deepest gratitude and appreciation to my parents, Ali and Robab, for their immeasurable love and sacrifices. They worked hard against all difficulties to make life easier for us and let me build my future with their infinite love and support.

RÉSUMÉ

Les systèmes de murs de refend en béton armé font partie des systèmes structuraux les plus couramment utilisés pour résister aux charges sismiques. L'utilisation de murs de refend dans la conception parasismique est répandue en raison de leur rigidité élevée et la facilité de construction. Ce système est encore plus avantageux pour les bâtiments de grande hauteur, car il est plus critique d'offrir un niveau de rigidité acceptable pour de telles structures.

De nombreux codes modernes, y compris les codes canadiens CNBC 2015 et CSA A23.3-14, utilisent une approche basée sur la force pour la conception parasismique des murs de refend. Bien que cette méthode soit relativement simple et ait été utilisée dans la pratique depuis longtemps, elle a ses propres inconvénients. Un inconvénient important est que le niveau de dissipation d'énergie doit être considéré tout au début du processus de conception en anticipant la ductilité du système. Dans cette approche, le niveau de ductilité effectivement mobilisée sous les charges de conception n'est pas vérifié et le système est conçu pour maintenir la capacité minimale pour un niveau présumé de ductilité. Les normes NBCC 2015 et CSA A23.3-14 énoncent des dispositions spécifiques pour la conception parasismique des murs de refend afin de maintenir le niveau présumé de ductilité.

Contrairement à la méthode de conception basée sur la force, la méthode de conception basée sur le déplacement sismique pourrait prédire le niveau de ductilité des murs de refend conçus, dès le début. Selon les approches basées sur le déplacement, dans les régions de sismicité modérée, tel que l'est du Canada, les déplacements maximales des murs de refend de plus grande hauteur sont souvent plus petits que le déplacement au point de début de plasticité, et donc la réponse sismique élastique est indiquée. Une telle prédiction ne concorde pas avec les hypothèses de la méthode basée sur la force qui suppose que la réponse est toujours inélastique.

Bien qu'en théorie les méthodes basées sur le déplacement permettent de prédire le niveau de ductilité, elles ont des difficultés pour prédire les efforts de conception pour les murs de refend à hauteur élevée dans les régions à sismicité modérée. Contrairement à l'ouest du Canada, les tremblements de terre de l'est du Canada ont une magnitude plus faible et sont riches en ondes à hautes fréquences. La combinaison d’une période fondamentale élevée et de l'exposition à des ondes sismiques à haute fréquence amplifie l'impact des modes supérieurs, ce qui complexifie davantage la prédiction de la réponse des murs de refend à hauteur élevée dans l'est du Canada.

Cette recherche examine les problèmes liés à l'utilisation des méthodes basée sur la force et basée sur le déplacement dans la conception parasismique de murs de refend à hauteur élevée dans l'est du Canada, particulièrement en ce qui concerne les déformations et la ductilité aux niveaux local et globale, puis propose des procédures pouvant améliorer la précision de l'estimation de ces paramètres.

Pour atteindre ces objectifs, dans un premier temps, une étude préliminaire a été réalisée sur deux bâtiments de 17 étages avec murs de refend en béton armé, situés dans l'est et l'ouest du Canada. Les murs de cisaillement ont été conçus conformément aux règles de conception basée sur la force (FBD) du NBCC / CSA A23.3 et la méthode actuelle de conception basée sur le déplacement direct (DDBD), et la différence spécifique des prévisions de conception entre l'est et l'ouest du Canada ont été discutés. Les efforts de conception de chaque approche ont été comparés aux résultats de l'analyse de l'histoire temporelle non linéaire (NTHA) pour des ensembles de mouvements au sol avec des contenus fréquentiels différents. Pour le mur de refend dans l'est du Canada, les résultats ont montré une surestimation du facteur de ductilité par la méthode FBD. Néanmoins, l'approche DDBD actuelle a sous-estimé l'effort de cisaillement et les moments fléchissant. La comparaison des résultats de la NTHA dans différents ensembles d'enregistrements de tremblement de terre a démontré que la courbe de déformation des murs de refend est très sensible à la fréquence des mouvements de sol imposés.

Dans les murs de refend en béton armé à rotule plastique unique à la base, la courbure à la base est le paramètre clé de la ductilité locale. Par conséquent, pour avoir de meilleures prédictions du niveau de ductilité, il est nécessaire d'avoir une prédiction adéquate de la ductilité locale. Les méthodes actuelles d'estimation de la courbure à la base, spécialement celles basées sur les prédictions de conception de la méthode DDBD, s'avèrent inexactes pour les murs en béton armé à hauteur élevée dans l'est du Canada. Pour résoudre ce problème, la courbure à la base des murs de cisaillement dans cette région doit être estimée. Une étude paramétrique a été réalisée sur plus de cent murs de refend afin d'identifier les paramètres ayant le plus grand impact sur le déplacement au sommet et la courbure à la base des murs de cisaillement dans l'est du Canada. Pour cette étude paramétrique, les NTHA ont été effectuées sur OpenSees sous des mouvements de sol simulés sélectionnés. Les résultats de l'étude paramétrique ont été utilisés pour déterminer une équation empirique permettant d'estimer la courbure à la base des murs de refend. La courbure de base prédite peut être utilisée pour calculer la ductilité locale des murs de cisaillement. La ductilité locale

pourrait être utilisée comme indicateur pour évaluer le niveau de réponse inélastique. Une version modifiée de la méthode DDBD utilisant la ductilité locale estimée dans le processus de conception a été proposée. Des facteurs analytiques d'amplification de cisaillement élastique dus aux modes supérieurs ont été suggérés pour répondre à la sous-estimation observée de des efforts de conception de la méthode DDBD. Des exemples de murs de cisaillement conçus selon l'approche proposée ont été comparés avec les résultats de la méthode NTHA et ont montré des résultats améliorés.

ABSTRACT

Reinforced concrete shear wall systems are one of the most commonly used structural system to resist seismic loads. The use of shear walls in seismic design is widespread because of their relatively high stiffness and their ease of construction. Shear wall system is even more beneficial for taller buildings because providing an appropriate level of stiffness for such structures is critical.

Many modern design provisions including National Building Code of Canada (NBCC 2015) and CSA A23.3-14 reinforced concrete design standard use force-based design approach for seismic design of shear walls. Although force-based method is fairly simple and have been used in practice for a long time, it has its own drawbacks. One important drawback of the force-based method is that the level of energy dissipation must be considered at the beginning of design process by anticipating the ductility of the system. In this approach, the actual level of mobilised ductility is not verified, and the system is designed to uphold the minimum capacity for a presumed level of ductility. In NBCC 2015 and CSA A23.3-14 there are specific provisions for seismic design of shear walls to maintain the presumed level of ductility.

Contrary to force-based design method, seismic displacement-based design methods permit to determine the level of ductility for the designed shear walls upfront. In regions of moderate seismicity, such as eastern Canada, the displacement-based approaches indicate that the maximum displacement demand for taller shear wall would be smaller than the yield displacement and thus, the common displacement-based methods would predict an elastic response. Such prediction is not in line with force-based method assumptions that the inelastic response is always achieved. Although in theory the displacement-based methods could predict the level of ductility, they have difficulties to accurately predict design forces for tall shear walls in regions with low to moderate seismicity. Compared to western Canada, in eastern Canada the earthquakes have lower magnitude and predominant high-frequency content. The combination of the long fundamental period of vibrations and the exposure to high-frequency ground motions, amplifies the impact of the higher modes which adds to the complexities in predicting the seismic response of tall shear walls in this region. This research investigates the issues involved with using force-based and displacement-based methods in design of tall shear walls in eastern Canada with specific focus on the deformation and ductility response at local and global levels and propose procedures to improve the accuracy of the estimations of these parameters.

As the first step to address these objectives, a preliminary study was carried out on two 17-storey shear wall buildings located in eastern and western Canada. The shear walls were designed according to NBCC/CSA A23.3 force-based design (FBD) and standard direct displacement-based design (DDBD) methods and the specific difference of the design predictions between eastern and western Canada were discussed. The design forces from each design approach were compared with the results of nonlinear time history analysis (NTHA) under ground motion sets with different frequency contents. For the shear wall in eastern Canada the results showed over-estimation of the ductility factor used in FBD method. On the other hand, the standard DDBD approach underestimated the design shear force and bending moments. The comparison of the results of NTHA under different sets of ground motion records demonstrated that the deformation response of the shear walls is very sensitive to ground motions frequency content.

In RC shear walls with single plastic hinge at the base, the base curvature is the key indicator of local ductility. Therefore, to have better predictions of the level of ductility, it is necessary to adequately predict the local ductility. The current methods to estimate the base curvature, specially those used in DDBD design, are found to be inaccurate for the taller RC walls in eastern Canada. To address this issue an objective was set to estimate the base curvature for shear walls in this region. A parametric study was carried out on more than hundred shear walls to identify the parameters that influence the most the top displacement and the base curvature of the shear walls in eastern Canada., Nonlinear time-history analysis (NTHA) were carried out in OpenSees under selected simulated ground motions. The results of the parametric study were then used to develop an empirical equation to estimate the base curvature. The predicted base curvature can be further used to calculate the local ductility of the shear walls, which is a good indicator to assess the level of inelastic response. A modified version of DDBD was proposed that uses the estimated local ductility in the design process. Analytical elastic shear amplification factors due to the higher modes were suggested to achieve an appropriate estimate of design force by DDBD. The seismic response of example walls designed according to the proposed approach were compared with the results of NTHA and showed improved results.

TABLE OF CONTENTS

LIST OF TABLES

LIST OF FIGURES

LIST OF SYMBOLS AND ABBREVIATIONS

c	Compression depth of the cross section
C	Coefficient that relates the base curvature to the top displacement (Dezhdar, 2012)
C_d	The ductility coefficient according to ASCE 7
DB	Displacement-based
DBD	Displacement-based design
DDBD	Direct displacement-based design
FB	Force-based
FBD	Force-based design
h_w, H_n	Height of shear wall
H_e	Height of the equivalent single degree of freedom system
H_i	Height of i^{th} level
I_e	Importance factor of the building according to NBCC
K_e	Effective stiffness of the equivalent single degree of freedom system
l_w	Length of shear wall
M_e	Mass of the equivalent single degree of freedom system
m_i	Seismic mass of i^{th} level
$M_{v\text{-}NBCC}$	Elastic amplification factor due to the higher modes according to NBCC
M_v	Elastic amplification factor due to the higher modes
M_w	Modal magnitude of the earthquake
N	Number of storeys
P_f	Axial compressive force at the base of the sear wall
q	Ductility factor according to EC 8
q_0	Behaviour factor according to EC 8

R	Analytical load reduction factor (Dezhdar, 2012)
R	Load reduction factor according to ASCE 7 OR the epicentral distance of the earthquake
R_d	Ductility related load reduction factor according to NBCC
R_o^{adj}	Adjusted over-strength related load reduction factor
R_o	Over-strength related load reduction factor according to NBCC
R_ξ	Damping reduction factor
$S_{(Ta)}$	Seismic design acceleration
SI	Stability index factor
T_1, $T_{Analitical}$	Fundamental period
T_a	Empirical design period according to NBCC
T_c	Corner period
T_d	Seismic design period
T_e	Effective period of the equivalent single degree of freedom system
V_d	Seismic design base shear
β	Coefficient that relates the base curvature of the shear wall to its top displacement
δ_u	Ultimate inelastic displacement at the top of the shear wall according to ACI 318
Δ_{de}	Design displacement of the equivalent single degree of freedom system
Δ_i	Total displacement at i^{th} floor
Δ_{max}	Maximum spectral displacement
$\Delta_{max,\xi=5\%}$	Maximum spectral displacement with 5% damping
Δ_{ye}	Yield displacement of the equivalent single degree of freedom system
Δ_{yi}	Displacement at i^{th} level at the yielding point
Δ_i	Inelastic portion of the total displacement at i^{th} floor

Δ_f	Elastic displacement of the shear walls according to CSA A23.3
Δ_t	Top displacement of the shear wall
Δ_y	Yield displacement of the shear wall
Δ_{ye}	Yield displacement of the equivalent single degree of freedom system
ϵ_{cu}	Concrete crushing strain
ϵ_{cu}	Yielding strain of reinforcement steel
μ	Global ductility factor, displacement ductility factor
μ_φ	Base curvature ductility factor
Ω_v	Inelastic shear amplification factor due to higher mode effects
φ_y	Yield curvature
γ_w	Nominal over-strength factor of the shear wall according to CSA A23.3
θ_{id}	Rotational demand at the base of shear wall according to CSA A23.3
θ_{ic}	Rotational capacity at the base of shear wall according to CSA A23.3
θ_m	Maximum allowed drift
θ_y	Drift at yielding point
ξ	Damping of the system
ξ_{eq}	Equivalent viscous damping of the system

CHAPTER 1 INTRODUCTION

Reinforced concrete (RC) shear wall systems are commonly used as the seismic force resisting system (SFRS) in high-rise buildings. The ease of design and construction as well as their efficient integration into common architectural layouts make them a popular choice for structural engineers. Depending on the level of seismic forces, as well as the layout and the height of the building, either simple or coupled shear wall systems could be used. Because of the higher share of the low-to-medium rise structures in building construction, seismic design provisions have been developed having this group of structures in mind and do not explicitly account for differences in seismic response of taller buildings. Not recognizing the particularities of seismic behavior of these structures may lead to designs that could be overly conservative or even unfeasible.

Canadian seismic design provisions use force-based design (FBD) methodology to determine design forces for building structures. It is assumed that in response to seismic loads, the structures dissipate seismic energy through inelastic deformations of dedicated structural elements. Design forces are first estimated from the elastic design spectrum, and subsequently modified by reduction factors to account for system over-strength and inelastic structural response. These factors, prescribed by design codes for different structural systems (Mitchell et al., 2003), are essential to initiate the design process. The FBD method is simple and direct but has several drawbacks. The procedure requires that the stiffness, fundamental period and the mobilized ductility be estimated in advance (Humar et al., 2011, Priestley et al., 2007) and falls short to establish the clear relationship between structural strength and inflicted damage. Numerous studies have been conducted in recent years to improve the accuracy of the FBD approach (Priestley and Amaris, 2002, Luu et al., 2013b, Boivin and Paultre, 2012b). However, the design assumptions of this approach heavily depend on first mode behavior which is difficult to justify for tall buildings. Such conceptual drawbacks still remain and are accentuated in the design of taller buildings, especially those with reinforced concrete (RC) shear walls.

An important research effort has been made to improve the force based seismic design method and account appropriately for higher modes effects for the taller RC shear walls. In Canada, the elastic higher modes shear amplification of base shear was introduced in 2005 edition of NBCC (NRC 2005) after the studies carried out by Humar and Mahgoub (2003). The inelastic effects of higher modes on shear forces and bending moments were recently studied by Boivin and Paultre (2012b)

and Luu et al. (2013b) for western and eastern Canada, respectively. While these studies focused mainly on the force amplification, in particular that of the shear forces, in the study by Dezhdar (2012) the impact of higher modes on the drift and curvature of cantilever shear walls in western Canada was also investigated. It was found that the requirements of CSA A23.3-14 based on the FBD procedure overestimated the base curvature and could not adequately establish the relationship between the maximum base curvature and the maximum top displacement. Considering that the ground motions in western Canada are dominated by low frequencies while the earthquakes in the east are rich in high frequencies (Atkinson, 2009), the effects of higher modes in eastern Canada are likely to be larger. Thus, for eastern Canada, the estimate of the curvature-displacement relationship would be even less accurate.

In low-to-moderate seismic zones, such as eastern Canada, taller shear walls are more likely to exhibit an elastic response to seismic loading. Such behaviour was observed by Luu et al. (2013a) based on the mean rotational ductility demand at the base of the wall. This response contradicts the predictions by the FBD method that relies on the assumption of the development of the full plastic hinge, and thereby overestimates the force reduction factors for such walls. Providing the minimum ductility capacity regardless of the type of structural response can become a limiting design criterion for taller walls, and potentially lead to uneconomical solution.

Contrary to the force-based design (FBD) in which displacement are verified at the end of the design process, displacements are essential design criteria in the displacement-based design (DBD). An important research effort has been deployed to develop design methods aimed to achieve desired displacements and/or inter-story drifts in the structure by Priestley et al. (2000 and 2007), Chopra and Goel (2001 and 2004), Aschheim (2002) and Tjhin et al. (2007). The direct displacement-based design (DDBD) method proposed by Priestley et al. (2007) is simple and efficient and can be easily implemented in practice. However, when applied to tall shear walls, DDBD has several downsides. Similar to the FBD, the procedure relies on the assumption that the first mode dominates the seismic response. Once determined, the seismic base shear has to be adjusted to account for higher mode effects. Humar et al. (2011) illustrated the use of the DBD design with the example of a 12-story RC shear wall building located in western North America. Effects of the higher modes were assessed by performing additional modal push-over analysis once the design was completed. In this study, it was possible to achieve a unique design because the structure was located in high-seismicity zone, and in the mid-range heights. Humar concluded that

the ductility assumed in the design codes can be rarely mobilised if the drifts remain below the code-specific drift limits or the drifts limits required to avoid instability caused by P-D effects. No other Canadian study explored the use of the DBD design for taller RC shear walls or structures located in eastern Canada.

In view of limited number of studies investigating seismic response of RC shear walls in eastern Canada and in absence of a detailed study on the deformation and ductility response of the tall RC shear walls in eastern Canada it appears pertinent to conduct a research addressing the issues discussed above.

1.1 Objectives

The main objectives of this PhD thesis are to study the seismic response of tall RC shear walls in eastern Canada, with focus put on their deformation response and to establish a relationship between global and local ductility indicators that could be used to improve seismic design procedures for this system. The methodology applied to achieve these objectives is detailed in the following section.

1.2 Research methodology

The research conducted in this study was regrouped around four distinct topics. The initial study was carried out to identify the shortcomings of available design methodologies in the context of taller RC shear wall seismic design, as well as specific differences in the seismic behaviour of these structures in eastern and western Canada. The attention is then directed to a detailed study of deformation response through the parametric study. Next, the results were used to develop a more appropriate relationship between the global and local ductility indicators (top displacement and base curvature). The developed relationship was then applied to improve displacement-based design procedure for this type of structure.

1.2.1 General study on the design predictions for the tall RC rectangular shear walls in Canada using forced-based and displacement-based design methodology

For the initial study, 17-storey shear walls in typical buildings located in Montreal and in Vancouver were designed according to NBCC 2015/CSA A23.3 force-based design (FBD) method and governing design parameters were identified. In parallel, DDBD method, proposed by Priestly et al (2007), was adapted for taller RC walls accounting for the possible elastic and inelastic approach. In the absence of explicit design displacement spectra in NBCC, displacement spectra were constructed following recommendations available in literature.

The seismic response of the walls was then studied using the nonlinear time history analysis using OpenSees. The models were calibrated following the recommendations available in literature (Luu et al, 2013 and ATC-72-1, 2010). The analyses were conducted for a set of twenty simulated ground motion records selected from the database proposed by Atkinson (2009).The sensitivity of the response to the frequency content of ground motions was evaluated. Two designs were compared by tracking the curvature ductility, lateral displacements, bending moments and story shears. Also, the impact of higher modes on seismic response of both regions was investigated.

1.2.2 A parametric study on deformation response of the shear walls in eastern Canada

In view of the findings from the initial study, a parametric study was carried out with focus on the deformation response of the tall RC shear walls in eastern Canada. The aim of this study was to identify the parameters which influence the most displacement and curvature response of such shear walls and to assess their specific impact on the top displacement and the base. Top displacement and base curvature were chosen as global and local deformation indicators respectively.

To carry out the parametric study, large number of rectangular shear walls had been designed with heights varying between 10- to 30-storeys. All shear walls were assumed to be located in Montreal, QC, on site class “C”. To obtain a variety of options with different geometrical properties and capacity-to-demand ratios, the shear walls were designed according to either FBD or DDBD

approaches. The level of axial compressive force was varied as well. To introduce different dynamic characteristics, the seismic mass was also varied for certain walls with the same geometry.

Although the focus of this research was on the rectangular shear walls, in order to investigate the possibility of expanding the conclusions to I-shaped shear walls, several I-shaped walls were also designed using the FBD approach and their response was compared to that of rectangular shear walls.

The designed shear walls were modeled in OpenSees for NTHA, that were calibrated using the available experimental test data on an 8-storey shear wall carried out at Polytechnique de Montreal (Ghorbanirenani et al, 2010). Additionally, the OpenSees modeling strategy was compared and calibrated with FE models in VecTor 2 for taller walls (20 and 25-storey shear walls) to confirm its accuracy especially regarding the prediction of base curvature and top displacement.

A set of thirteen simulated ground motions (Atkinson 2009) were chosen to perform the parametric study out of which eight records with relatively low frequency content and five records with high frequency contents. The records were selected and scaled following the guidelines provided in NBCC 2015. The response to the simulated ground motion records was compared with the response to the historical ground motions compatible with the governing earthquake scenarios in eastern Canada. The results of NTHA were assessed using different statistical values (i.e. mean, median, 84^{th} percentile etc.). The results of the NTHA were compared with the design predictions for both FB and DDB designed walls and the sources of the discrepancy were investigated.

Once identified, the most influential parameters were then considered to develop a relationship between the two key deformation responses, the top displacement and the base curvature.

1.2.3 Development of a relationship between the base curvature and the top displacement

In this part of the study, a function relating the top displacement to the base curvature is proposed. This function should improve the deficiencies of the base curvature prediction based on current FBD and DDBD approaches and lead to a more accurate estimate of the base curvature for the tall shear walls located in eastern Canada. The proposed relationship is then applied to walls designed in the parametric study and design predictions from the proposed relationship are compared against the estimates obtained from original design as well as the results of NTHA. The proposed

relationship is then further validated on nine different shear walls with heights between 10 to 30-storeys.

1.2.4 Modification of the existing DDBD based on the proposed relationship between the base curvature and the top displacement

The proposed relationship to predict the base curvature is then used to put forward a modified DDBD methodology, better adapted to design of taller RC shear walls. A study was carried out to estimate the elastic shear amplification factor due to higher mode appropriate for use with this method. The proposed procedure was then used to design different shear walls with varying heights. The design predictions were compared with the results of NTHA to investigate the accuracy of the proposed method.

1.3 Organization of the thesis

Chapter 1 introduces the problematics, sets objectives of the study, discusses the methodology adopted and describes the organisation of the thesis. The review of the literature pertinent for the project is presented in Chapter 2.

In Chapter 3, the initial study carried out on two shear wall buildings located in Montreal and Vancouver, is presented. This preliminary study introduces the reader to specific challenges regarding the design of tall shear walls and examines the fundamental differences in response of the shear walls in eastern Canada and western Canada.

The extensive parametric study used to identify the parameters that influence the most the deformation response of taller shear walls is described in Chapter 4. The relevant information regarding the NTHA, including the calibration of the analytical model and selection and scaling of the ground motion records are explained in this chapter.

Chapter 5 of this thesis presents the proposed statistical formulation that relates the base curvature to the top displacement. Later in this chapter a modified DDBD approach is proposed and its applicability is examined using NTHA.

Last chapter of this thesis, Chapter 6, includes the summary and conclusions of the research and provides the suggestions for the future studies.

CHAPTER 2 LITERATURE REVIEW

2.1 Seismic design of shear walls according to Canadian design provisions

The design of structural reinforced concrete (RC) shear walls according to Canadian design codes (NBCC, 2015 and CSA A23.3, 2014) follows a force-based approach. In NBCC (2015), the inelastic seismic base shear is calculated using the following equation:

Equation 2-1 $$V_d = \frac{S(T_d) M_V I_e W}{R_D R_0}$$

where T_d is the design fundamental period of the structure, $S(T_d)$ is the spectral acceleration at the design period with a probability of exceedance of 2% in 50 years; M_v is the factor accounting for the increase in base shear due to higher mode effects; I_E is the importance factor, W is the seismic weight, and R_d and R_o are the ductility and over strength-related force reduction factors, respectively. R_d factors are specified in NBCC for various structural systems and they quantify the energy dissipated through inelastic deformations. To find the demand forces, either static or dynamic analysis can be used. The seismic base shear, determined from dynamic analysis, must be calibrated to the base shear determined by equivalent static force method following the rules established for the regular and irregular buildings. Once the forces are determined, the estimates of total displacements can be obtained by multiplying the elastic displacements caused by the design force V_d by R_dR_o. This approach based on the equal displacement principal, which stipulates that the total displacements of inelastic and elastic systems are approximately equal. Newmark and Hall (1982) showed that for medium-to-long period structures ($T \geq 0.5$ s), the equal displacement principle does apply and that the ductility-related force modification factor, R_d, can be considered equal to the global ductility ratio, μ.

For regular buildings with RC shear walls used as the primary lateral load resisting system, it is assumed that most of the earthquake energy is dissipated through flexural inelastic rotations at a region at the base of the shear wall commonly known as the plastic hinge. The design procedure prescribed by CSA A23.3 (2014), incorporates the capacity design principles, and should provide a wall with an adequate resistance, stiffness and ductility. The section at the base of the wall is first designed to have an adequate flexural resistance for the bending moment introduced by seismic

loading. The design bending moments for the sections above the plastic hinge, are amplified by the ratio of the section's flexural resistance at the base of the wall and the bending moment demand at the top of the plastic hinge. The design shear forces are also found by the capacity design approach through amplifying the shear demands by the ratio of the nominal or probable bending moment capacity to the bending moment demand at the base of the shear wall, for ductile and moderately ductile walls, respectively. The ductility requirements are verified next. These include the verification of the minimal quantity of concentrated and distributed vertical and horizontal reinforcement and the construction details, the verification of stability of compression zone, and comparison of the inelastic rotational demand and the rotational capacity in the plastic hinge region. The verification of the inter-storey drifts against the limits described by NBCC completes the design process.

2.2 Seismic deformation of RC shear walls

Although there have been many studies addressing the seismic force response of RC shear wall structures, the studies on the deformation response of this type of structures are relatively limited. One of the most comprehensive studies on this topic in Canada was carried out by White and Adebar (2004) with the objective of investigating the rotational and displacement demands in simple and coupled shear walls, using nonlinear time history analysis. The findings of this study provided the bases for the ductility provisions of CSA A23.3 in 2004. The study was done for 10 to 40 storey high walls using a set of ten strong ground motion records with predominantly low frequency contents, representative of earthquakes in western North America.

The study showed that simple walls developed smaller rotational and displacement ductility demands compared to coupled walls because the participation of the elastic displacement in total displacement in simple cantilever shear walls is usually more significant. Even though the ground motion records were dominated by low frequencies, the impact of the higher modes on the deformation response was noticeable because of the wall height. White and Adebar (2004) assumed that the inelastic displacements of a shear wall were proportional to the inelastic rotation around the center of the plastic hinge (see Figure 2-1).

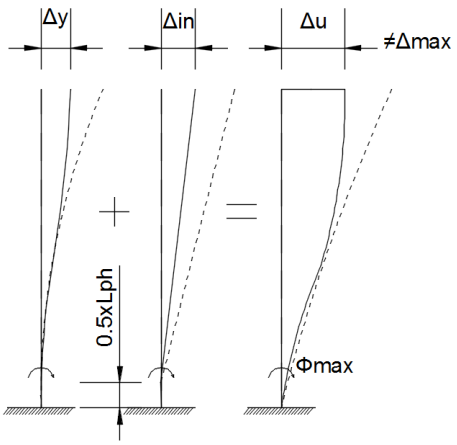

Figure 2-1: Total deformation of the shear wall as the summation of elastic and inelastic portions after White and Adebar (2004).

Consequently, the elastic deformation profile of the shear wall can be found by deducting the inelastic deformation from the total deformation profile. It is presumed that these elastic deformations include the higher mode contribution and inelastic deformation can be simplified as a rigid body rotation at the mid-height of the plastic hinge. It was assumed that although due to higher mode impacts, the maximum base rotation and top displacement do not occur at the same instant, the inelastic response can be derived from deducting the elastic portion from the total displacement. The total displacement is derived by multiplying the elastic displacement by the ductility factor.

Although White and Adebar (2004) noted that for the taller walls, the maximum rotation at the base and the maximum top displacement did not occur at the same instant, their proposed method assumed that there is a direct geometrical relationship between the base rotation and the top displacement. Because of its simplicity and reasonable accuracy for the low-to-intermediate height walls, their method was adapted by CSA A.23 and is being used in current version of the code (A23.3 2014). However, as it was pointed out before, this study addressed the walls located in western North America for which the impact of the higher modes is not as significant as in eastern North America. For tall shear walls located in eastern Canada, the wall ductility assumed in the force-based approach may not be fully mobilized implying that estimating the ultimate displacement form the elastic deformation could be very conservative and inaccurate.

Dezhdar and Adebar (2012) continued the research on the relationship between the base rotation and the top displacement of cantilever walls using a statistical approach through a parametric study.

Similar to the study by White and Adebar (2004), their study focused on western Canada. The seismic response of a total of fifteen shear walls with heights varying between 10 to 50 storeys was studied using non-linear time history analysis. The inelastic shear wall response was modeled using a trilinear moment-curvature law and the concentrated plasticity simulation. The analysis was carried out for a set of fifty-three ground motion records representative of western North America selected and scaled to achieve the compatibility with NBCC design spectrum over a selected period range.

After evaluating the base rotation and the top displacement response of the shear walls, the authors proposed the following equation to relate the top displacement and the base curvature:

Equation 2-2 $$\varphi_d = C * \frac{\Delta_t}{h_w l_w}$$

in which φ_d is the demand curvature, Δ_t is the top displacement, and h_w and l_w are respectively the height and the length of the shear wall. The coefficient *C* is a statistical parameter introduced by the authors to correlate the base curvature and the top displacement. The proposed coefficient is inversely proportional to the force reduction factor (*R*), thus directly proportional to the global ductility μ. In their study, the reduction factor (*R*) is not the presumed reduction factor of the NBCC code (R_d), but is the ratio of the inelastic base shear to elastic base shear force that was calculated for each shear wall. The expressions for the upper and lower bound values of C are based on the mean and the mean plus one standard deviation results and are respectively as follows

Equation 2-3 $$C = 1.8 - 0.017 * \frac{h_w}{R} > 0.8$$

$$C = 2.8 - 0.022 * \frac{h_w}{R} > 1.0$$

The first equation should be used if lower wall ductility is anticipated while the second one is appropriate for walls that develop higher ductility demand. The authors showed that the proposed equation provided a good accuracy in estimating the base curvature for shear walls up to 20-storeys high. For taller walls, the impact of higher modes is very significant, and the scatter of the results obtained for base curvature increases. Consequently, it becomes more difficult to put forward a unique equation to cover all shear walls with different geometry and design properties.

2.3 Design provisions related to global ductility, rotational ductility demand and base rotational capacity

NBCC (2015) defines three options that can be considered in seismic design of non-coupled reinforced concrete shear walls which are related to the global system ductility: conventional construction (R_d = 1.5 R_o =1.3), moderately ductile shear walls (Rd = 2.0 Ro =1.4) and ductile shear walls (Rd = 3.5 Ro =1.6). Height limitations are imposed for walls of conventional construction as a function of the location (40m and 30m for eastern and western Canada, respectively).

CSA A23.3 (2014) provides specific design and detailing requirements to ensure that the desired system ductility is achieved while maintaining the adequate resistance and avoiding any instability. However, like in other force-based methods, there are no explicit verifications at the end of the design process to confirm to what degree the assumed ductility is effectively mobilized by the seismic demand. To provide the capacity for ductile deformation, CSA A23.3-14 prescribes specific reinforcement detailing for ductile and moderate ductile walls, these being more stringent for ductile shear walls. Concentrated vertical reinforcement has to be on the edges of the shear wall as well as at the corners and the intersections with other walls in order to achieve a more efficient and ductile performance by the shear wall. Also, a minimum quantity of vertical and horizontal reinforcements must be provided. Longer development and overlap lengths are required for the reinforcement to guaranty the sufficient bond between the steel rebar and the concrete during an earthquake. The maximum distance between the bars is limited for a better inelastic performance. The vertical concentrated reinforcement must be tied to avoid flexural buckling failure modes and provide the necessary confinement for concrete. Depending on the level of ductility, the distributed vertical reinforcement should also be tied to prevent the flexural buckling of these rebars under compression.

While the global ductility ($\mu=R_d$) is not verified explicitly during the design process, verification of local ductility at plastic hinge is required by CSA A23.3-14 (clause 21.5.7.2&3). The design must demonstrate that the inelastic rotation of the shear wall, θ_{id}, at the base does not exceed the rotational capacity of the section, θ_{ic} ($\theta_{id} \leq \theta_{ic}$). θ_{id} and θ_{ic} can be calculated from the following equations:

Equation 2-4 $$\theta_{id} = \frac{\Delta_f * R_o * R_d - \Delta_f * \gamma_w}{h_w - \left(\frac{l_w}{2}\right)} \geq (\theta_{id})_{min}$$

Equation 2-5 $$\theta_{ic} = \frac{\epsilon_{cu} * l_w}{2c} - 0.002 \leq (\theta_{ic})_{max}$$

where l_w is the length of the wall, h_w is the total height, R_d and R_o are the related force reduction and over-strength factors, respectively, Δ_f is the displacement at the roof level at yielding under inelastic seismic load, γ_w is the ratio of the nominal flexural resistance to the factored flexural moment at the base, c is the depth of compression zone of the concrete section, and ϵ_{cu} is the maximum concrete compression strain. $(\theta_{id})_{min}$ ensures a minimum ductility for buildings with small inelastic drifts and $(\theta_{id})_{min}$ is equal to 0.003 and 0.004 for moderately ductile and ductile walls, respectively. $(\theta_{id})_{max}$ is taken as 0.025 for the two ductility levels to account for the possibility that the tensile strain capacity of the reinforced bars limits the inelastic rotational capacity of the shear wall. By combining the demand and capacity equations and assuming (h_w/l_w=5) the formulation of the local ductility requirements can be stated in term of the ratio of the length of the compression zone to the length of the wall as follows (Adebar, Mutrie, and DeVall, 2005):

Equation 2-6

For moderate ductile walls:

$$\frac{c}{l_w} \leq 1/(1 + 300 * (\frac{\Delta_f * R_0 * R_d}{h_w}) * (\frac{2.8 - \gamma_w}{1.5})) \leq 0.40$$

For ductile walls:

$$\frac{c}{l_w} \leq 1/(1 + 430 * (\frac{\Delta_f * R_0 * R_d}{h_w}) * (\frac{5.6 - \gamma_w}{4.3})) \leq 0.33$$

In American standards (ASCE 7, 2015 and ACI 318, 2017) two categories of shear walls are defined in relation to the level of ductility: Ordinary reinforced shear walls and Special reinforced shear walls. In ASCE (2015), instead of the two reduction factors (R_o and R_d) prescribed by NBCC (2015), only one force reduction factor (R) is represented which is equivalent to (R_o*R_d). Contrary to the Canadian code in which the ductility factor is assumed to be the same as the reduction factor, in ASCE a separate ductility factor (C_d) is presented. The force reduction (R) and ductility (C_d) factors for each level of ductility are given in Table 2-1. The bearing wall systems are those in which bearing walls are the major elements to support the vertical loads, and frame systems are those in which frames support the vertical gravity loads. In general, the reduction factors for frame

systems are larger than those for the bearing wall systems as they have better performance in dissipating the seismic energy. For bearing systems, the ductility (C_d) and load reduction factors (R) are equal, but this is not the case for frame systems. It is noted that the loads reduction and ductility factors in ASCE 7 (2015) are noticeably larger than those in the Canadian code (R_oR_d). However, to compare these factors with NBCC 2015, attention must be paid to the difference of the strength reduction factors between the codes.

Table 2-1: Ductility properties of shear wall structures in ASCE 7-15

Structural system	R	C_d
Bearing Wall System, Special reinforced shear walls	5	5
Bearing Wall System, Ordinary reinforced shear walls	4	4
Building Frame System, Special reinforced shear walls	6	5
Building Frame System, Ordinary reinforced shear walls	5	4.5

R: Load reduction factor

C_d: Ductility factor

The ASCE 7 (2015) does not allow the use of ordinary walls in areas with high seismic risk and specifies a limit of 48m (160ft) for systems using special shear walls only. For taller walls in these regions, it is obligatory to use a dual system that is a combination of shear walls and moment resisting frames, capable to resist at least 25% of the total seismic forces. There is no height limit either for ordinary or for special reinforced shear walls in areas of low seismic risk.

In ACI 318-(2017) the available rotational capacity at the base of the shear wall is verified only for special shear walls using Equation 2-7; for ordinary shear walls it is only required to provide special confinement detailing. This control is regardless of the system supporting the vertical loads (i.e. bearing wall or frame system).

Equation 2-7 $$\frac{c^*}{l_w} \leq \frac{1}{600*\left(\frac{\delta_u}{h_w}\right)} \leq 0.238$$

where c^* is the compression depth, h_w is the height of the shear wall and δ_u is the ultimate inelastic displacement at the top of the shear wall. For comparison, this equation can be rewritten in CSA A23.3 format as shown in Equation 2-6, taking into account the fact that the concrete resistance factor in ACI code is equal to 1.0 while in CSA A23.2 (2014) it is 0.65, (Adebar et al., 2005):

Equation 2-8 $$\frac{c}{l_w} \leq \frac{1}{390*\left(\frac{\Delta_f * R_0 * R_d}{h_w}\right)} \leq 0.37$$

In New Zealand standards (NZS 1170, 2004 and NZS 3101, 2006) three types of shear walls are defined as a function of the level of ductility of the shear wall buildings, namely nominal ductile shear walls, limited ductile shear walls and ductile shear walls. The equal displacement approximation is considered applicable for the structures with fundamental periods greater than 0.7s. The maximum ductility factor for each system is shown in Table 2-2. The aspect ratio of the walls influences the value of the ductility factors and consequently, walls with low aspect ratios have smaller ductility factors due to shear failure effects.

The maximum permitted compression depth in ultimate state, that does not require confinement reinforcement, is defined as:

Equation 2-9 $$\frac{c}{l_w} \leq \frac{0.1*\phi_{ow}}{\lambda}$$

where λ is 1.0 for limited ductile walls and 2.0 for ductile walls and ϕ_{ow} is the over strength factor. NZS-3101 limits the maximum curvature ductility (at the ultimate strength of the section) in the plastic hinge region to 6 for limited ductile walls and 14 for ductile walls.

Table 2-2: Ductility properties of shear wall structures in New Zealand code (NZS 1170, 2005)

Structural system	μ
Nominal ductile walls	1.25
Limited ductility walls	3.0
Single cantilever ductile walls	$4/\beta_a$
Two or more cantilever ductile walls	$5/\beta_a$
Two or more couple ductile walls	$5/\beta_a < \mu = (3A+4)/\beta_a < 6/\beta_a$

$R=\mu$ for T > 0.7sec. and for soil class A, B, C, D

$1 \leq \beta_a = 2.5 - 0.5A_r \leq 2.0$

A_r: Aspect Ratio of the wall
for walls with aspect ratio more than 3 ($A_r \geq 3$) β_a is 1.0

A: Degree of coupling of the coupled walls, $1/3 \leq A = [(T_w * L')/M_{ow}] \leq 2/3$

Similar to NBCC (2015) and CSA A23.3 (2014), Eurocode 2 (2001) and Eurocode 8 (2008) consider two levels of ductility for seismic design: namely moderate ductility and high ductility. Eurocodes use the equal displacement assumption for periods larger than the corner period of the

displacement spectrum (T_c). Corner period is the period at the upper limit of the constant acceleration region of the spectrum. Similar to the New Zealand code, the ductility factors for the shear walls with low aspect ratios are reduced. The behaviour factor ,q_0, which is equivalent to force reduction factor in the Canadian and the American codes, is defined as the following:

Equation 2-10 $$q = q_0 * k_w$$

The coefficients q_0 and k_w are given in Table 2-3. The displacement behaviour factor (q_d) for shear walls with a fundamental period larger than the spectral corner period is equal to q_0.

Eurocode 8 stipulates that the rotational capacity of plastic hinge regions be such that the maximum strain in concrete does not exceed the maximum allowable strain ϵ_{cu}. In addition, the plastic hinge curvature ductility capacity shall not exceed the following values:

Equation 2-11 $$\mu_\varphi = 2 * q_0 - 1 \text{ if } T_1 \geq T_C$$

$$\mu_\varphi = 1 + 2 * (q_0 - 1) * \frac{T_c}{T_1} \text{ if } T_1 < T_C$$

where q_0 is the behaviour factor used in the analysis and T_1 the fundamental period of the building, both defined for the plane in which bending takes place, and T_C is the corner period.

Table 2-3: Ductility properties of shear wall structures according to (Eurocode 8, 2008)

Structural system	q_0
Cantilever wall system Moderate Ductility	3
Cantilever wall System High ductility	4.0*(α_u/α_1)

For systems with only two uncoupled walls per horizontal direction: α_u/α_1=1.0

Other uncoupled wall systems: α_u/α_1=1.1

Wall-equivalent dual, or coupled wall systems: α_u/α_1=1.2

$0.5 \leq k_w=(1+\alpha_0)/3 \leq 1$

α_0: Aspect Ratio of the wall

2.4 Higher modes impact on seismic response of shear walls

Filiartault et al. (1994) carried out one of the first studies in Canada on the impact of the higher modes on the response of RC shear walls. It was proposed to apply two different amplification

factors on elastic forces; one for shear forces and the other for bending moments. This approach with some modifications is currently used in New Zealand standard (NZS 1170.5, 2004) which takes into account both elastic and inelastic amplifications due to higher modes effects. NBCC (2015), considers the impact of the higher modes on the elastic response based on the approach proposed by Humar and Rahgozar (2000). In this method, the same higher mode amplification factor (M_v) is applied to the elastic base shear and the bending moment. The elastic base shear is then reduced by the over-strength (R_o) and ductility (R_d) reduction factors to represent the inelastic response of the structure (Equation 2-1). Because the higher modes have more significant impact on the shear force compared to the bending moment, a modification must be made by applying a moment reduction factor (J) to the bending moment. The values of coefficients M_v and J specified in NBCC depend on the type of the structural system, the value of the fundamental structural period and the seismic region. The amplification of the shear is closely related to the spectral shape and differs for different regions. As the ground motion records in eastern Canada have a dominant high frequency content, the impact of the higher modes in eastern Canada is more significant than in western Canada.

Although the impact of the higher modes on the elastic response of the structures have been recognized and addressed in design practice, in recent years important research efforts have been made to evaluate and estimate the impact of the higher modes on the inelastic response of shear walls. Boivin and Paultre (2012) carried out an extensive parametric study on 47 shear walls to investigate the inelastic amplification of shear forces and bending moments for shear wall structures located in western Canada. The key parameters in this study were height, aspect ratio, section profile, over-strength factor (γ_w) and site class. Although authors briefly reviewed the curvature ductility demands, the main focus of this study was on the demand shear force and bending moments. From the outputs of this parametric study, it was proposed that the inelastic shear amplification due to the higher modes be expressed by a coefficient related to R_oR_d/γ_w ratio and the fundamental period of vibration. Boivin and Paultre (2012) also proposed a new capacity design envelope for bending moments above the plastic hinge region which are amplified by a similar factor related to R_oR_d/γ_w ratio and the fundamental dynamic period.

Luu, Léger and Tremblay (2013) performed another study on the inelastic higher modes amplifications which focused on the response of shear walls located in eastern Canada. A parametric study was carried out on 35 shear walls with varying heights (between five to twenty-

five storeys), over-strength factors, ductility levels (ductile or moderate ductile) and site classes. Based on the results of this study, Luu et al. (2013) proposed an equation for shear amplification as a function of the fundamental period and the over-strength factor of the shear wall. Also, similar to Boivin and Paultre (2012), they observed the potential of formation of the plastic hinges in the upper levels of the wall and recommended that the capacity design bending moment envelope be further amplified to avoid such behaviour.

The current version of CSA A23.3 (2014) considered the inelastic amplification effects of the higher modes on shear forces along the height of shear walls. The inelastic shear amplification shall be considered for shear walls with period larger than 0.5s in eastern Canada and with periods more than 1.0s in western Canada. is calculated as the following:

Equation 2-12 $$\Omega_v = 1 + 0.25 * \left({R_o * R_d}/{\gamma_w} - 1 \right) \leq 1.5 \text{ and } \geq 1.0$$

Whereas Ω_v is the inelastic shear amplification factor due to higher mode effects, R_o and R_d are the over-strength ductility reduction factors and γ_w is the nominal over-strength factor of the shear wall.

Since the impact of higher modes on the global displacement profile particularly for the regions with strong earthquakes are usually not significant, most of the studies on higher modes impacts and the corresponding code provisions have commonly focused on the impacts on the forces. To the author's knowledge, the most important study regarding the impact of higher modes on deformation response is carried out by Kreslin and Fajfar (2011) which will be discussed later in this chapter in the section regarding the recent progress in displacement-based design approaches.

2.5 Experimental studies on slender shear walls

Because of the practical difficulties involved with building and testing large specimens, the number of experimental tests on tall shear walls is limited in the literature.

Ibrahim and Adebar (2000) performed a quasi-static test on a ¼ scaled specimen of a 80m shear wall. The point of application of the controlled displacement was selected to be at the two-third of the height of wall as an equivalent to an inverse triangular load distribution. The intent of this research was to determine an effective stiffness for slender shear walls appropriate for seismic design. The length of the wall and its thickness were respectively 1.52m and 101mm and it had a dumbbell shape. The displacement-controlled loading protocol was designed to represent the

seismic demand in Vancouver, BC. The results of this study served as the basis to propose upper and lower bound limits for the effective stiffness of slender shear walls, later integrated in 2004 edition of CSA A.23.3.

In Canada, the most recent and major experimental test has been performed by Ghorbanirenani et al (2010) at Polytechnique de Montreal. In this test, the dynamic response of an eight-storey (20.97m) shear wall was studied by performing shake table tests on two reduced scale shear wall specimens (1:2.33) subjected to seismic ground motions representative of the seismic hazard in eastern Canada. The length and thickness of the scaled specimens were respectively 1400 mm and 60mm. The ground motion records were applied to the walls in increments. The ground motions applied to the first specimen varied between 40% to 120% of the design level and to another specimen the ground motion records were incremented in the range between 100% to 200% of the design levels. The results showed a significant impact of the higher modes on the response of the tested shear walls. The response of the shear walls at the design level of earthquake was predominantly elastic and the rotation at the base of the shear wall did not significantly surpass the yield rotation. The test showed signs of inelastic behaviour at levels above the plastic hinge indicating a potential for the formation of the second plastic hinge in upper levels of the shear walls. It was noted that before entering the inelastic domain, the concrete shear resistance of the wall's cross-section significantly contributed to the overall shear capacity of the wall's cross-section.

Other experimental tests using shaking table have been carried out for western North America. Panagiotou & Restrepo (2011) confirmed the significance of the higher modes impact on the response of the RC walls.

An experimental study performed by Escolano-Margarit, Pujol, and Benavent-Climent (2012) consisted of quasi-static monotonic tests performed on two shear wall specimens, with and without confinement reinforcements. The test was characterised based on the seismic demands in western North America. The results showed that the level of the curvature ductility at the base could be significantly large. For a drift level, ranging between 1.2 and 1.5 percent, a curvature ductility of 25 to 30 was recorded in the specimen with confined reinforcement.

2.6 Nonlinear time history analysis of RC shear walls

2.6.1 Ground motion records

The earthquakes in eastern Canada are of moderate intensity and generally have low energy in lower frequencies while the major portion of their power is associated with high frequencies. The available historical ground motion records are commonly very weak either due to low-energy or low sensitivity of the recording instruments. For taller structures, for which the fundamental periods are long, using the historical records is thus questionable. For this reason, using artificial records for eastern Canada to conduct time-history analysis is a widespread practice amongst researchers.

Atkinson (2009) provided sets of records compatible with target UHS (Uniform Hazard Spectrum) given in NBCC 2005 for various Canadian locations. For each location, the sets of records are given for different soil classes and each set includes forty records with different magnitudes and epicentral distances. For eastern Canada, two major earthquake scenarios are considered; M6 scenarios with short epicentral distances representative of high frequency earthquakes that excite higher modes and thus amplify their impact on structural response, and M7 scenarios representative of earthquakes which have longer epicentral distances and lower frequency content and usually produce the largest flexural demand forces and deformations. For western Canada three main sources of seismic hazard can be identified, namely crustal, in-slab and interface earthquakes events. As the magnitude increases, the energy of these earthquakes increases, and their dominant frequency content shifts from high frequency to low frequency. Atkinson (2009) recommended a procedure for selecting and scaling of these simulated records. For each set of records a period range over which the selection of the records is desired is first defined. The period range for each set should be selected considering an appropriate to the earthquake scenario. For example, for the high frequency and weak ground motion records the period range shall be selected in high frequency range to cover the second and third mode frequencies, while for stronger motions with lower frequencies, the period range shall be selected in low frequency range to cover the first mode frequency. For each set in its relevant period range, the records with lowest standard deviation compared with the target UHS (with best shape match) would be selected and then scaled to the mean ratio of the UHS to record spectrum over the selected period range. Tremblay et al. (2015) in a comprehensive set of guidelines suggested two methods for selection and scaling of ground

motion records using NBCC 2015; one based on a single unique target spectrum over the period range and the other based on using multiple target spectra over the selected period range. The first suggested method is in fact a generalized version of the recommended procedure by Atkinson (2009) with similar steps. The guidelines by Tremblay et al. (2015) have been integrated in 2015 edition of the NBCC commentary.

2.6.2 Analytical modeling

The advancement in computational tools and methods has allowed more accurate modeling for RC shear walls. Although in previous decades nonlinear analyses were mainly limited to static push-over methods, in current research studies use of nonlinear time history analysis (NTHA) of RC shear walls is a very common. Different approaches are in use which vary based on the efficiency and the level accuracy. Some of the more common modeling approaches are concentrated plasticity models using predefined plastic hinges, fiber section modeling and distributed plasticity based on 2D or 3D finite element modeling. Each of these methods have their benefits and deficiencies. 2D and 3D finite element approaches are usually most accurate among the other methods as they can model the shear-flexure-axial force interaction and give a better prediction of the response at local levels. However, they are very time costly and the modeling procedure could be complicated. Using of concentrated plastic hinges, on the other hands, is usually much less time consuming. However, its accuracy is basically dependent on the accuracy of the plastic hinge force-deformation law and normally are not able to directly consider interaction between shear-bending and axial forces. Fiber section models are one step more efficient than the concentrated plastic hinge models since they integrate bending-axial force interactions and can lead to fairly accurate results when the levels of shear stresses are not significant.

Amaris and Priestley (2002) performed a study on the higher mode effects in RC shear walls. The study was carried out by NTHA of shear walls between two to twenty storeys. They used the concentrated plasticity modeling technic for NTHA. The models were developed in Ruaumoko program (Carr, 1996). For each storey, based on the axial forces, bilinear moment-curvature functions were defined and applied to the model. A modified Takeda hysteretic rule was used to define a nonlinear hysteretic relation between the bending moment and the curvature. Rayleigh damping coefficients were determined considering 5% damping at the first mode and 4% damping at the second mode. To calculate the Rayleigh damping matrix, the tangent stiffness was used. In

this study five artificial ground motions were used to perform NTHA. The ground motions were matched and scaled to EC8 code.

Boivin and Paultre (2012) used two different modeling approaches for their parametric study on RC shear walls in western Canada. The first model was developed in the 2D finite element program VecTor2 (Wong, Vecchio and Trommels 2004, 2013) which employs the modified compression field theory and smeared cracking approach for modeling RC membranes. The VecTor2 model allows considering both shear and flexural inelastic response of the RC wall. The other group of models were developed in OpenSees using fiber sections modeling strategy. Force-based beam-column elements were used with nonlinear materials defined for concrete and steel. For rebars, Steel02 material law was used which accounts for the strain hardening and the Bauschinger effect. For concrete, Concrete03 material law based on modified Park-Kent model was utilised and the modified Bentz model was employed to consider tension stiffening effects. The shear deformations were modeled as elastic. Authors did not report what percentage of the initial shear stiffness was used as the elastic shear stiffness. The damping of the models was set to 2% for the first and the last (based on the number of degrees of freedom) dynamic modes of the MDF system. Generally, five integration points were used for the beam-column elements, but three points were used whenever a convergence issue occurred. In this study, Boivin and Paultre used forty simulated ground motion records, ten for each of four selected earthquake scenarios, from Atkinson's database (2009).

Luu et al. (2013) performed an extensive parametric study on numerical modeling of RC shear walls as a part of their research to calibrate shear wall models to be used in a parametric study on force amplifications due to higher modes. They studied the impact of parameters like lumped and smeared reinforcement modeling, reinforced concrete tension stiffening, viscous damping ratio and its modeling approach and the shear stiffness in fiber modeling using OpenSees and finite element modeling using VecTor2. For this purpose, the results of a shaking table experimental test (Ghorbanirenani et al., 2010) were used. The numerical models were developed using fiber section approach in OpenSees and finite element method in Vecotr2. The concrete and steel material laws were the same as what was used by Boivin and Paultre (2012). Five integration points were used for the elements of the OpenSees model. The authors concluded that a better match with experimental data was achieved when the tension stiffening effects in concrete were ignored. For damping, to achieve a better match with the test results it was suggested to use 2% damping at the

first and the second modes for the OpenSees model and 1.5% at first and the third modes for the VecTor2 model. For calculation of the damping matrix during NTHA, using the last-committed stiffness matrix was found to be the most efficient method. It was reported that for best results, non-uniform values of shear stiffness should be assigned along the height of the wall to take into account a realistic shear deformation. It was suggested to use 25% of the gross section shear stiffness at the base of the shear wall and 5% at upper one forth of the height. These values are slightly larger compared to 10% of the gross-section shear stiffness suggested by ATC 72-1 (PEER, 2010) for modeling of new structures. Both OpenSees and VecTor2 showed a good accuracy in predicting the deformation and forces of the tested shear walls. However, in the OpenSees model, shear force results showed high sensitivity to the assumed shear stiffness.

2.7 Seismic displacement-based design of shear walls

In the last three decades the increase of interest in performance-based design motivated the development of new design methods for building structures based on the performance criteria. In performance-based design, the performance criteria are usually described in form of strain, displacement, drift or some other deformation parameters. An important research effort has been deployed to develop design methods aimed to achieve desired displacements and/or inter-story drifts in the structure by Priestley et al. (2000 and 2007), Chopra and Goel (2001 and 2004), Aschheim (2002). Contrary to the force-based design (FBD) in which displacements are verified at the end of the design process, in the displacement-based design (DBD), displacements are essential design criteria. In seismic displacement-based design the structure is designed to reach a specific design displacement during the design seismic event. Thus, the main goal of such method is to find the optimum stiffness which would lead to the desired design deformation, under the selected earthquake hazard level.

In the following text, an overview of the displacement-based design method is provided as well as selected implementations by prominent researchers.

2.7.1 Direct displacement-based design method (DDBD)

In displacement-based design, satisfying deformation demands is the key design objective, and the demand forces are calculated based on the desired structural deformations. Most commonly, it is assumed that the deformation profile is governed by the fundamental mode of vibration, and

therefore the target displacement of the equivalent SDF system can be derived. This displacement, in combination with the appropriate design displacement spectrum, is usually used to estimate the desired stiffness of the equivalent SDOF system. Once the structural stiffness and design target displacement are known, the seismic design base shear and the seismic force profile can be determined.

2.7.2 Direct displacement-based design using elastic spectra

The direct displacement-based design (DDBD) method proposed by Priestley et al. (2007) is simple and efficient and can be easily implemented in practice. In this approach the design is based on a linear equivalent single degree of freedom (ESDF) system with its damping and stiffness properties calibrated to represent the inelastic response of the structure. The stiffness of the equivalent elastic system is the secant stiffness of the inelastic system and the impact of the inelastic response on the seismic demand is represented based on an equivalent viscous damping for the elastic SDF system.

The DDBD design approach based on modified elastic spectra (Priestley and Kowalsky, 2000) is illustrated in Figure 2-2.

The multi-degree of freedom (MDF) inelastic system is replaced by an elastic ESDF system characterized by the secant stiffness at the target displacement. Additionally, the elastic displacement spectrum is modified by considering an effective equivalent viscous damping. The fictitious damping accounts for the energy dissipated through inelastic deformations and it depends on the assumed dynamic response of the seismic resisting elements and their hysteresis response. The design displacement spectrum is then derived by adjusting the elastic spectrum for a given effective damping. For a target design displacement of ESDF system, Δ_{de}, the effective period T_e can be determined from the design displacement spectrum. For a given mass, the effective stiffness K_e of the substitute structure can then be determined from T_e. Subsequently, the design seismic base shear is obtained as the simple product of K_e and Δ_{de}.

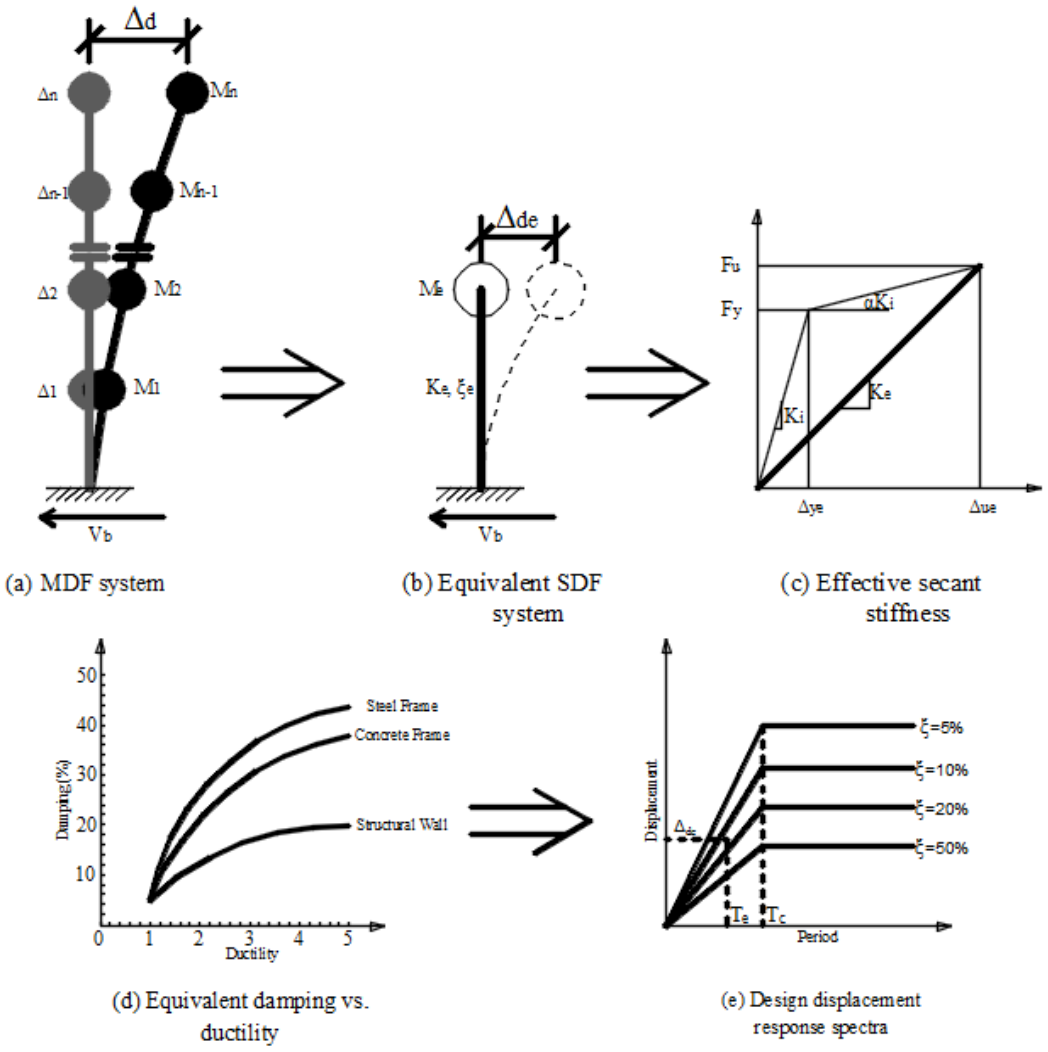

Figure 2-2: Fundamentals of direct displacement-based design (Priestley et al. 2007)

Assuming that the design displacement spectrum for the selected design location is available, DDBD of simple RC shear walls implements following steps; The geometry of the wall, in particular the wall length, and the inelastic deformation profile are presumed at the beginning of the design process. Commonly a reverse triangular deformed shape is considered for the inelastic deformation, assuming the dominance of the inelastic rigid body deformation after forming the plastic hinges. A target design top displacement is specified next, as a function of the desired performance criteria for the selected hazard level. The displacement profile is then updated based on the target top displacement and the MDF system is transformed to ESDF system (Figure 2-2-b). The effective mass (M_e), the effective height (H_e) and the target design displacement (Δ_{de}) of the equivalent SDF systems are calculated following the basics of structural dynamics. To find the

level ductility the yield displacement of the ESDF system should be estimated. For shear walls the following expression is proposed (Priestley et al. 2007):

Equation 2-13 $$\Delta_{ye} = \gamma_y * \varphi_y * H_e^2$$

where φ_y is the yield curvature of the system and γ_y is a coefficient proposed to be between 0.28 to 0.33 by different researchers (Paulay 2001 and Priestley 2007). For a given ductility, the equivalent viscous damping, ξ_{eq} should be estimated. Priestley et al. (2007), based on Takeda model for shear wall structures, propose the following equations for equivalent viscous damping. The elastic design displacement spectrum is modified by a reduction factor (R_ξ) defined by Equation 2-14.

Equation 2-14 $$\xi_{eq} = 0.05 + 0.444\,(\frac{\mu-1}{\mu\pi})$$

Equation 2-15 $$R_\xi = (\frac{0.10}{0.05+\xi_{eq}})^{0.5}$$

From the modified spectra, for a given design target displacement, the period of the equivalent elastic SDF (T_e) can be determined. For known values of T_e and M_e, the equivalent secant stiffness (K_e) is determined from the following:

Equation 2-16 $$K_e = 4\pi^2 \frac{M_e}{T_e^2}$$

The design base shear (V_d) is obtained from the product of the effective stiffness (K_e) and the design displacement of ESDF (Δ_{de}). The design base shear is distributed along the height of the shear wall using the shear force profiles from either an equivalent static or a response spectrum dynamic approach and the seismic demand shear force and bending moments are determined to design the wall sections.

2.7.3 Displacement-based design method using inelastic spectra (DBDIS)

This approach was mainly developed by Chopra and Goel (2001, 2004, 2011) and is the major alternative to DDBD. The first steps outlined for DDBD approach regarding the transformation of the structure to a single-degree-of freedom system are common for other DBD approaches such as DBD using inelastic spectra. In this method, a constant ductility inelastic spectrum is used unlike the modified elastic spectra used in DDBD.

The inelastic spectrum can be given in the form of a displacement (Figure 2-3) or an acceleration spectrum which provides the maximum displacement or yield acceleration for a structure with a

specific initial elastic period. The inelastic spectrum is derived from the elastic spectra by applying a reduction factor. The reduction factor is related to the level of ductility of the structure and varies as a function of periods of vibration.

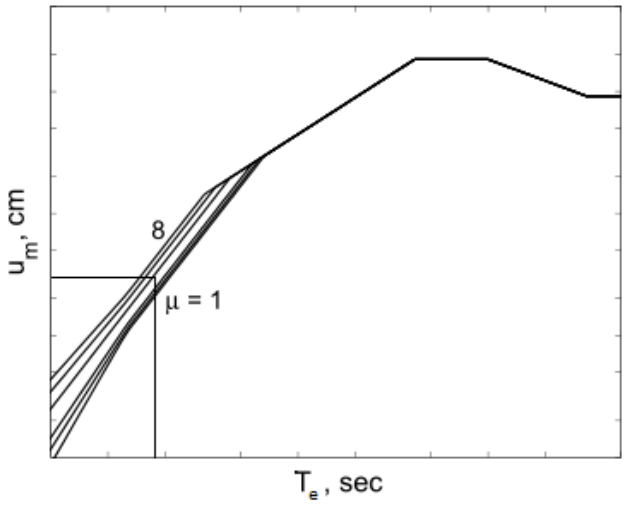

Figure 2-3: Example of inelastic displacement spectra (Chopra et al., 2001)

Similar to DDBD, the design displacement and the ductility factor of the SDF system are calculated first. Then for the calculated design displacement and ductility, from the inelastic spectra the initial elastic period of the structure is derived and accordingly the initial stiffness of the system is calculated, next. The required yield strength of the system is calculated by multiplying the initial elastic stiffness by the estimated yield displacement. After the preliminary section design, the initial stiffness of the global structure would be compared with the desired initial elastic stiffness calculated during design. An iterative trial and error procedure is then used until the stiffness of the system and the desired stiffness from design match with acceptable accuracy.

In general, the accuracy of both methods ultimately depends on the accuracy of the ductility reduction factor and/or the equivalent viscous damping being used for DBDIS and DDBD respectively. The proposed DBDIS method by Chopra and Goel gives different reduction factors for different period ranges contrary to the uniform reduction factor used by DDBD. Chopra and Goel argue that, compared to the DDBD, the inelastic spectra approach gives a better estimation of the inelastic response of the structure particularly for structures with large inelastic response. According to Chopra and Goel (2001), compared to DBDIS, the DDBD approach could under estimate the displacements and ductility of the structure. However, if limited plasticity develops in the structure, the difference between the two approaches is not significant.

2.7.4 Displacement-based design using yield point spectra

The Yield-Point Spectra (YPS) method proposed by Aschheim (2002) is another interpretation of the DBD procedure using inelastic spectra. The design spectrum used in this method is based on the uniform ductility similarly to the one used in DBDIS procedure. However, in YPS method the design spectrum is constructed for the yield displacement of the ESDF versus its yield strength.

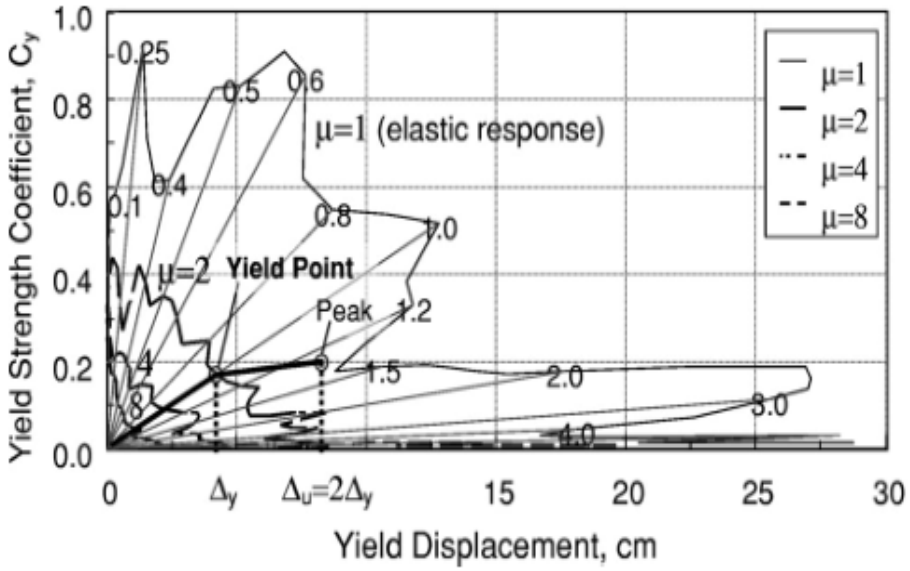

Figure 2-4: Example of yield pint spectra (Asschheim 2002)

When the ultimate design displacement is known, by predicting the yield displacement the ductility of the system can be calculated. The ductility and the predicted yield displacement of the system are then used to derive the required yield strength from the YPS.

The approach to construct the YP spectra is similar to DBDIS based on inelastic reduction factors which are applied to the elastic spectra. The reduction factors, like DBDIS, can vary for different period ranges for a uniform level of ductility. Although YPS is proposed to be used as a direct approach by design engineers, to achieve an acceptable accuracy, similar to DDBD and DBDIS, an iteration procedure must be implemented.

2.7.5 Displacement design spectrum for eastern Canada

Although the 2015 edition of NBCC provides spectral accelerations for periods up to 10 s, and thereby improves the data for design of structures with longer fundamental periods, the design

displacement spectra are not readily available for use in design practice. Nevertheless, the spectral displacement could be derived from spectral acceleration ($\Delta(T)=T^2/4\pi^2*S(T)$). This approach is adopted by most of the international design codes (except for Eurocode 8 which uses a more precise spectral displacement shape). For the Canadian UHS, however, because a linear interpolation between the spectral accelerations is advised by simple conversion of the acceleration spectra to displacement spectra, the desired bilinear shape for the displacement spectra cannot be achieved (see Figure 2-5). In order to approximate the shape of the displacement spectra, it is required to determine an appropriate value of the corner period and the maximum design displacement for the selected design location. The corner period denotes a period after which the spectral displacements reach the maximum displacement and remain constant.

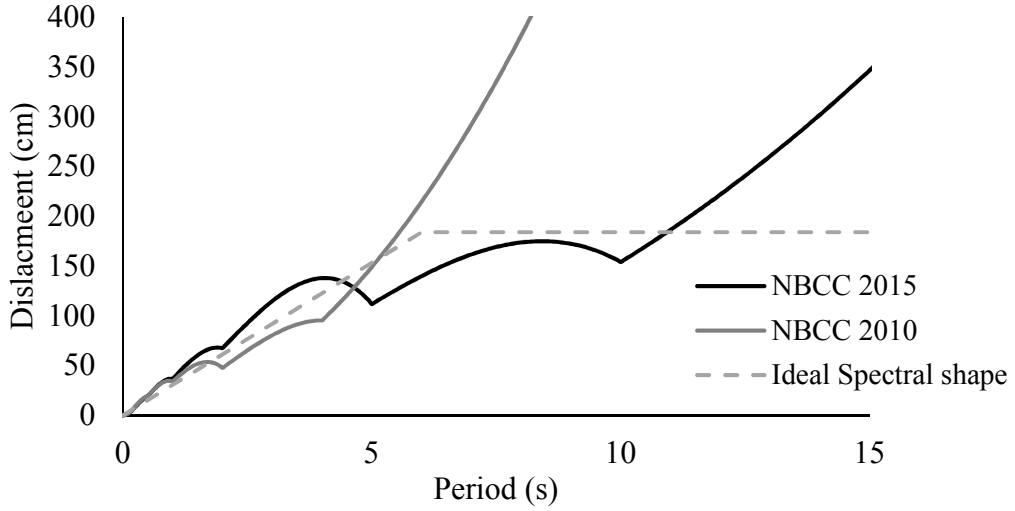

Figure 2-5: Displacement spectra derived by converting NBCC acceleration spectra (2475 years return period)

Corner period is a site specific seismological variable which mainly depends on the modal magnitude of the governing earthquakes. Various procedures are suggested to determine corner periods and are implemented in international seismic norms. In ASCE 7 (2015) the corner period is ranging from 4s for magnitudes between M_w=6 and 6.5 to 16s for magnitudes between M_w=8 and 8.5. In the New Zealand seismic code, NZS1170.5 (2004) the value for the corner period is fixed at 3 s for all locations. In Eurocode 8 (2004), the design displacement spectrum has a slightly different shape for long periods (Smerzini, Paolucci, Galasso, & Iervolino, 2012). Two spectral shapes (Type 1 or Type 2) are given considering the surface-wave magnitudes of the governing earthquakes. For M_s smaller than 5.5 the corner period is 1.2 s and for Ms larger than 5.5 the corner

period is 2 s. The spectral displacement reaches the maximum spectral displacement at the corner period, remains constant up to 4.5 s or 6 s (depending on the ground category) and then linearly reduces to the peak ground displacement at the period of 10s. The displacement spectra remain constant for periods larger than 10 s.

To estimate the corner period for displacement spectra, two well-known equations are available from Faciolli et al. (2004) and Crouz et al. (2006). Both equations are based on the modal magnitude of the design earthquake scenario. Faccioli 's equation is derived using the analysis of selected data of strong motions from Taiwan, Japan, Italy and Greece and according to Priestly can be conservatively used for earthquake magnitudes larger than M5.7. The equation is:

Equation 2-17 $T_c = 1.0+2.5(M_w - 5.7)$

According to Priestley (2007), Faciolli suggested the following equation to estimate the maximum spectral displacement (refer to Priestley, 2007):

Equation 2-18 $$\Delta_{max} = C_s \frac{10^{(M_w - 3.2)}}{r}$$

in which M_w is the modal magnitude of the governing earthquake and *r* being the epicentral distance in km. C_s for firm soil class is equal to 1.0.

The proposed equation by Silva (Crouse, Leyendecker, Somerville, Power & Silva, 2006) is developed based on the ground motion data of North America region:

Equation 2-19 $T_c = 10^{(-1.25+.3M_w)}$

The above equation is the base for the suggested corner periods in ASCE 7-2015. To the author's knowledge no other equation for the maximum spectral displacement has been suggested for North America.

2.8 Recent progress in displacement-based design

In recent years, several studies addressed deformation demands and displacement-based design of RC shear walls. Sulivan and Fox (2015) proposed a simple version of the DDBD (Priestley et al., 2007) for designing of the RC shear walls according to Eurocode 8. They used the maximum allowed plastic rotation from EC8 as the main criteria to calculate the design displacement. To control the P-Δ they proposed to limit the stability index of the SDF structure to 0.3. The proposed

method was applied to twenty case study shear walls which all were eight-storeys. The walls were designed for different design spectra with different corner periods and maximum spectral displacements. The design results were compared with the results of NTHA. The proposed approach showed to be always conservative with relatively well predictions of the demands. Although, the proposed approach was used to design shear walls in regions with low seismicity in some case studies, because the shear walls were fairly short, the predicted response was inelastic for all the case studies. They proposed that DDBD does not lead to unique design for tall shear walls with large periods. The proposed method does not explain how tall shear walls with predicted elastic response should be designed.

Fox, Sullivan, & Beyer (2015) performed a study on the deformation demands from DDBD, nonlinear static and nonlinear dynamic analysis of an eight-storey shear wall structure. The structure consisted of six simple RC shear walls with different lengths and configurations to model asymmetric stiffness in plan. For comparison, nonlinear response was modelled using both lumped and distributed plasticity for which the difference was found to be minor. Authors reported reasonable accuracy from DDBD and nonlinear static analysis. However, it was noted that DDBD needed more development in the region with fundamental period around and beyond the corner period, which is the case for the taller shear walls. Also, it was shown that these simplified design methods do not accurately consider the impact of higher modes on the deformations particularly after the yielding point.

Kreslin and Fajfar (2011) proposed a modified evaluation method for evaluating the response of shear walls by considering the effects of higher modes. The method assumes that the higher mode effects in the inelastic and the elastic ranges are equal. The authors proposed to amplify the target displacement of the push-over analysis by a higher mode amplification factor. This factor is calculated from the ratio of the elastic displacement from response spectrum analysis to the elastic displacement from the first mode. However, this method was suggested as a companion simple assessment to other more accurate approaches and was not suggested to be used for the final design.

Canadian studies reported in the literature that address the use of DBD for seismic design of RC shear walls include that from Alexieva (2007) and Humar, Fazileh, Ghorbanie-Asl, & Pina (2011). Alexieva (2007) performed a study on three shear wall structures with 6-, 12- and 18-storey heights. The shear walls were designed according to three displacement-based methods described in

Sections 2.7.2 to 2.7.4, namely DDBD, DBDIS and YPS, for 75, 475 and 2500 years seismic hazard levels. The walls were located in Montreal and Vancouver as the representatives of eastern and western Canada. NTHAs at each hazard level were carried out and the analyses results were compared with the design predictions. The study showed that the three approaches lead to relatively similar design forces. Alexieva recognized that with increase in height, because of more important impact of higher mode impacts, the accuracy of the methods reduces. For design spectra, Alexieva did not consider the maximum displacement demand limit for design which resulted in design displacement proportionally increasing with the design period. This assumption may be overly conservative for eastern Canada region.

Humar et al. (2011) performed a displacement-based design of a 12-storey shear wall building in Vancouver with simple rectangular walls. The DDBIS method proposed by Chopra and Goel (2004) was used to design the walls. The results of the study showed that a significant part of the provided ductility capacity, anticipated by NBCC 2010 FBD approach, was not mobilized. The design was governed by the global drift to limit the P-Δ effects. The impact of the higher modes on the displacement, inter storey drifts and shear forces was considered by doing a multi-mode push-over analysis after the preliminary force estimation. The ductility demand from the presented DBD approach is much smaller from that specified by the code. The maximum ductility of 1.57 compare to the proposed 3.5 code ductility demand confirms the findings from the previous studies that the code specified ductility capacities are rarely mobilized. From multi-modal push over analysis, it was found that the impact of the higher modes on the displacement and inter-storey drifts was not significant. However, the impact of the higher modes on the shear forces was substantial.

2.9 Summary

In this chapter the existing approaches to estimate the seismic deformation and the level of ductility for walls structures were discussed. The force-based design method incorporated into the Canadian code and other modern codes were reviewed along with the displacement-based design methods.

Most of the previous studies, presented in this Chapter, addressed low-to-moderate height RC shear walls located in the areas of high seismicity and only few investigate the use the displacement-based approach. Specific dynamic characteristics of the tall shear walls will cause the amplification

of seismic response due to higher mode effects which will lead to different seismic behaviour compared to that reported in the previous studies. On the other hand, the ground motions in eastern Canada are of lower intensity and have high frequency content which differs greatly from the ground motions typical of western Canada and amplifies even more the importance of the higher modes on the response of the shear wall. Since ductility of the system is a function of the deformations, the level of ductility for the tall shear walls in regions like eastern Canada could be affected. The taller the shear wall, the level of ductility reduces to up to a point that the overall response can be considered as elastic. Unlike FBD methods, DBD method can predict such behaviour through the course of design. However, DBD methods have their own challenges regarding the design of tall shear walls with predicted elastic response. The available Canadian studies presented in this Chapter used somewhat conservative assumptions to determine displacement spectra and this issue needs to be further addressed.

CHAPTER 3 COMPARISON OF FORCE-BASED AND DISPLACEMENT-BASED SEISMIC DESIGN OF TALLER REINFORCED-CONCRETE SHEAR WALLS

In this chapter, the force-based and displacement-based seismic design methods were applied to design RC shear walls in 17-storey buildings located in Montreal and Vancouver with objective to investigate the applicability of design methodology to taller RC wall design. Two design methods are compared using the results of nonlinear time history analyses (NTHA). The advantages and the limitations of the two methods are discussed. For the study presented in this chapter, the FB designed shear walls were designed according to NBCC 2010 and CSA 23.3-14 and to construct the displacement design spectrum for DDBD, the maximum spectral displacement was derived from the UHS of NBCC 2010. During the course of the research project, the 2015 edition of NBCC with updated design UHS became available. Although the changes would impact both FB and DDB designs, the conclusions of this chapter are unaffected by these changes. The studies presented in the next chapters of this dissertation are in compliance with NBCC 2015.

3.1 Force-based seismic design of tall shear walls

In an exploratory study which served as basis to define this research project it was observed that the for the shear walls under high level of axial stress the requirements for controlling the ductility capacity are likely to govern the design. To further investigate the importance of this design requirement for RC wall design, 12-, 14-, and 20-storeys moderately ductile walls were designed for Montreal building considering the floor geometry as shown in Figure 3-2. The walls are under high compressive force stress ($0.12*f'_c$) and have varying lengths. Aspecial effort was made to minimize the flexural over-strength at the base of the wall.

In all cases, the rotational demand was governed by the minimum value prescribed by the CSA A23.3 (2014) standard ($(\theta_{id})_{min}=0.003$). For 12- and 14-storeys walls, the length selected to satisfy strength requirements was sufficient to provide adequate rotational capacity at the base. However, as illustrated in Figure 3-1, for 17- and 20-storeys structures the rotational demand exceeded the maximum possible capacity of the section and thus it was necessary to increase the length of the wall to meet this requirement. This, in turn, resulted in increased flexural over-strength at the base

equal to 11% and 21% for 17- and 20-storey wall respectively. Lengthening the wall solely to provide the minimum rotational capacity results in a higher over strength, which influences directly design of capacity-protected zones and may alter the desired seismic response of the wall.

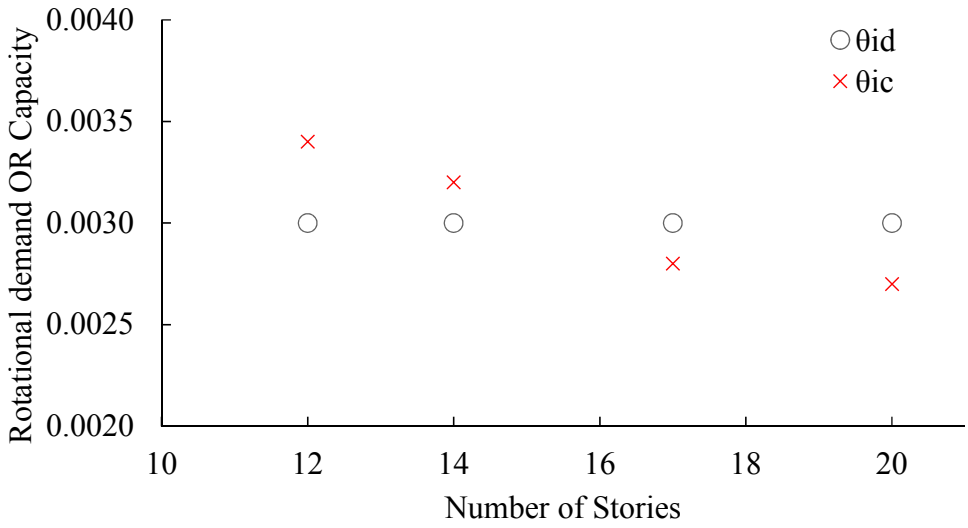

Figure 3-1: Base rotational demand and capacity of sample shear walls according to CSA A23.3

This study showed that, for shear walls taller than 17 storeys, satisfying inelastic rotational demand may become a major design challenge. Thus, to investigate further the feasibility of CSA-A23.3-14 procedures for seismic design of taller RC shear, a study was carried out on the example of 17-storey office building with simple rectangular shear walls. The building was assumed to be located in Montreal (eastern Canada) and Vancouver (western Canada) and designed according to NBCC2010 and CSA A23.3-14. The plan of the building is shown in Figure 3-2. In each direction, four rectangular perimeter walls provided the resistance against seismic forces. The walls are detailed as moderately ductile in Montreal and ductile in Vancouver as would be commonly done in practice. It should be noted that the original design of the building included a combination of the internal C-shape RC walls and rectangular RC walls on the edges of the plan which is a practical solution for tall buildings. However, since the purpose of this study was to investigate the deformation of the rectangular shear walls, the internal C-shaped shear walls in the original plan were replaced with rectangular shear walls. The number of the shear walls in each direction was selected to provide level of stiffness similar to that of the combination of the C-shaped and rectangular RC walls in the original design.

The seismic loads are determined from a 3D response spectrum analysis (RSA) performed using ETABS (CSI 2015). Accidental torsion is considered by applying eccentricity equal to 5% of the building's dimension in each direction as permitted by NBCC for regular structures. The dynamic seismic base shear is calibrated to 80% of design base shear, calculated by the equivalent static method. For the two sites, the fundamental periods obtained from the modal analysis exceed the code-suggested empirical values by a large margin and thus the design period corresponded to the minimum limit permitted by NBCC ($T_d = 2*T_{empirical}$). Because of this limitation, the minimum shear does not govern the design.

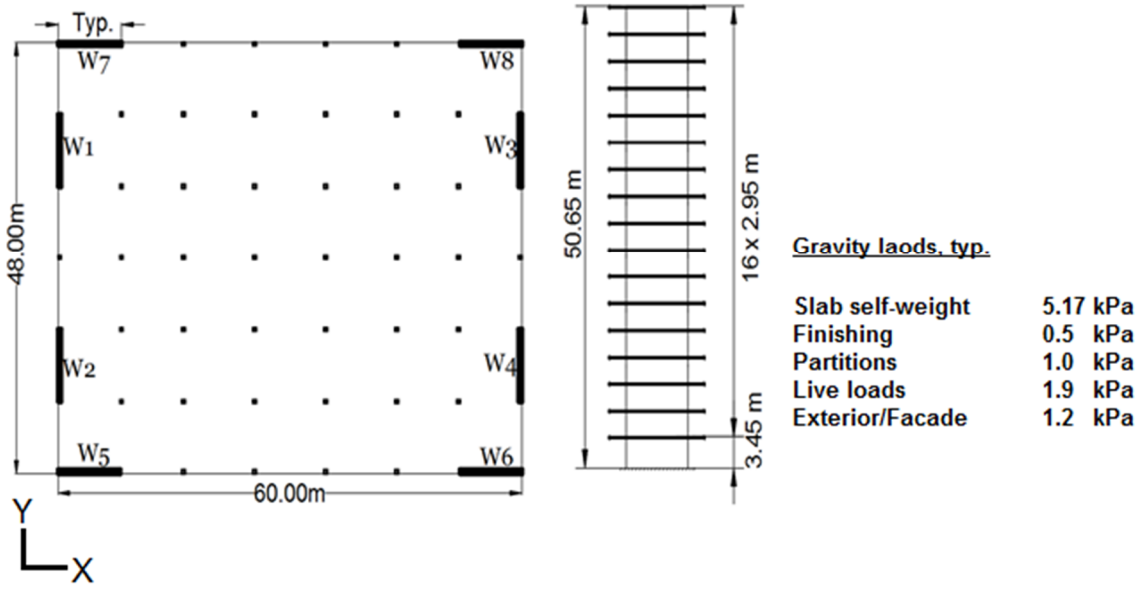

Figure 3-2: Studied building: plan view, wall elevation and gravity loads

The results of the seismic load calculations are summarized in Table 3-2. Because of the difference in the assumed level of ductility, the design base shears of the two buildings are similar even though the spectral accelerations for Vancouver are significantly larger. Larger torsional stiffness and accidental torsion in the Y direction causes more significant amplification of bending moment and base shear force for walls W_1 to W_4. The amplification is more pronounced for Montreal; 43% and 19% increase in bending moment and shear force, are respectively recorded in the Montreal building compared to 25% and 16% increase in the Vancouver building. W_1 to W_4 have the largest design forces and are selected and discussed for the study. In the following text W_{MTL} and W_{VCR} are used to denote the selected walls in Montreal and Vancouver buildings, respectively. The

typical detailing and selected reinforcement of the shear wall cross sections for W_{MTL} and W_{VCR} are shown in Figure 3-3 and Table 3-1. It should be noted that the confinement reinforcement detailing for each shear walls is different depending on level of ductility demands.

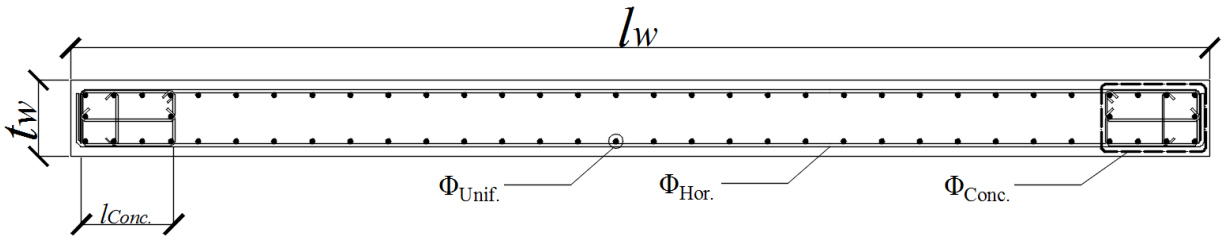

Figure 3-3: Typical section for the designed shear walls

Table 3-1: The cross-sectional reinforcement of the designed shear walls (Units: mm)

Location	Design case	Levels	l_w	t_w	$\phi_{Unif.}$	$l_{Conc.}$	$\phi_{Conc.}$	$\phi_{Hor.}$	Confinement detailing
W_{MTL}	DDBD	base to 7th	6500	400	15M@200	800	2x8 30M	15M@200	N/A
		8th to 12th	6500	400	15M@200	800	2x8 25M	10M@250	N/A
		13th to 17th	6500	400	10M@200	800	2x8 20M	10M@250	N/A
	FBD	base to 7th	8000	400	15M@200	800	2x8 25M	15M@200	Moderate ductile
		8th to 12th	8000	400	15M@200	800	2x8 25M	15M@250	Moderate ductile
		13th to 17th	8000	400	15M@200	800	2x8 25M	10M@250	Moderate ductile
W_{VCR}	DDBD	base to 7th	8000	400	15M@200	1100	2x10 30M	15M@150	Ductile
		8th to 12th	8000	400	15M@200	1100	2x10 25M	15M@200	Ductile
		13th to 17th	8000	400	15M@200	1100	2x8 20M	15M@250	Ductile
	FBD	base to 7th	8000	400	15M@200	1100	2x10 30M	15M@150	Ductile
		8th to 12th	8000	400	15M@200	1100	2x10 25M	15M@200	Ductile
		13th to 17th	8000	400	15M@200	1100	2x8 20M	15M@250	Ductile

For all analyses and designs the compressive concrete strength (f'_c) is 30 MPa and the yielding strength of steel is 400 MPa. The ultimate strain of concrete is equal to 0.0035 as per CSA A23.3-14. Minimum reinforcement requirements did not control the designs. Shear reinforcement along the height of the wall and flexural reinforcement outside the plastic hinge region were determined according to capacity design requirement. For both site locations the curtailing of the reinforcement was done at 7th and 12th floors. On the other hand, providing adequate inelastic rotational capacity

was a critical design parameter for the walls in the two locations. The elastic overall drifts were small enough so that the minimum inelastic rotational demand had to be respected. For W_{MTL} augmenting the wall length to 8 m proved to be the most efficient way to increase the inelastic rotational capacity of the section at the base. In fact, according to Equation 2-5 for tall shear walls, the length-to-compression depth ratio, l_w/c, is smaller resulting in low values of θ_{ic} that are often below the minimum rotational demand $\theta_{id(min)}$. In such cases, two options are possible to increase the rotational capacity of a shear wall section. Either the design compressive strain of the reinforced concrete can be increased by providing confinement reinforcements or the wall can be lengthened. Increasing the length of the wall is the preferred option because of the construction difficulties associated with providing the confinement reinforcement.

Table 3-2: Seismic design information of $W_{1\sim4}$ in Montreal and Vancouver

Design information	**Montreal (MTL)**	**Vancouver (VCR)**
Length (m)	8	8
First, second and third periods (sec)	4.13, 0.7, .0.27	4.13, 0.7, .0.27
Design period (sec) ($Ta=2*T_{emperical}$)	1.9	1.9
Spectral acceleration at the design period, $S(T_a)$	0.06	0.19
Higher mode effects amplification factor (M_v)	1.91	1.16
R_0 & R_D	1.4 & 2.0	1.6 & 3.5
Building design base shear (kN)	16895	17600
Maximum roof drift at the edges of the building	0.45%	1.11%
Maximum inter-story drift at the edges of the building	0.63%	1.71%
Axial gravity load at the base, 1.0E+1.0D (kN)	12011	12011
Axial gravity load at the base, 1.0E+1.0D+1.0L (kN)	12525	12525
Base shear for $W_{1\sim4}$ (kN)	4365	4020
Bending moment for $W_{1\sim4}$ (kNm)	61890	75970
Bending over-strength factor (γ_w)	1.3	1.3
Shear amplification due to the inelastic higher mode effects (Ωv)	1.29	1.50

For the shear walls of the building located in Vancouver, length of the walls required to ensure that the minimum rotational capacity at the base found to be unpractical. Simple rectangular walls are not the most efficient option for tall structures in severe seismic zones. I-shaped and C-shaped shear walls provide larger flexural strength, and rotational ductility capacity and would be likely selected. For the purpose of this study, however, it was decided to keep simple walls and ignore the minimum rotational demand requirement for W_{VCR} walls. The study showed that providing

adequate inelastic rotational capacity was a critical design requirement, both in Montreal and Vancouver.

Because the rotational demand is determined assuming that the full wall ductility is mobilised, it is of interest to determine what is the realistic level of ductility attained and, as a result, judge on the pertinence of this design criterion for tall wall design. Thus, to investigate further the efficiency of CSA-A23.3-14 procedures for seismic design of taller RC shear walls, the seismic response of 17-storey wall designed for Montreal and Vancouver is examined using non-linear time history analysis. The results of this study are presented in Section 3.5.

3.2 Direct displacement-based design procedure for tall RC shear walls

The existing DBD methods are not straight-forward when applied to taller shear walls. With increase in height, the yield displacement of the system, based on the first mode of response, increases and at some point, exceeds the maximum UHS demand displacement. Consequently, the shear wall does not enter the inelastic domain and the overall response remains elastic. In this case, the classic DBD methodology can not lead to a unique design and in theory many solutions are possible. Even though, as discussed in Chapter 2, in recent years research efforts have been deployed to define more adapted DBD procedures, additional work is required. In this thesis, the DBDD procedure proposed by Priestley et al. (2007) was used. For the design of tall shear walls in Canada, when was needed, adjustment were made to the Priestley's method which will be pointed out in the text. The main steps of design are outlined below:

a) Determine the design displacement of the system and its deformation profile: Two criteria are considered: (i) the design displacement is set equal to the maximum top displacement prescribed by NBCC 2010, and (ii) the design displacement is set equal to the displacement corresponding to the maximum allowable inelastic rotation at the base of the wall. The second criterion ensures that the inelastic rotation at the base does not exceed the capacity of the section. Note that in order to start the design process, the length of the wall must be assumed.

The displacement profile corresponding to the first criterion can be established assuming the predominant first mode response and using the maximum allowable drift from NBCC 2010:

Equation 3-1 $$\Delta_i = \Delta_{yi} + (\theta_m - \theta_y) * H_i = \frac{\varphi_y}{2} * H_i^2 \left(1 - \frac{H_i}{3H_n}\right) + \left(\theta_m - \frac{\epsilon_y * H_n}{l_w}\right) * H_i$$

where Δ_i is the displacement at the i^{th} storey, Δ_{yi} is the displacement at the yield point, H_i is the height of the i^{th} storey measured from the base, and H_n is the total height of the wall; θ_m is the maximum allowed drift and θ_y is the roof drift at the yield point. θ_m is taken equal to 2.5% for buildings with normal importance as per NBCC 2015.

To define the displacement profile corresponding to the second criterion, the rotational capacity, θ_c, of the wall can be calculated from the maximum allowable curvature of the base, φ_m, equal to:

Equation 3-2 $$\varphi_m = \frac{\epsilon_{cu}}{c} = \frac{\epsilon_{cu}}{\alpha_c l_w}$$

where ϵ_{cu} is the design crushing strain of concrete, c is the depth of the compression zone under the factored bending moment and axial force, l_w is the length of the wall, and $\alpha_c = c/l_w$. Adebar et al. (2005) suggest limiting α_c to 0.33 and 0.40 for the ductile and moderately ductile shear walls, respectively, in order to provide a minimum rotational capacity at the base.

If the compressive depth of section is limited to above-mentioned limits, the elastic component of the maximum curvature can be estimated by the following equation (Priestly and Kowalsky 1998):

Equation 3-3 $$\varphi_y = \frac{2 * \epsilon_y}{l_w}$$

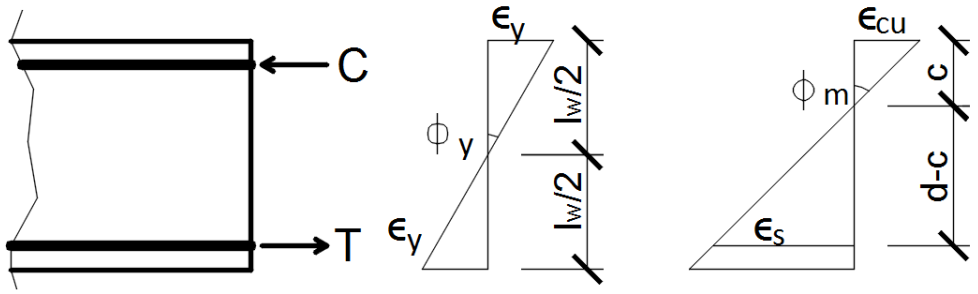

Figure 3-4: The yield and maximum curvature of a shear wall section according to CSA A23.3-14

The displacement profile based on the minimum rotational capacity can then be calculated as:

Equation 3-4 $$\Delta_i = \Delta_{yi} + \Delta_{pi} = \frac{\epsilon_y}{l_w} * H_i^2 \left(1 - \frac{H_i}{3H_n}\right) + (\varphi_m - \varphi_y) * L_p H_i$$

In the above equations, ϵ_y is the steel reinforcement yield strain, and L_p is the length of the plastic hinge that can simply be taken equal to l_w (Bohl and Adebar 2011). In this equation the maximum allowable curvature is based on the crushed strain in concrete. The maximum curvature based on the maximum strain in reinforcement steel, taken as 0.05 according to CSA A23.3, is neglected because it does not govern design of the tall shear walls which have large level of axial force at the base section.

The final design displacement profile of the MDOF system is established using the minimum of the two aforementioned criteria. This deformation profile is used to calculate the demand shear and bending moments along the height of the wall. For taller walls, the displacement profile corresponding to the minimum rotational demand is most often the governing design displacement.

b) Transform the MDF system to an equivalent SDF system: Equivalent SDF system properties are calculated assuming an inelastic deformation profile based on the first dynamic mode using the following equations:

Equivalent design displacement (Δ_{de}):

Equation 3-5 $$\Delta_{de} = \frac{\sum_{i=1}^{n}(m_i * \Delta_i^2)}{\sum_{i=1}^{n}(m_i * \Delta_i)}$$

Equivalent mass (M_e):

Equation 3-6 $$M_e = \frac{\sum_{i=1}^{n}(m_i * \Delta_i)}{\Delta_{de}}$$

Equivalent height (H_e):

Equation 3-7 $$H_e = \frac{\sum_{i=1}^{n}(m_i * \Delta_i * H_i)}{\sum_{i=1}^{n}(m_i * \Delta_i)}$$

ESDOF yield displacement:

Equation 3-8 $$\Delta_{ye} = \frac{\varphi_y}{2} * H_e^2 \left(1 - \frac{H_e}{3H_n}\right)$$

ESDOF ductility:

Equation 3-9 $$\mu_{DDBD} = \frac{\Delta_{de}}{\Delta_{ye}}$$

c) Construct the modified design spectra: The modification of the elastic design displacement spectrum to include the effects of inelasticity is done by applying a reduction factor

as proposed by Priestley et al. (2007). Assuming a 5% elastic damping for the structural and non-structural elements, the equivalent viscous damping ξ_{eq} for RC shear walls based on Takeda model is proposed as:

Equation 3-10 $$\xi_{eq} = 0.05 + 0.444\,(\frac{\mu-1}{\mu\pi})$$

And the modification factor, R_{ξ}, is determined from the following formula:

Equation 3-11 $$R_{\xi} = (\frac{0.10}{0.05+\xi_{eq}})^{0.5}$$

d) Conduct the preliminary assessment of the seismic response: At this step the seismic response of the shear wall can be estimated. Different scenarios are possible:

a. If the design displacement of the equivalent SDF system, Δ_{de}, is smaller than the maximum spectral displacement, $\Delta_{max,,\xi=5\%}$, and the two exceed the yield displacement, Δ_{ye}, the seismic response of the system will be predominantly inelastic. The preliminary ductility is estimated from Equation 3-9. In this case DDBD gives a unique value of design base shear because the required stiffness of the system is precisely defined.
b. If $\Delta_{max,\xi=5\%}$ is larger than Δ_{ey} but smaller than Δ_{de}, the response of the system will be inelastic. This is an indication that initial values of Δ_{de} and μ were overestimated because it is impossible that the design displacement exceeds the maximum spectral displacement. Thus, the iterative procedure has to be applied to finalise the design.
c. If $\Delta_{max,\xi=5\%}$ is smaller than Δ_{ey}, the response of the system will be predominantly elastic, because the yield point of the structure will not be reached. The design displacement is set equal to the maximum spectral displacement, and no modification of the elastic design spectra is required. In this case, the design does not lead to a unique solution, and the required stiffness of the system is not clearly defined. Such case is frequently encountered for the tall RC shear walls in regions with low or moderate seismicity.

e) Refine the estimation of the stiffness of the equivalent SDF system: During this phase, the bending reinforcement at the base of the wall and the level of concrete confinement are validated through an iterative procedure. For tall shear walls, a minimum reinforcement necessary to satisfy ductility requirements could be used as a starting point to define reinforcement details of an equivalent SDF system. Nonlinear push-over analysis is carried out next, and the resulting force-displacement diagram is idealized with a bilinear graph by minimizing the summation of

differences between the push-over curve and the idealized graph in the range up to the design displacement Δ_{de}. The idealized graph gives precise information on yield displacement, initial and secant stiffness, and thus design shear can be derived. The obtained values are compared with the preliminary estimations and the procedure is repeated until convergence is achieved.

f) Final estimation of the design parameters and calculation of the design forces: Using the final yield displacement of the equivalent SDF system, the system ductility is determined, and the design displacement spectrum is modified. If the inelastic response is predicted by design, the effective period (T_e) at the design displacement is read from the relevant displacement spectrum (Figure 2-2). The effective secant stiffness of the equivalent SDF system, $k_e = 4\pi^2 m_e/T_e^2$ is compared to that obtained from the bilinear force-displacement graph to confirm consistency. If convergence is not achieved, the reinforcement section detailing is modified for the next iteration. Finally, design base shear V_d is determined by multiplying the effective stiffness, k_e by the design displacement of the structure, Δ_{de}.

If the elastic response is predicted for a specific value of design displacement, a unique value of T_e cannot be found and therefore different design solutions are possible. Although, in theory in such situation any wall section and reinforcement details can be proposed, other requirements need to be considered to achieve a safe design. For tall walls, the P-Delta effects become a critical design criterion and set the limit for the minimum stiffness of the wall. In this study, the stability index, SI, was initially estimated from the following equation:

Equation 3-12 $$SI = \frac{M_e * g * \Delta_{ed}}{V_d * H_e}$$

In NBCC, this index is limited commonly to 0.4 to prevent excessive flexibility and avoid stability problems. The final verification of the stability index at every story must be done once the design of the wall is completed.

To complete the design base shear calculations, the higher mode effects and the impact of the system over-strength must be considered. In this study, the methodology available in NBCC 2010 and CSA A23.3-14 are adopted and the appropriate higher mode amplification coefficients (M_v and Ω_v) are selected. When the predicted wall response is elastic, the inelastic amplification factor Ω_v is not applied. The calculated base shear force is then distributed along the height of the shear wall using the force profile obtained from the response spectrum analysis (RSA).

3.2.1 Design displacement spectra

In NBCC 2010, design displacement spectra are not readily available but can be derived from acceleration spectra. However, because of the limitation imposed on design acceleration for periods exceeding 4 s, the displacements keep on increasing as periods increase (Figure 2-5). In order to develop more realistic displacement spectra, the shape of acceleration spectra given in ASCE 7 (2010, 2015) was adapted to the Canadian seismic context. Detailed presentation of the procedure can be found in the Sadeghian and Koboevic (2014). The maximum spectral displacement, Δ_{max}, is calculated from the acceleration spectrum using the following equation:

Equation 3-13 $$\Delta_{\max} = \frac{T_c^2}{4\pi^2} * S_{(T_c)}$$

where T_c is the corner period, and $S(T_c)$ is the spectral acceleration at the corner period. NBCC does not provide guidance to determine Tc, so appropriate values were defined for this study. To calculate the T_c, initial estimates were obtained using the expressions proposed by Faciolli. (2007, Equation 2-17) and Crouse et al. (2006, Equation 2-19) in function of the modal earthquake magnitude, M_w. To apply these equations, the dominant M-R scenarios (Vancouver M=9, R=152 km; Montreal M=6.875, R=30 km) were identified using hazard desegregation maps at the periods close to the first modal period of the studied structures (T = 4.13 s). However, for Montreal, the data available from the Geological Survey of Canada (GSC 2010) and the US Geological Survey (USGS 2015) are provided only for fundamental periods up to two seconds, and thus the desegregation map for spectral acceleration at 2 s was used. For Vancouver, in the absence of data for periods longer than 2 seconds in GSC database, the data was extracted form USGS database. The dominant scenarios were identified from USGS data for periods of T = 4 s and T = 5 s. Accordingly from the equations from Priestley (2007) and Silva (Crouse at al, 2006), the corner periods (T_c) for Vancouver are respectively 9.25 s and 28.18 s while for Montreal 3.94 s and 6.49 s . The two equations yielded significantly different T_c, particularly for Vancouver, so for further comparison, the corner periods were determined from elastic displacement spectra of simulated and historical records (Sadeghian and Koboevic 2014). Final values selected for this study were 16s and 6s for Vancouver and Montreal, respectively, which is consistent with the values assigned by ASCE 7-15, in the US regions close to the two cities. For selected corner periods, the maximum spectral displacements derived from Equation 3-13 based on NBCC 2010 UHS are 1.353 m and 0.203 m for Vancouver and Montreal, respectively.

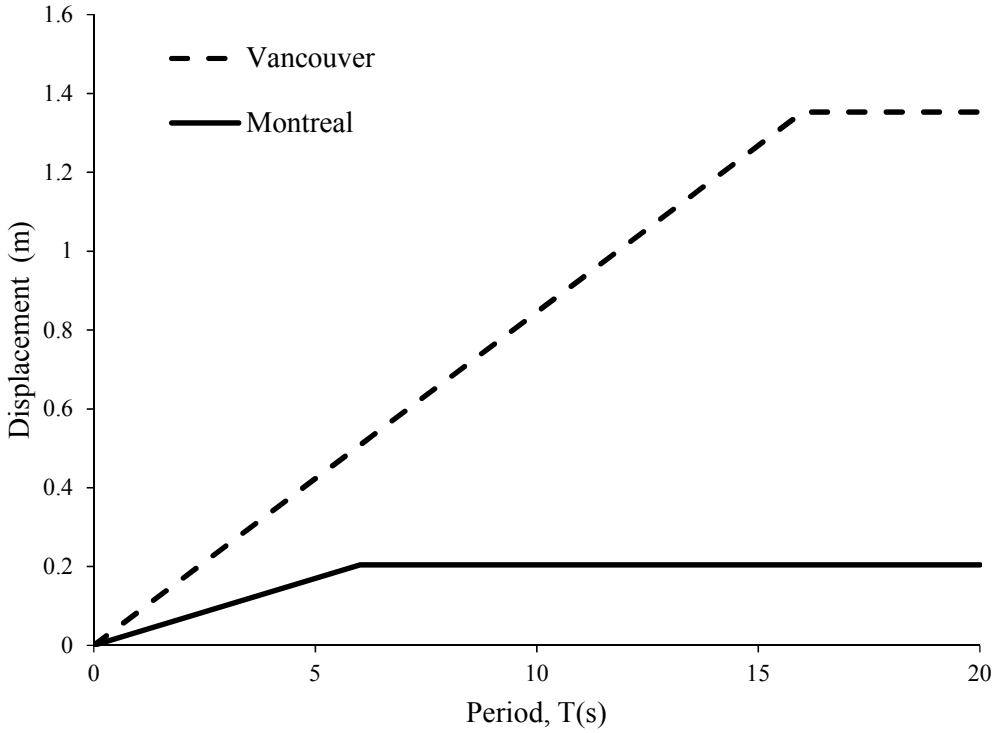

Figure 3-5: Design displacement spectra based on NBCC 2010 UH acceleration spectra

In comparison, the maximum spectral displacement form Equation 2-18 (Priestley et al., 2007) for Vancouver and Montreal are respectively 4.150m and 157mm. For Vancouver, both values (1.35m and 4.15m) are very large and choosing either value would not impact the design. For Montreal the larger Δ_{max} (0.203m) will lead to a more conservative design. Therefore, the maximum spectral displacements used for design were 1.353 m and 0.203 m for Vancouver and Montreal, respectively.

3.3 Direct displacement-based design of the shear walls under study

The aforementioned design procedure is applied to the design the structures under study. The summary of initial designs for Montreal (W_{MTL}) and Vancouver (W_{VCR}) before step (e) is given in Table 3-3 (a).

For W_{MTL}, both Δ_{ye} and Δ_{de} are larger than the maximum spectral displacement ($\Delta_{max,5\%}$= 204mm). Thus, a predominantly elastic response is anticipated ($\mu = 1$). The design displacement is set equal to the maximum spectral displacement. The rotational demand obtained based on the maximum

spectral displacement is smaller than the rotational capacity of the section. Therefore, unlike the FB designed wall, no increase of length was required to meet the ductility requirements. For 6.5m length, the preliminary stability index (SI) of the shear wall is equal to 0.25, which is judged acceptable, and thus no further modification of the stiffness is required.

For W_{VCR}, Δ_{ye} and Δ_{de} are smaller than $\Delta_{max,5\%}$. Therefore, the inelastic response is expected for this wall. The selected length of 8 m is identical to that obtained in FBD since the demand design forces are relatively close. The preliminary ductility factor is 2.96, which falls in between the NBCC ductility levels associated with moderately ductile walls (R_d=2) and ductile walls (R_d=3.5).

With the preliminary design completed, the iterative procedure is performed. Note that the NBCC 2015 elastic higher mode amplification factors (M_v), are applied in all cases while the inelastic higher mode shear amplification factors, Ω_v, as specified in CSA A23.3-14, are considered when the inelastic wall response was anticipated by design. The over-strength factors R_o are adjusted to exclude the impact of the strain hardening already considered in the model. Characteristic parameters of the final designs as well as the fundamental periods for W_{MTL} and W_{VCR} are given in Table 3-3(b). Because of the significant inelastic response, to provide adequate ductility the section of W_{VCR} is detailed like a ductile shear wall according to CSA A23.3-14. To determine the shear forces and bending moments along the height of the walls, the shear force and moment distribution from elastic RSA was used. Therefore, there was no need to apply the J factor specified in NBCC.

Table 3-3 Direct displacement-based design parameters

(a) Preliminary design

	l_w	t_w	Me	He	Δ_{ye}	Δ_{de}	$\Delta_{max,\xi=5\%}$	μ	ξ_{eq}	R_ξ	$R_\xi * \Delta_{max,\xi=5\%}$	SI
W_{MTL}	6.5	0.4	7642	36.86	0.28	0.50	0.20	1.00	0.05	1	0.20	0.25
W_{VCR}	8.0	0.4	7875	36.64	0.17	0.50	1.35	2.96	0.13	0.75	1.01	0.40

Units : m, tons

(b) Final design

	K_e	Δ_{ye}	Δ_{de}	T_e	μ	ξ_{eq}	V_{DDBD}	M_v	R_o^{adj}	$V_{d\text{-}total}$*	$V_{d\text{-}per\ wall}$**	$M_{d\text{-}w1\sim w4}$**	Max. S.I. Final***	Ω_v
W_{MTL}	8140	0.23	0.20	6.09	1.00	0.05	1663	1.91	1.3	9772	3203	49404	0.20	1.0
W_{VCR}	4520	0.17	0.50	8.29	2.96	0.14	2276	1.16	1.3	8120	2360	44625	0.40	1.5

* $V_{d\text{-}total}=(V_{DDBD}*M_v*N_w)/R_o$, N_w: Number of walls in each direction

** Analytical shear and bending moment at the base of the walls $W_1 \sim W_4$ including the amplifications from accidental torsion: 25% amplification for Montreal and 15% for Vancouver.

*** Maximum stability index of the stories.

3.4 Comparison of design from DDBD and FBD methods

Building seismic base shear obtained by DDBD for Montreal is 57% and for Vancouver is 46% of its FBD counterpart. In the FBD approach, the limit imposed on the period leads to much larger design seismic acceleration and base shear, whereas in the DDBD approach such conservative limits are not imposed. Subsequently, the DDBD design forces for $W_{1\sim4}$ for the two sites are smaller than the FBD design forces. For Montreal, the DDBD wall is more slender than the FBD wall (6.5m vs. 8m wall length). However, for Vancouver, because of the larger displacement demand, the lengths of the DDBD walls and FBD walls are similar. The over-strength factor for W_{MTL} and W_{VCR} designed by the DDBD approach are 1.32 and 1.96, compared to 1.25 and 1.23 calculated for FBD walls, respectively. For Montreal, contrary to FBD, DDBD did not predict a significant inelastic response, so no additional confinement reinforcement was required by design. Also, because of the absence of a plastic hinge at the base of the wall, the capacity design procedures need not to be followed. For Vancouver, on the other hand, DDBD predicted the formation of a plastic hinge and high ductility demand. Therefore, the capacity design is applied, and the ductile detailing specified in CSA A23.3-14 is implemented. The roof drifts at the edges of the building for the DDBD design, equal to 0.63% and 1.24% for Montreal and Vancouver, respectively, exceeds FBD drift predictions by 40% for Montreal and 10% for Vancouver. The results obtained for the inter-storey drift show the same trend.

Overall, the demand forces and displacements from DDBD for the two design sites are much smaller than the design forces and displacements from the FBD method. The difference is more pronounced for the Montreal site for which the DDBD approach lead to more slender wall, as well as no special ductile detailing.

3.5 Non-linear time history analysis

3.5.1 Selection and scaling of ground motion records

Ground motion records for nonlinear time history analysis are initially selected on the basis of the M-R scenarios that contribute most significantly to the seismic hazard at the design location. Special attention is given to ensure that the periods of the vibration modes that significantly contribute to the building's dynamic response are covered. Because of the lack of historical records

for eastern Canada, simulated records, compatible with NBCC 2010 design spectra, were used for the two design locations (Atkinson 2009). De-aggregation data (GSC and USGS) are used to determine the governing earthquake scenarios. For Montreal, 10 records are selected from M=6 R=10 to 30 km scenario to cover a range higher periods and 10 records from M=7 R = 15 to 100 km scenario to cover the fundamental period of the structure. For Vancouver, 5 records from M6 R=10 to 30 km scenario and 5 records from M7 R=15 to 100 km scenario are selected to cover higher-modes periods and 10 records from M9 R=110km to 200km to cover fundamental structural period. The selection and scaling of the records is done following the approach described by Atkinson (2009). The summary of selected scenarios and period ranges used in the calibration for each design is given in Table 3-4. Each design is analysed for a set of 20 records. For Montreal, FBD walls were studied for the set consisting of record groups I and II-FBD, while DDBD walls were examined under records from group I and II-DDBD. For Vancouver, FBD walls were studied for the set consisting of record groups III, IV and V-FBD while DDBD walls were examined under records from group III, IV and V-DDBD. For FB designed walls, both in Montreal and Vancouver, the design was based on NBCC design spectrum, in which the spectral accelerations for periods larger than 4 s are limited to the spectral value defined at 4 s period considering a minimum acceleration limit for periods larger than 4 s. Therefore, the ground motion records were selected and scaled to achieve compatibility with this spectrum. Note that for DDB designed walls, the 4 s limit period was not applied to achieve compatibility with the displacement spectra used in design (see Figure 2-5).

Table 3-4 Summary of selected records for NTHA of the shear walls for the office building

Site location	Record group	Number of the selected records	Earthquake magnitude	Epicentral Distance (km)	Selection and scaling period range (sec.)	Minimum design spectral acceleration applied?
Montreal	I	10	M6	10 - 30	0.2~1.0	N/A
	II-FBD	10	M7	15 - 100	3.0~6.0	Yes
	II-DDBD	10	M7	15 - 100	3.0~6.0	No
Vancouver	III	5	M6.5	10 - 30	0.2~1.0	N/A
	IV	5	M7.5	15 - 100	0.2~1.0	N/A
	V-FBD	10	M9	110 - 200	3.0~6.0	Yes
	V-DDBD	10	M9	110 - 200	3.0~6.0	No

3.5.2 Numerical model

2D-nonlinear time history analysis was carried out using OpenSees (PEER, 2012). The walls were modeled using one force-based nonlinear beam-column element per floor. The element section was discretized into fibers for which the nonlinear material stress-strain response was defined. Distinct fibers were attributed for confined and unconfined concrete zones and for the steel reinforcement. The fiber section model considers the bending moment-axial force interaction, but the shear-bending or shear-axial force interactions cannot be represented. Concrete behaviour was modeled using the uniaxial Kent–Scott–Park model with linear tension softening (Concrete02). To determine the material parameters, the material law based on modified compression field theory proposed by Vecchio et al. (1986 and 2000) was used. For unconfined concrete, the ultimate strain, ε_{cu}, was taken equal to 0.0035 as prescribed by CSA A23.3, and the ultimate concrete compressive strength was assumed to be 30 MPa. For the reinforcing bars, the Giuffré-Menegotto-Pinto hysteretic material (Steel02) was employed to describe the inelastic behaviour.

The parametric study was conducted to determine the adequate number of integration points for the analysis. After examining the structural periods, the wall base shear and storey shears, the overturning moments and the roof displacements, three integration points per element were selected as a rational compromise offering adequate accuracy, convergence and reasonable computational time. This selection is in line with the practice reported in the literature (Boivin and Paultre, 2012, a). 5% damping for first and third mode was assigned, and the initial stiffness option was used to constitute the damping matrix. For W_{MTL} models, for which a lesser inelastic response was anticipated, the strain hardening was taken equal to 1.2% as suggested by (Ghorbanirenani 2010), while for W_{VCR} models with an expected high inelastic response, the strain hardening was taken equal to 2% (ATC72-1, 2010).

The studied shear walls are slender with an aspect ratio of about 7 and the shear stresses are small. Therefore, a linear elastic model for the shear deformation of the wall elements was considered acceptable. For the same reason, the moment-shear interaction was ignored in the model as suggested in the literature (ATC72-1, 2010). The model was calibrated using the available experimental data (Ghorbanirenani 2010) following the procedure described in (Luu et al., 2013a). A non-uniform shear stiffness pattern was assigned. The values used for Montreal are those

recommended by Luu. For Vancouver, the same shear stiffness profile was applied with its values adjusted according to data available in the literature (ATC72-1, 2010).

3.5.3 Discussion of results

The response of the studied walls is examined by tracking curvature ductility, lateral displacements, bending moments and story shears. Comparison between the two designs is done using median results, but 84th percentile results are reported when necessary. The impact of the frequency content of selected ground motion records on the structural response was also investigated.

Figure 3-6 (a) and (b) compare the normalized median curvature ductility obtained for W_{MTL} and W_{VCR} walls, respectively. The maximum curvatures obtained for each record are normalized by the yield curvature given in CSA A23.3-14 ($\varphi_y=2*\epsilon_y/l_w$). The resulting curvature ductility for the two groups of records is also shown. For W_{MTL} wall, the two designs show the similar, predominant elastic response. As expected, the maximum median curvature ductility developes at the base, reaching 0.7 and 0.83 for DDB and FB designs, respectively. These results are consistent with the experimental findings reported by Ghorbanirenani et al. (2011). The 84th percentile exceeds the yield curvature by about 65 percent for the two designs. Even being larger than 1, this level of local ductility can still be associated with an elastic response. Paulay and Priestley (1992) showed that for the RC shear wall with the aspect ratio between 6 and 8, which corresponds to the walls considered in this study, it is necessary to reach the curvature ductility at the base of about 4 in order to develop a global displacement ductility $\mu=R_d=2.0$. Thus, while according to the FBD, moderately ductile wall response was anticipated and adequate detailing in plastic hinge region was required, the DDBD correctly estimated the elastic wall response and justified the omission of ductile detailing in the final wall design.

For the two designs, high-frequency records (groups I and III, see Table 3-4) induces significant higher mode response, with larger curvature ductility recorded at the base of the structure and at about two-third of the wall height. The potential to form a second plastic hinge exists in the upper storeys, however developed curvatures do not exceed the yield curvature and are indicative of predominant elastic response. For the two designs under the low-to-intermediate set of records (Groups II, IV and V) the first mode dominated the response. However, the potential to introduce the second plastic hinge can still be observed at the locations where the details of the reinforcement

curtailing cause step changes in the resistance of the section, which may result in an increased demand-to-capacity ratio at these locations.

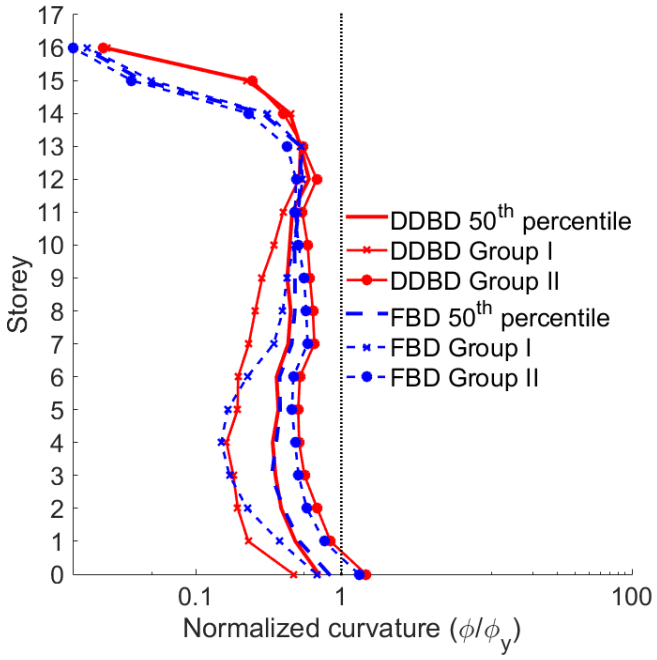

(a)

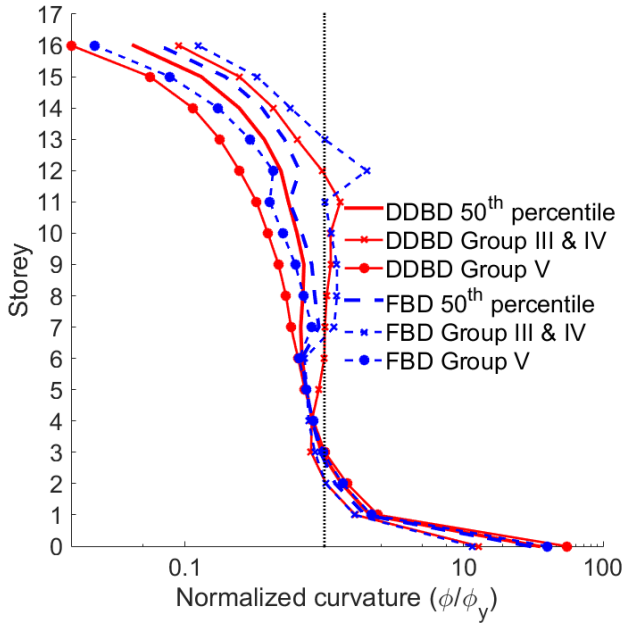

(b)

Figure 3-6: Curvature profile for shear wall in (a) Montreal and (b)Vancouver

For W_{VCR} wall, the inelastic response at the base of the wall was significant for the two designs. Figure 3-6 (b) shows that the normalized median maximum curvature ductility at the base reaches values of 34.5 and 29.7 for DDB and FB design, respectively. The 84th percentile results exceed the yield curvature by a large margin for the two designs. The recorded median values are significantly higher than those discussed by Paulay and Priestley (1992) who associated the curvature ductility of around 9 to the global displacement ductility equal to $\mu=R_d=3.5$ for RC shear walls with similar length-to-height wall ratio. Nevertheless, these results are in line with the values reported in numerical studies by Boivin and Paultre (2012a). Quasi-static cyclic loading tests conducted by Escolano-Margarit et al. (2012) on large-scale RC structural walls also showed that, for the comparable drift level, ranging between 1.2 and 1.5 percent, a curvature ductility of 25 to 30 can develop in a properly confined shear wall.

The impact of frequency content of the record on the resulting curvature is very significant; intermediate and low frequency records induced about ten times larger curvature at the base compared to high-frequency records. For the two designs, the first mode dominated the wall response to low-frequency records, while the response to intermediate and high-frequency records shows the contribution of higher modes in the curvature profiles. The participation of higher modes is more pronounced under high-frequency records and is more notable for FB-designed wall for which the effects of higher-mode amplification in the upper storeys, combined with the more abrupt transition in reinforcement curtailing, may lead to the development of a second plastic hinge at two thirds of the wall height. The median curvature value observed at this location under high-frequency records reaches the value of 1.71.

The computed median lateral displacement profiles for the two designs are shown in Figure 3-7 (a) and (b) for W_{MTL} and W_{VCR} walls, respectively. 84th percentile results are also illustrated for more complete comparison with design predictions. The results are normalized by the wall height. Because no limits were imposed on the period in the response spectrum analysis as permitted by NBCC for the calculation of displacements, for FBD, the total displacements are determined for the analytical period. DDB design predicted elastic wall response in Montreal and inelastic in Vancouver, thus the values plotted in Figure 3-7 and Figure 3-8 represent elastic and total displacements for final wall designs in two design locations, respectively. Note that, for both locations, the displacement profile for DDB design is obtained by presuming the first mode deformed shape. Figure 3-7 shows that for two W_{MTL} walls, median and 84th percentile roof

displacements are well below the maximum code limit of 2.5% reaching the values of about 0.25% and 0.5%, respectively. In Vancouver, larger roof displacements were recorded, but still well within the code limit (1.2% and 1.7% for median and 84th percentile values, respectively).

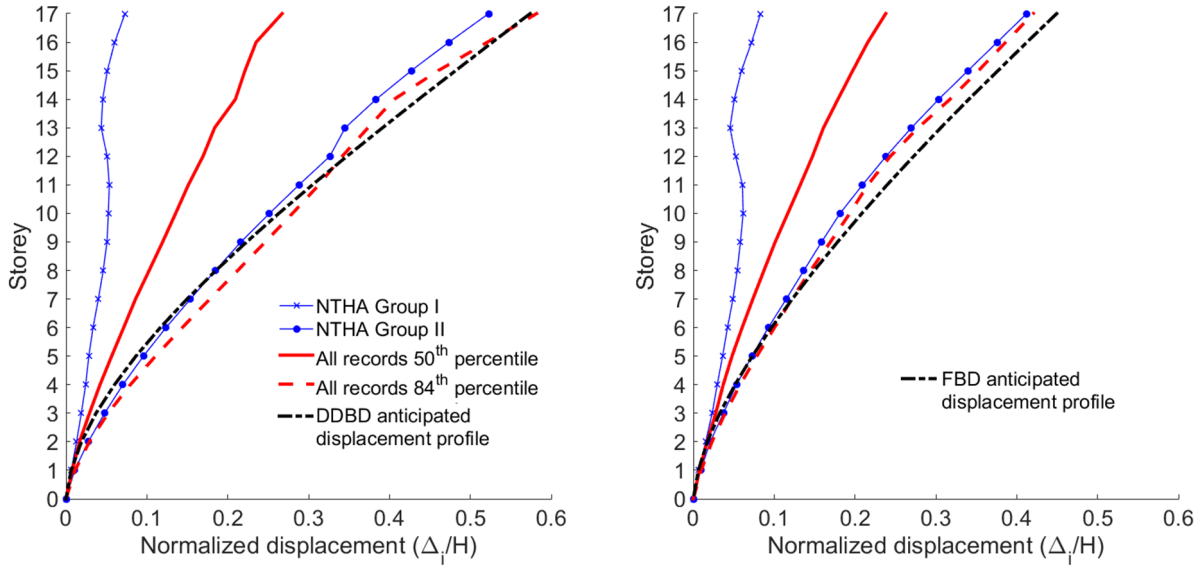

(DDBD) (FBD)

Figure 3-7 Displacement profile for shear wall in Montreal based on normalized displacement (Δ_i/H)

For both design locations, frequency content of ground motions greatly influences the displacement demands. High-frequency records induces smaller displacement demand, particularly in Montreal, the difference being slightly more pronounced for force-based design. For this location, design predictions are equal to the 84th percentile values and are approximately two times larger than the median results. Because in DDBD, displacements are key design parameters, for successful design, the displacement demand from various possible ground motions should be properly estimated. As seen in Figure 3-7, the DDBD method is successful in predicting displacement profile as it provides the envelope of displacement demand for two record sets. For W_{MTL} designed by FBD method, design estimate of total displacements matches 84th percentile values from NTHA and largely surpasses the median value. However, contrary to DDBD method, in FBD method inelastic wall response is anticipated, so although the amplitudes of the displacements are well predicted, their nature is not. Median results are close to elastic displacement but fall far below those induced by low frequency records.

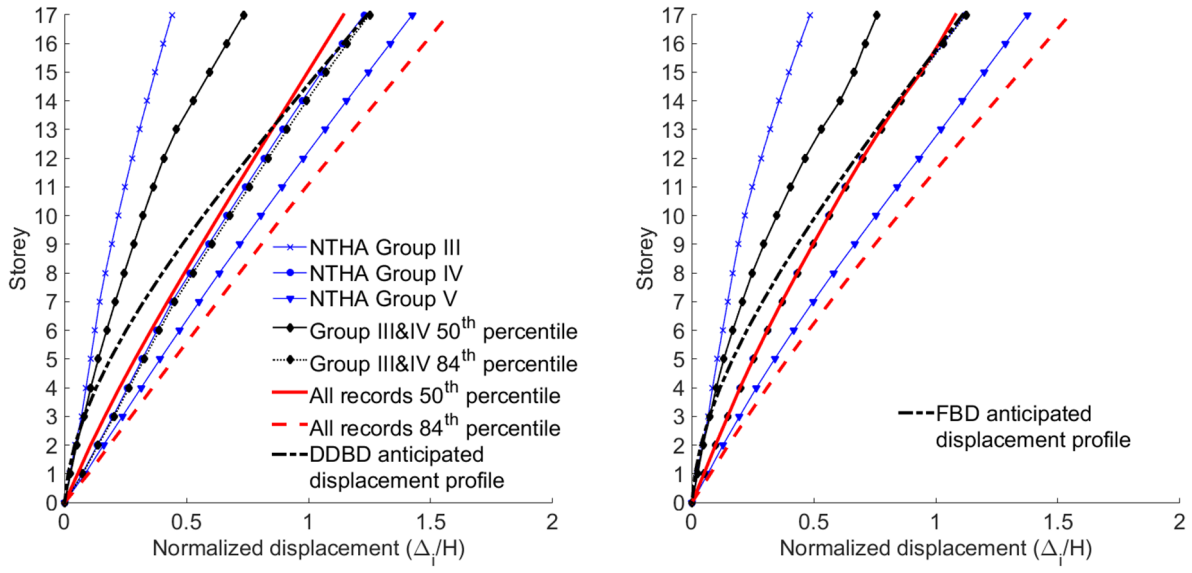

(DDBD) (FBD)

Figure 3-8 Displacement profile for shear wall in Vancouver based on normalized displacement (Δ_i/H)

The trend observed in Vancouver for the complete records suite differs from that seen in Montreal. This difference is attributed to the impact of M9 records that induced significant displacement demand with a median value exceeding design prediction by maximum 24 percent. Because of the height of the wall, a minor inelastic rotation of the plastic hinge at the base can lead to a significant top displacement. In that regard, the fiber models have limitations, because the propagation of the plastic hinge cannot be properly represented. Figure 3-8 shows that for DDDB W_{VCR} design predictions are close to the median results for the whole record set and the 84th percentile results for high to intermediate records (groups III and IV), with demand being slightly overestimated in the upper storeys and underestimate in the lower storeys. Note that one of the records for DDBD design caused excessive displacements and its contribution was not accounted for in the 84th percentile results. FBD W_{VCR} design exhibited similar displacement response. Thus, in Vancouver, none of the two design methods was able to predict significant displacement demand caused by low frequency ground motion records.

By inspection it was established that the time of occurrence of the maximum roof displacement and the maximum base curvature did not coincide for any of studied cases. Both DDBD and FBD

heavily rely of the assumption that the two parameters are directly related and occur simultaneous which is clearly not the case for taller walls.

In Figure 3-9 and Figure 3-10, the median distribution of the bending moments obtained from NTHA for two design methods and two selected locations is compared to design predictions. The results, normalized by the tributary seismic weight and the wall height, are given for each record group as well as for the complete set of records. For each design method (FBD and DDBD) the distribution of the shear force and bending moments is derived from RSA and is calibrated with the design base shear for each design case.

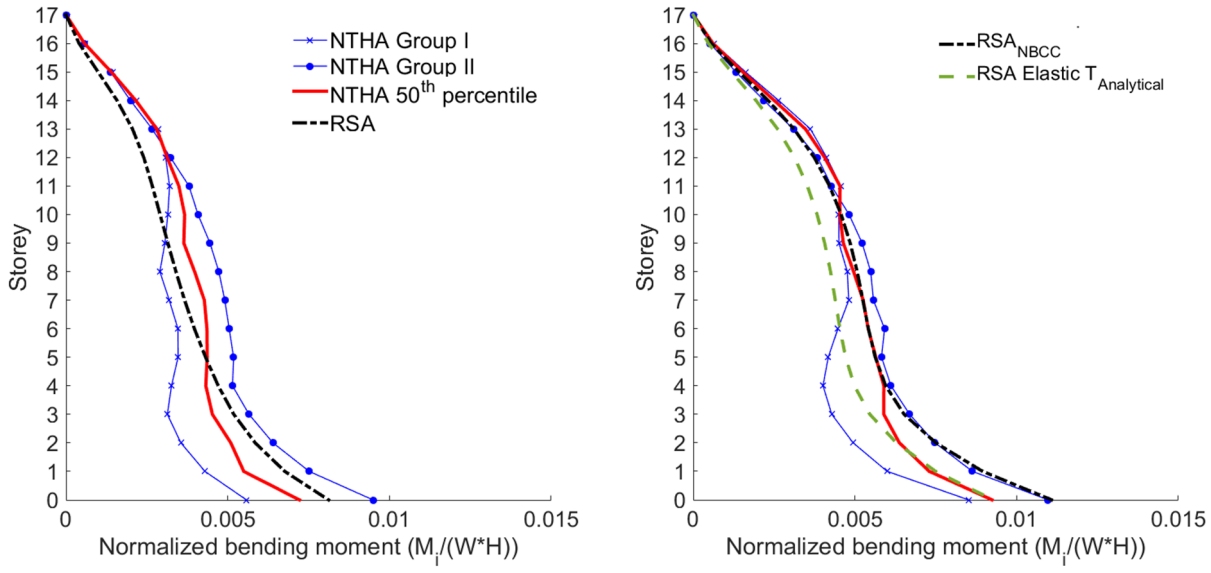

(DDBD) (FBD)

Figure 3-9: Bending moments profile for Montreal

For the W_{MTL} wall, design values for FBD were also determined assuming the elastic response and using the analytical period of vibration from modal analysis ($T_{Analytical}$). Note that for this case, the limit on design period imposed by NBCC was not applied. For FBD W_{MTL} wall, the median bending moment at the base for complete record set is about 20% below the design values. However, the median curvature at the base, shown in Figure 3-6, implies elastic wall response, so the comparison with design values that account for inelastic response may not appropriate. When the median NTHA results are compared to the elastic design predictions, a good match is observed. A closer inspection of NTHA results for separate record groups shows a significant difference in the

response. While high frequency records (Group I) did not impose any inelastic demand at the base, low frequency records (Group II) induces inelastic response, and the median results for this record group at the base compare well with inelastic design predictions. Outside the plastic hinge region, the median bending moments exceeds elastic design predictions up to 15th storey by a maximum of 20 percent. This may be attributed to the more important contribution of higher mode to the response in that part of the wall which is visible in the median demand from the high frequency record group (Group I). Inelastic design predictions are very close to the values obtained from NLTH analysis for Group I records, indicating a possibility to form a second plastic hinge in this region. For FBD W_{VCR} wall, the bending moments at the base for all ground motion groups reaches the plastic bending moment of the section. This, combined with the high curvature recorded at this location, suggests that formation of the plastic hinge took place. Outside the zone of plastic hinge, starting from 9th storey up, the demand caused by intermediate and low frequency records is very close to the capacity design envelope, which suggests possible second hinge formation in the upper storeys.

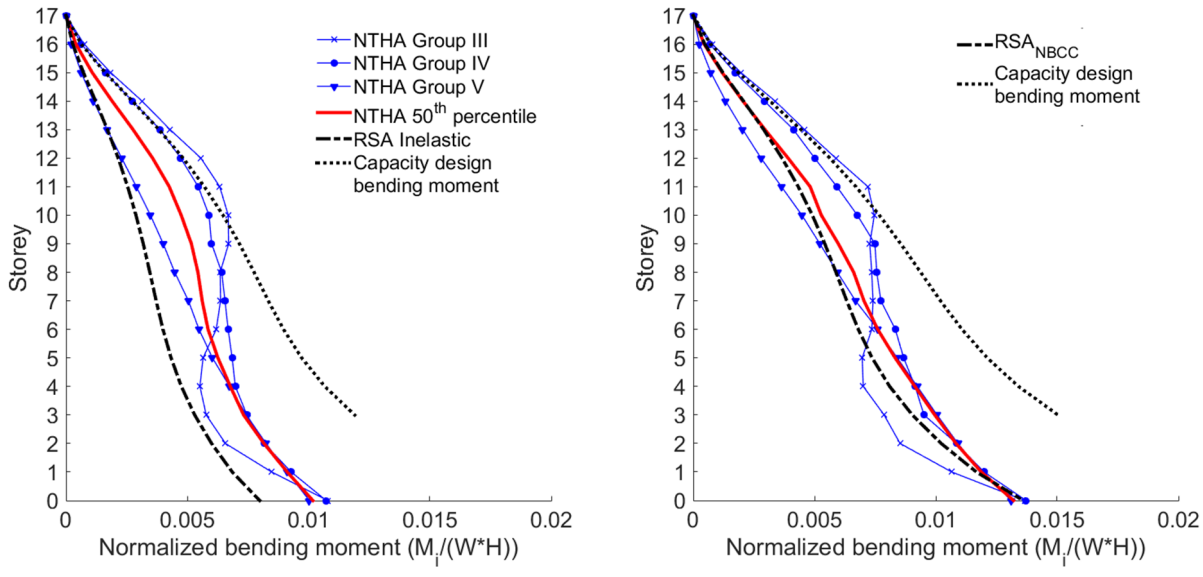

(DDBD) (FBD)

Figure 3-10: Bending moments profile for Vancouver

For W_{MTL} wall designed by DDBD method, design bending moment at the base exceeds the median bending moment for complete record set but is smaller than the median bending moment for the ensemble of low frequency records by about fifteen percent. Strength requirements does not govern

the design of this wall; the section is in fact sized to provide a minimum stability index of 0.2, so the actual capacity of the section at the base surpasses the median demand from the low frequency records by about five percent. Note that 7 out of 10 low frequency records induce limited inelastic response at the base. Design predictions are conservative up to the 5th storey; for the storeys above, median bending demand is about 60 percent higher. Thus, an amplification of design forces in the upper storeys would be necessary to account for the effects of the higher modes. Similar to W_{MTL} wall, for DDBD W_{VCR} wall, providing required stiffness to limit the stability index is a governing design criterion. The design bending moment at the base matches well NTHA median demands induced by the complete record set as well as the median demand produced by individual record groups. Because the inelastic response was anticipated for this wall design, bending moments demand outside of the plastic hinge region are determined using capacity design approach. In Figure 3-10, the capacity design moment envelope appears adequate for the median bending moment demand. However, for the high-frequency records (Group III), the median demand is about 15 percent higher than the design estimates and suggests a potential plastification of the wall.

The comparison of the storey shear forces obtained from RSA to the outputs of NTHA for two designs is shown in Figure 3-11 and Figure 3-12 for Montreal and Vancouver, respectively. Capacity design envelope is also illustrated were appropriate. For all four cases studied, RSA shear forces demand includes NBCC 2010 M_v factor to account for elastic effects of higher modes. For FBD wall in Montreal as well as DDBD and FBD walls in Vancouver, the shear amplification caused by inelastic higher mode effects (Ω_v), as defined by CSA A23-14, is also considered.

For W_{MTL} wall, the DDBD approach underestimates the shear force demand at the base by about 50 percent in comparison to the median of the complete record set. For this wall, DDBD predicted elastic response, thus the shear force demand included only the amplification caused by the elastic effects of higher modes. FBD predictions of shear forces have a better coherence with NTHA results. There is a conservatism built into the value of FB design base shear which is due to the NBCC limits imposed on the fundamental period. This is not present in the DDBD shear force and thus DDBD need an extra shear amplification to cover the impact of the higher modes on shear forces. If median level considered, FBD wall shows an elastic response, so the increase of RSA shear forces to account for the inelastic higher modes amplification is in fact not justifiable. For the low frequency Group II records, which induces inelastic wall response, the median response is still about 6 percent higher than predicted shear force design demand. Overall, the capacity shear

envelope slightly underestimates the amplification at the base but provides adequate estimates elsewhere.

For W_{VCR} wall, DDBD approach also underestimates the median shear force demand at the base but to a lesser extent (20 percent). In the upper storeys a better match is recorded. The capacity design is implemented in design of this wall; however, the capacity design shear envelope is below the median demand from high and intermediate frequency records (Groups III and IV) by about 27 and 10 percent respectively. The use of higher mode amplification factors proposed in NBCC force-based design procedure cannot be directly extended to DDBD procedure as they do not produce adequate predictions of shear force demand. This subject requires a further study.

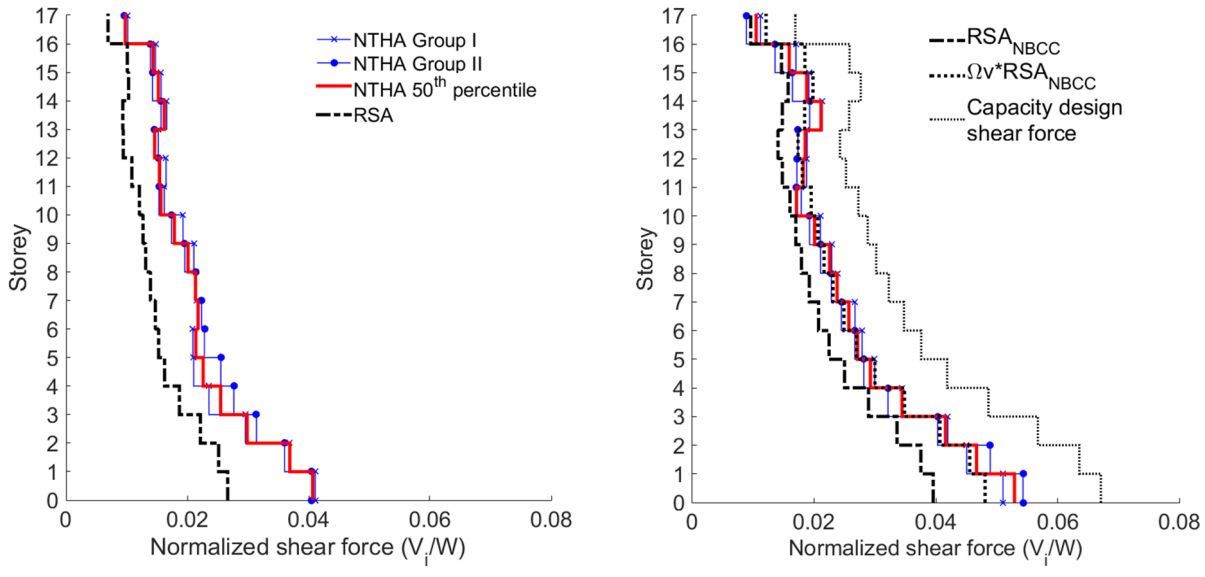

(DDBD) (FBD)

Figure 3-11: Shear force profile for Montreal

For W_{VCR} wall designed by FBD method, median NTHA results for the whole record set are below estimated shear force demand. The frequency content of the record has an enormous impact on the response; median demand produced by high and intermediate frequency records surpasses design shear force values by 20 and 3 percent, respectively, while it is about 30 percent lower for low frequency records. Capacity design shear envelope provides s conservative estimates for all record groups, including the high frequency records (Group III), for which the largest shear forces are recorded.

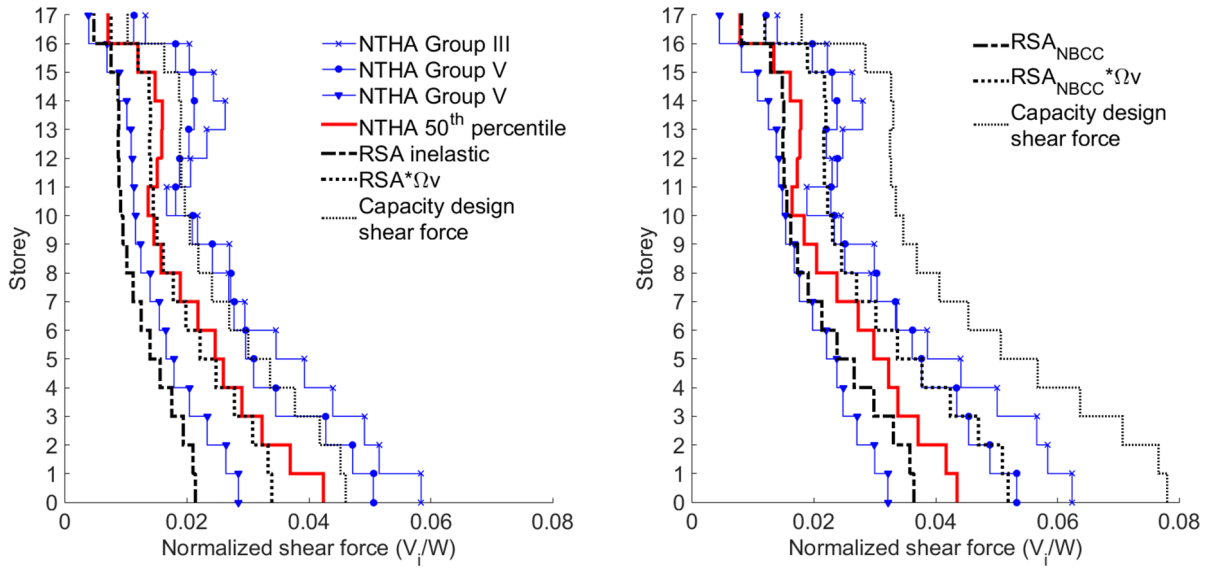

(DDBD) (FBD)

Figure 3-12: Shear force profile for Vancouver

3.6 Conclusions

A forced-based design method and a direct displacement-based approach to seismic design of taller RC shear walls were compared on the example of a 17-storey shear wall structures located in Montreal (QC) and Vancouver (BC), Canada. Canadian seismic design requirements for RC shear wall design were critically assessed in the context of taller wall design. The application of direct displacement-based design methodology for seismic design of taller buildings was presented, and the construction of the design displacement spectra was discussed. Seismic behavior of the walls was assessed using nonlinear time history analyses for suites of simulated ground motions compatible with design spectra. Special attention was devoted to study the sensitivity of the response to the frequency content of ground motions. Two designs were compared by tracking the curvature ductility, lateral displacements, bending moments and story shears.

For the two locations, ensuring an adequate rotational capacity is the important design constraint when the NBCC force-based design procedure is applied. In Montreal, the length of the wall had to be increased to provide the required rotational ductility capacity; nevertheless, the results of the NLTHA shows that the response of the wall is nearly elastic. In Vancouver, it was not possible to provide the rotational capacity required in the design with simple shear walls of reasonable length.

For this location, the ductility anticipated in the design was fully mobilised under intermediate- to high-frequency records, and significantly surpassed for low-frequency records.

For both FB and DDB shear wall designs in Montreal, the observed levels of base curvature ductility indicated very limited inelastic response, significantly smaller than the one predicted by NBCC Rd factor. Results of NLTHA show that FBD underestimated the value of seismic base shear. This can be attributed to the combination of inadequate elastic higher mode amplification and the over-estimation of the level of inelastic structural response.

It was found that the seismic response of the walls was very sensitive to the frequency content of ground motions. For both location and two design methods, low frequency records induce inelastic response at the base of the structure although to a much lesser extent in Montreal W_{MTL} walls. Displacement response showed the same trend. High frequency records, on the other hand, induced more significant demand in the upper levels, confirming the potential to develop second plastic hinge at this location. Although this tendency was more pronounced for Montreal structures, it was also observed for Vancouver walls particularly at the levels where the transition in reinforcement curtailing is present.

The amplification factors provided in NBCC that are used in this study for FBD and DDBD, underestimate the higher modes amplification of the base shear for both location, but especially for the shear wall in Montreal. This discrepancy is more pronounced for the walls design using DDBD approach showing the need for assign higher shear amplifications when this method is used.

The use of DDBD method to design walls in high seismicity region like Vancouver, for which the significant inelastic seismic response is anticipated, seems straight forward. However, when the elastic structural response is anticipated, DDBD method did not provide the unique solution because the yield displacement of the system exceeded the maximum spectral displacement.

Both FBD and DDBD approach heavily rely on the assumption that the seismic response of the structure is dominated by the fundamental mode of vibrations. To relate local and global ductility demand, it is commonly assumed that the maximum roof displacement and the maximum base curvature occur simultaneously. The results of NLTHA confirmed that for the shear walls under study, the two parameters did not occur simultaneously for any of the studied cases. The comparison of two design approaches shows that, although both methods have their advantages, they lack accuracy when dealing with high-rise simple concrete shear walls in regions with low

and moderate design earthquakes. Very limited data is available in the literature on deformation response of taller RC shear walls in eastern Canada, yet this information is essential for tailored seismic design regardless if the methodology is forced-based or displacement-based. For this reason, the study reported in following Chapters, focuses on this subject.

CHAPTER 4 PARAMETRIC STUDY ON SEISMIC DEFORMATION OF TALL SHEAR WALLS IN EASTERN CANADA

When a tall RC shear wall building structure is exposed to a moderate seismic event, the inelastic portion of the base rotation usually reduces as the height of the wall increases. On the other hand, the top displacement will be limited to a maximum demand displacement. This causes a non-uniform relationship between the top displacement and base rotation which varies in function of the height of the shear wall. This phenomenon can be significant depending on the level of seismicity and the shape of the seismic design spectrum. In addition, the impact of higher modes becomes more prominent and could affect both the top displacement and the base rotation at the plastic hinge.

These particularities of seismic response of tall RC shear wall makes the definition of global ductility challenging. On one hand the direct proportionality between the base rotation and the top displacement no longer holds, and on the other hand, the estimation of the yield displacements based on the fundamental mode becomes questionable.

The abovementioned characteristics of seismic response are illustrated on an example of a 25-storey shear wall building located in Montreal on C class site. The building has a 30 m x 30 m plans and, in each direction, has four shear walls symmetrically distributed on the edges. The typical wall was designed as moderately ductile using NBCC 2015 and CSA A23.3-14 design procedures. The height of the shear wall is 75m, its length is 9m and its thickness is 450mm. The fundamental period of the shear wall considering the cracked section properties is 3 s. The predicted top displacement according to NBCC 2015 FBD is 194mm and the estimated base curvature according CSA A23.3-14 procedure is 0.00069 (1/m).

The nonlinear time history analysis was carried out using OpenSees model similar to that descried in Chapter 3, Section 3.5.2, with some modifications made to damping and shear stiffness specifications. 2% damping at the first and third modes were used as the parameters of Rayleigh damping for this analysis. The modeling strategy, calibration and validation of the model are discussed in more detail later in Section 4.3.1. Two ground motion records were selected for the analysis, one simulated (Atkinson, 2009) and one historical (Northridge). The simulated record has relatively predominant high frequency content, while the Northridge record is dominated by the

low frequencies. Although not typical of eastern Canada, the Northridge record was selected to compare the impact of the ground motion frequency content on the deformation response of the shear wall. The records were scaled to the NBCC UHS in the period range between 2.5 and 4 s following the procedure described in NBCC (2015) and Atkinson (2009). This period range was selected to cover the elastic uncracked period of the shear wall and account for the potential increase of the period due to inelastic wall response. Analyses was also carried out for amplified simulated ground motion (150% and 200%).

For each ground motion record, the time history response of the base curvature and top displacement of the shear wall are shown respectively in Figure 4-1 and Figure 4-2. In Figure 4-1 the base yield curvature is also shown to indicate the state of the inelastic response. The yield base curvature was determined according to CSA A23.3 as $2\epsilon_y/l_w$ and it is equal to 0.00044 (1/m).

Under the 100% simulated ground motion record, the maximum base curvature (0.00023, 1/m) is around the half of yield curvature which indicates elastic wall response. This is contrary to the moderate inelastic response anticipated by design (R_d = 2). Under 150% of simulated ground motion, the base curvature reaches the yielding threshold and the curvature ductility is around one. When the amplitude of the simulated ground motion is doubled (200%), the base curvature largely exceeds the yield curvature and the curvature ductility increases to 2.4.

Displacements, however, do not increase in the same way as the base curvature with increasing level of seismic excitation in the same way as the base curvature. Under the 100% simulated record, the maximum top displacement of the shear wall is 205mm which surpasses the maximum spectral displacement (186mm for 2% damping). For this comparison it is more rational to use the spectral displacement for the damping compatible to that used in NTHA. The maximum spectral displacement at 5% damping (155mm) is different from the value given in Section 3.3 (203mm) because the UHS spectra of 2015 version of NBCC have been changed compare to NBCC 2010. The maximum top displacement from the time history analysis is close to the displacement predicted by design (194mm). When the excitation is increased by 50%, the maximum top displacement approximately doubles (436mm). Further augmentation of the excitation (200%), does not result in the proportional increase in the top displacement (507mm).

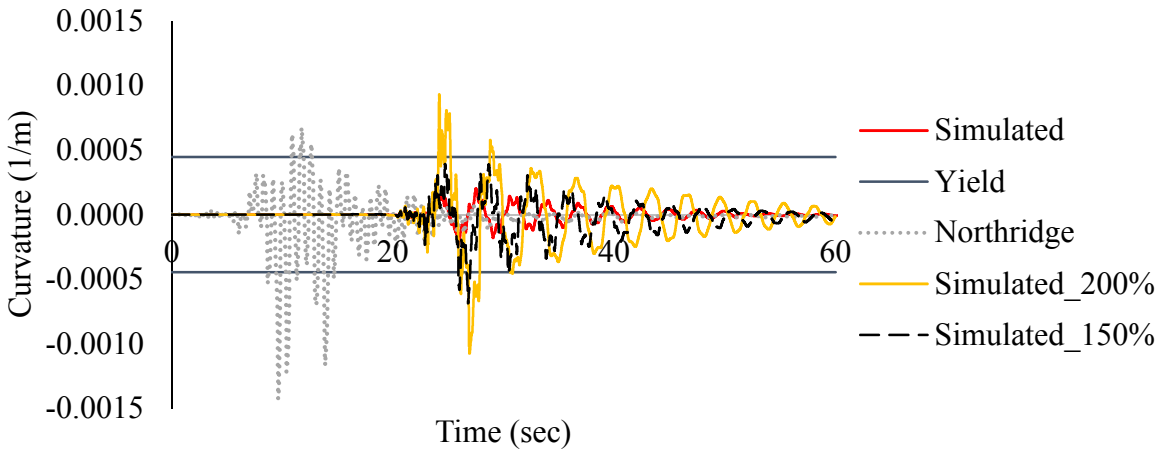

Figure 4-1: Time history response of the base curvature of the example shear wall to various ground motions.

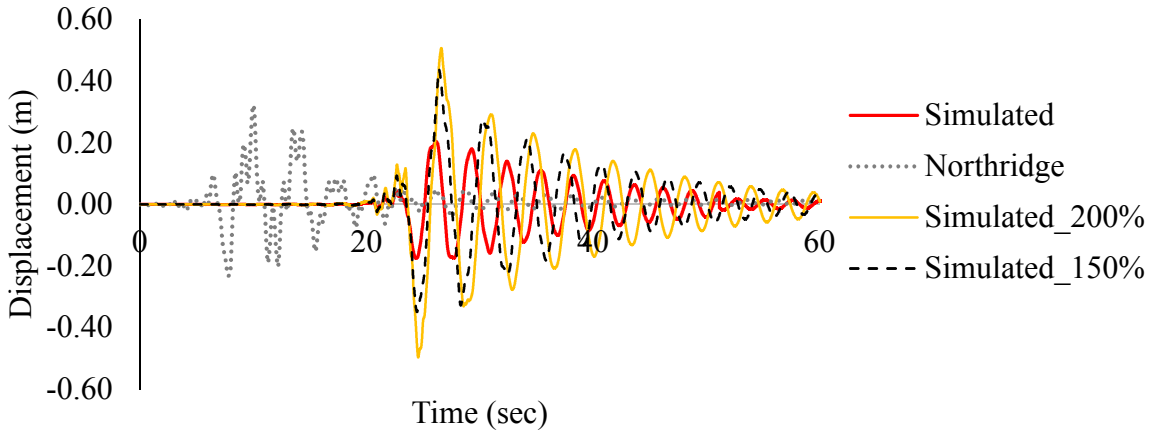

Figure 4-2: Time history response of the top displacement of the example shear wall to various ground motions.

Another observation that can be made from Figs. 4-1 and 4-2 is that the maximum curvature and maximum displacement do not occur at the same instant. For example, the maximum curvature under the original non-amplified simulated record occurs at 25.92s whereas the maximum displacement is recorded at 26.13s. This phase delay of the occurrence of the maximum deformation responses is the indication of the impact of higher modes.

The maximum top displacement recorded for Northridge ground motion (230mm) is comparable to that induced by the 100% simulated record. However, the maximum recorded base curvature is

equal to 0.0014 1/m and exceeds that determined for the simulated record by a large margin, indicating an important inelastic activity in the plastic hinge. Thus, it appears that the frequency content of the ground motion record has a significant role in the base curvature prediction.

In common design practice, for simplicity, the design base curvature of shear walls is estimated considering that the first mode dominates both elastic and inelastic structural deformation, that the plastic hinge fully develops at the base, and that the top displacement and base curvature are directly proportional. While these assumptions may be adequate for low-to-intermediate height RC shear walls, the above example illustrates that for taller walls such hypothesis are not valid and may result in inappropriate estimates of deformation response parameters. Design verification of maximum inelastic rotation at the base of the RC ductile shear walls are prescribed in many modern concrete design standards, including CSA A23.3 and are heavily dependent on the assumed base curvature-to-top displacement relationship. It was illustrated in Figure 3-1 that the design of tall shear walls with high axial stresses could be governed by the maximum inelastic rotational capacity of the wall. The procedure to calculate inelastic rotational capacity conservatively encompasses the response of the short- to medium-rise structures which are located in regions with high intensity earthquakes with predominant low-to-intermediate frequencies. In addition to problems that arise in force-based approach to design of RC shear walls for seismic loading, a proper estimate of deformation profile is a key element of success in application of DDBD method to this type of structures.

It thus seems pertinent to investigate more in-depth issues related to base curvature prediction and their consequences on design in the zones of moderate seismicity.

4.1 Design of RC shear walls for the parametric study

In order to establish a more realistic relationship between the base curvature and the top displacement for taller rectangular RC shear walls located in eastern Canada, a parametric study was carried out first to investigate the influence of various parameters and identify the most important ones.

In this study, a hundred rectangular shear walls were designed considering five different heights, varying between ten to thirty storeys. The walls are assumed to be located in Montreal, QC, and funded on class C site. Forty out of hundred walls are designed using NBCC 2015 and CSA A23.3-

14 provisions for moderately ductile shear walls while the remaining walls are designed using the DDBD method proposed by Priestly et al. adapted to tall walls in regions with moderate seismicity as discussed in Chapter 3. In the further text walls designed using A23.3 provisions are referred to as FB designed walls as the design procedure is forced based, and those designed using DDBD approach will be referred to as DDB designs. The displacement spectrum used for Montreal is the one described in the previous chapter with corner period, $T_{c,}$ equal to 6.0s. The maximum spectral displacement, Δ_{max}, for 5% damping is considered equal to 155mm to cover all the design cases between 6 to 10 seconds. The number of DDBD designed walls is bigger compared to those conformant to A23.3 design procedure because the former method offers a greater flexibility and results in greater number of design options.

To facilitate design, the MATLAB code was developed to integrate the analysis and capacity design both for A23.3 force-based design procedure and DDBD procedure.

For FB design the Matlab code call OpenSees program to perform modal analysis. The modal shapes and periods are then used to perform RSA in the developed Matlab code and to determine the seismic demand according to NBCC 2015. The results of RSA would be used to distribute the seismic demands. Finally, the capacity design forces for shear design and flexural design outside of the plastic hinge region are calculated as specified by A23.3. To calculate the capacity of shear wall sections, the Matlab code uses OpenSees by producing OpenSees input files, call OpenSees to run the section analysis and then extract the outputs. The code controls that all RC sections at all levels have adequate shear and bending capacity to handle the design demands. Such framework is beneficial when it is necessary to achieve a certain value of a design parameter (for instance, a specific over-strength factor, specific displacement profile, etc.) as it is possible to do iteration based on try and error approach until the solution is reached. As the process is automated, it is also possible to complete design faster for a large number of shear walls with different geometric characteristics.

Similarly, a framework was developed in MATLAB to perform DDBD. The Matlab code first transforms the structure to an equivalent single degree of freedom (ESDF). OpenSees program is then called to carry out a pushover analysis. A bilinear regression procedure is applied to the obtained pushover curve in order to determine the secant stiffness at the design displacement point which is then compared with desired secant stiffness (K_e). Through a try-and-error procedure,

automated in Matlab, the reinforcement of the base section is changed until a convergence for the stiffness is reached. The design base shear, calculated using K_e , is then distributed along the height using the profile obtained from RSA. Final design will be carried out considering the level of mobilised ductility. If the predicted global ductility from DDBD is less than or equal to one, the elastic design approach according to CSA A23.3 is selected. For shear walls with ductility more than one, the capacity design approach for moderate ductile walls (according to CSA A23.3) is applied. The whole process is automatized which significantly cuts down on design time and allows to realise numerous variant designs.

Following parameters are examined: height expressed by the number of storeys, axial force (P_f), longitudinal reinforcement ratio for the section at the base (ρ_s), wall length (l_w) and dynamic mass (M) which represents the variation of the fundamental period (T_1) for a selected wall height. Note that ρ_s is representative of γ_w in FBD approach because larger reinforcement ratio results in larger flexural strength while is does not affect the bending moment demands. In current FBD methods the demands are commonly independent from the reinforcement contents. Various wall lengths were assumed for each height, but they were all kept in the range of dimensions common in practice. When applicable, the period of the shear walls was not limited to the empirical period as it would normal be done in practice. Tables 4-1 and 4-2 provide a summary of designed walls and the values of different parameters examined. The information regarding the predicted ductility, wall base flexural over-strength factors, γ_w for FB designs and limiting stability indexes for DDB designs are also listed.

As seen in Table 4-2, DDBD approach predicted elastic response with ductility factor equal to one for shear walls taller than 10 storeys. For ten-storey shear walls the predicted response is inelastic, however the anticipated mobilised ductility is smaller than the one predicted by NBCC and A23.3 for all walls regardless of the height ($\mu=R_D=2$).

To ensure realistic wall dimensions for DDB designs, the stability index s was limited to 0.4, the maximum value recommended by NBCC 2015 to guarantee a sufficient stiffness to building systems. Because of the predicted elastic response from DDBD approach, the top displacements for the DDB designed walls are generally smaller compared to the assumed inelastic top displacement for the FBD options. On the other hands, the absences of the limitation imposed on

the design period used to calculate the design spectral acceleration, DDBD approach leads in general to smaller seismic design force compare to the A23.3 forced-based design procedure.

Table 4-1: FB designed shear walls design information (total 40 shear walls)

No. Storeys	Wall length (m)	Fundamental period (sec)	Reinforcement ratios*	Axial stress **	Global ductility factor (R_D)	Wall base flexural overstrength γ_w
10	5, 5.5, 6	1.5, 1.99, 2.38	0.46% to 1.21%	8%, 12%	2.0	1.35 to 1.92
15	6, 6.5, 7	2.56, 3.39, 4.05	0.44% to 1.11%	8%, 12%	2.0	1.23 to 1.64
20	6, 7, 8	3.4, 4.5, 5.38	0.48% to 1.20%	8%, 12%	2.0	1.22 to 2.32
25	7, 8, 9	4.14, 5.47, 6.54	0.47% to 1.23%	8%, 12%	2.0	1.20 to 2.52
30	9, 9.5, 10.5	4.68, 6.19, 7.4	0.47% to 1.44%	8%, 12%	2.0	1.25 to 2.75

Table 4-2: DDB designed shear walls design information (total 60 shear walls)

No. Storeys	Wall length (m)	Fundamental period (sec)	Reinforcement ratio*	Axial stress ratio **	Global ductility factor (μ)	Stability index
10	5, 6, 7	3.23, 2.65, 2.1	0.5% to 1.2%	8%, 12%	1.12 to 1.72	0.06 to 0.12
15	6, 7, 8	5.59, 4.72, 3.44	0.5% to 1.2%	8%, 12%	1.0	0.08 to 0.20
20	7, 8, 9	6.49, 5.30, 4.7	0.55% to 1.15%	8%, 12%	1.0	0.10 to 0.22
25	8, 9, 10	7.78, 6.51, 5.87	0.55% to 1.55%	8%, 12%	1.0	0.12 to 0.25
30	8, 9, 10	11.16, 9.32, 8.37	0.55% to 1.55%	8%, 12%	1.0	0.25 to 0.40

*Average reinforcement ratio (concentrated plus distributed reinforcement at the base for each wall length)

**$P_f/(f'_c*A_c)$

Although this project focuses on the deformation response of the simple rectangular walls, it might be argued that in tall buildings a mix of rectangular walls, core walls, C-shaped or I-shaped shear walls are used to provide adequate lateral stiffness and strength for the structure. As the flexural response of core walls and C-shaped walls could be approximated by equivalent I-shaped, nine I-shaped shear walls with 20-, 25- and 30-storey height w designed according to NBCC force-based

method and their responses were compared to those of simple rectangular walls of corresponding height and first period. The design information of the shear walls are given in Table 4-3.

Table 4-3: FB designed I-shaped shear walls design information

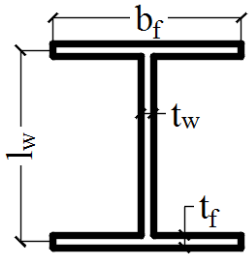

	Geometric properties of I section					
	l_w (mm)	**t_w(mm)**	**b_f (mm)**	**t_f (mm)**	**T_1(s)**	**P/(Ac*f'c)**
20-1	6000	500	2000	400	4.48	8%
25-1	6000	800	3000	400	5.57	8%
30-1	6500	800	4000	450	6.31	8%
20-2	6000	700	1700	400	5.24	8%
25-2	6000	850	3000	400	6.53	8%
30-2	6500	900	3500	450	7.70	8%
20-3	6000	700	1700	400	5.24	12%
25-3	6000	850	3000	400	6.53	12%
30-3	6500	900	3500	450	7.70	12%

Considering that the length of walls has little variation (6 and 6.5m), larger bending capacity is achieved by increasing the dimensions of the flanges. Also, an adequate shear capacity is controlled through the augmentation of the web thickness. The effort was made so that the fundamental periods of the designed walls be as close as possible to the period of corresponding FB designed simple walls with the same height. This was achieved by adjusting the seismic mass.

4.2 The ground motion characteristics, selection and scaling

In previous chapter it was explained that in lack of enough earthquake records with adequate energy in eastern Canada simulated records are the most appropriate available ground motion for NTHA. Unlike the study presented in the Chapter 3 for which NBCC2010 UHS design spectra were used, the parametric study presented herein is conducted using NBCC 2015 UHS design spectra as this new edition of the document become available in the course of the project. Therefore, a new set of 13 ground motion records from simulated ground motion database (Atkinson, 2009) is selected and scaled to achieve compatibility with NBCC 2015 design spectra.

The first group consists of eight records with the low frequency dominated content with modal magnitude of M7. The ground motion records are selected based on the M-R scenario that dominates seismic hazard for Montreal at fundamental periods larger than two seconds (M=6.875 & R = 30km). The low frequency records are selected to match the NBCC design spectrum for period range between two to ten seconds. This period range was retained as it covers the fundamental periods of the shear walls under study, from the elastic fundamental period of shortest walls to inelastic, elongated period of the tallest walls.

The second group of records consists of five high frequency dominated ground motion with modal magnitude of M6 (R=16.9 to 30.7 km). These records were selected to match the periods of the second mode of designed walls (0.2 to 1.5 s) and cover the high frequency range of NBCC spectra. The ground motion records were increased by 15% to account for the effect of accidental torsion that was considered in their design.

In addition, for comparison purposes, three historical ground motion records were selected. Because the historical earthquakes recordings in eastern Canada do not show sufficient energy to excite tall structures, the selected historical records come from other regions. The attention was made to select ground motion records with spectral shape as close as possible to NBCC design spectrum in period range between two to ten seconds and show a good visual match in short period range. It was found that the acceleration spectrum from 2001 M6.8 Nisqually earthquake had the closest match with reasonably low standard deviations. The three selected records belong to this earthquake event. In this selection magnitude and distance scenario of the design earthquake from available disaggregation diagrams (CGS 2010) at the fundamental period is used. The historical records were scaled to UHS in period range between two to ten seconds.

Each set of selected records were scaled to NBCC 2015 UHS acceleration spectrum for Montreal in the relevant period range. The guidelines provided in NBCC 2015 (Tremblay et al., 2015) and Atkinson (2009), as explained in section Chapter 13.5.1 were followed in scaling of the records.

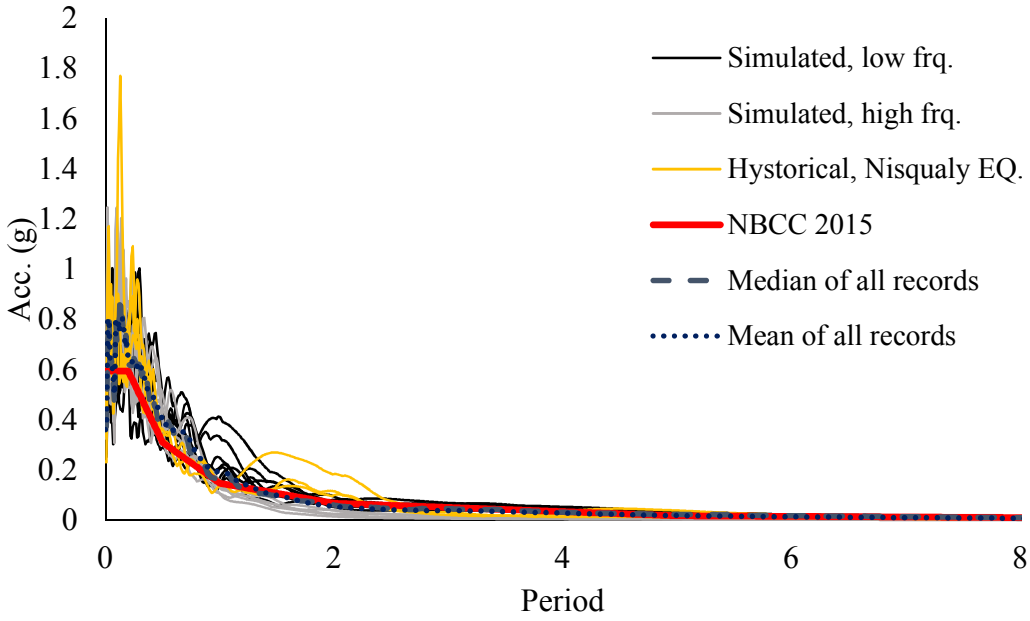

Figure 4-3: The acceleration spectrum of the scaled ground motion records used for the parametric study in comparison with NBCC 2015 design spectra for Montreal

The spectra of the scaled simulated and historical records are shown in Figure 4-3. It can be seen that the accelerations of high frequency records fall consistently under the NBCC spectrum for longer periods. On the other hand, the acceleration of low frequency records in high frequency range is both above and under the design spectrum. The low frequency simulated records typically surpass the NBCC design spectrum around the period equal to one second. This would not significantly impact the time history analysis results because the lower bound of period range of interest for low frequency records is two seconds. The spectral accelerations of historical records are larger that design spectral accelerations for periods between 1 to 2.5 seconds but show a reasonably acceptable match in other period ranges.

4.3 Analytical modeling

4.3.1 OpenSees model

The nonlinear time history analysis is performed using a two-dimensional model with fiber sections developed in OpenSees (OS) platform. (see Chapter 3). As prescribed by CSA A23.3, the ultimate strain for unconfined concrete, ϵ_{cu}, is taken equal to 0.0035 and the ultimate concrete compressive

strength is assumed to be 35 MPa for all shear walls. Modified Park stress-strain relationship (Park, Priestley, & D. Gill, 1982) used to represent confined and unconfined concrete. Results of the parametric study indicated that five integration points along the element give accurate results while assuring a reasonable duration of the analysis in view of large number of required analysis for different wall designs. The schematics of the fiber modeling of OS model is shown in Figure 4-4.

The shear walls examined in this study according to Priestley (2007) can be considered slender ($h_w/l_w > 4.4$) and thus the shear stresses will generally be very small. Luu et al (2013) showed that the variation of shear stiffness has a small impact on the important deformation parameters such as the top displacement and base curvature. Therefore, it was concluded that it was acceptable to use a linear elastic model for the shear deformation of the wall elements. Also, following the same reasoning and considering the recommendations from the literature (ATC72-1, 2010), the moment-shear interaction is ignored in the model .

Recommendations from the literature, issued from numerical and experimental studies were used to validate the OS model. Luu et al calibrated OS models developed the rectangular ductile shear wall against the results of experimental test of an eight storey shear walls designed for eastern Canada (Ghorbanian et al 2010). It was shown that using Park et al. (1982) stress-strain relationship for confined and unconfined concrete, 25% of the gross shear stiffness and 2% Rayleigh damping in 1^{st} and 2^{nd} mode and ignoring the tension stiffening resulted in good match with the experimental data. ATC72-1 (2010) confirms the use of less than typical 5% viscous damping for NTHA analysis of taller shear walls but recommends to 10% of the gross shear stiffness uniformly along the height of the wall which seems appropriate for the shear walls located in western North America but overly low for eastern North American locations.

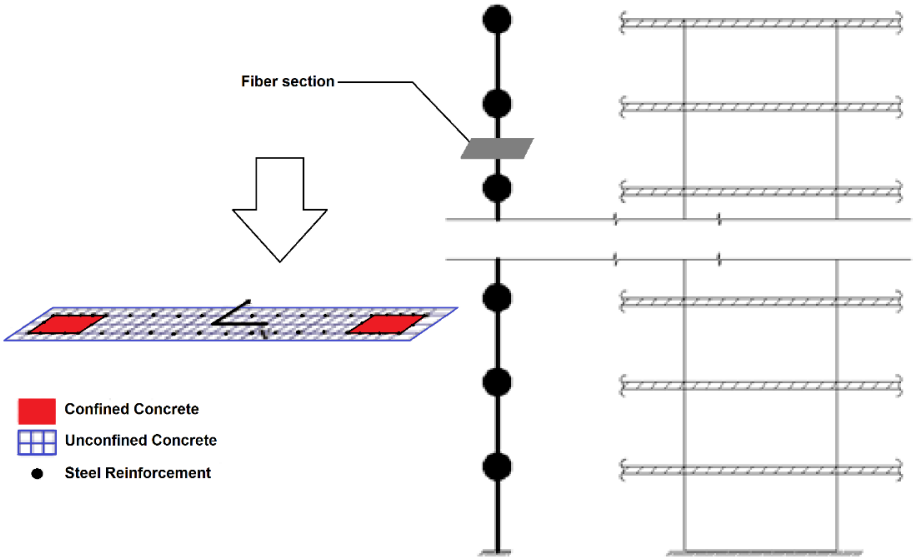

Figure 4-4: OpenSees fiber modeling schematic

For more extensive validation of OS model, particularly related to the estimation of the shear distribution for taller walls, Luu et al. used VecTor2 (VT2) finite element package (Wong & Vecchio, 2002), a plane stress finite element program based on compression field theory developed by Vecchio and Collins (1986). For the eight-storey shear wall, tested by Ghorbanian et al, OS models showed slightly better match than the VT2 models, however, for 20 and 25-storey walls certain discrepancies in shear force estimates were observed when OS model was used. Because the focus that research was to study inelastic higher mode impact on the shear forces, Luu et al. suggested that for the taller walls, for which no experimental data was available, using VT2 is more accurate modeling strategy because it considers the shear-bending-axial force interaction. However, performing analysis with VT2 is very time consuming and would limit the number of the walls that could be considered in the parametric study as seen in previous studies (Luu et al., 2013 and Boivin et al. 2012).

For this research study, the OS model based on parameters suggested by Luu et al. was used for 10 and 15 storey shear wall models. For taller walls, a comparison between OS model and VT2 models was done by comparing the response of two FB shear wall designs, 20 and 25-storey height to assess the result of OS model. The schematics of VT2 models are shown in Figure 4-5. The lengths of the walls are respectively 7m and 9m. In OS models modified Kent–Park model was used for concrete and a Menegotto-Pinto material, with Bauschinger effect, was selected for the reinforcements. Luu et al. suggested that in order to achieve the best match with the experimental

data the tension stiffening of the concrete material should be ignored. For VT2 models, as suggested by (Luu et al. (2013), Hognestad parabolic material model was used for pre-peak and Modified Kent-Park model used for post-peak compression behaviour. For compression softening Veccio model was used and, like the OS model, no tension stiffening was considered. The reinforcements were modeled using smeared reinforcement option and the steel material included the Bauschinger effects. In both models 2% damping was applied to the first and the third mode for the Raleigh damping in both OS and VT2 models. Nonlinear time history analyses were performed for a set of eight simulated records, the low frequency set of simulated ground motion records as explained in 4.2. As seen in Chapter 3, the records with lower frequency contents cause higher flexural demands and are expected to show larger top displacement and base curvature demand. For OS models, the calibration parameter used by Luu et al. for 10 and 15 storey walls were considered except that the 2% viscous damping was applied to the first and third modes to determine Rayleigh damping coefficients as it showed better match between OS and VT2 models. However, similarly to what was observed by Leger and Dussult (1992), the small variation in modal damping used for Rayleigh damping had little impact on the response of the walls under the study.

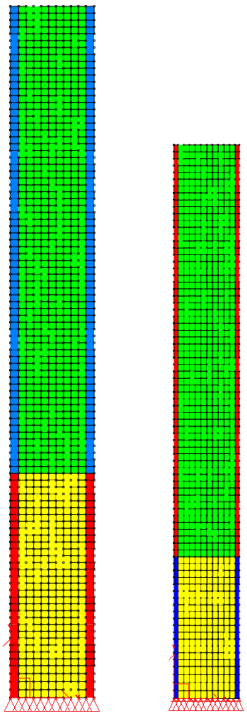

Figure 4-5: VT2 model for 20 and 25-storey shear walls

In Figure 4-6 the average of the maximum displacements obtained for eight ground motions is for OS and VT2 models and both wall heights match well. Since the base curvature is not readily available from VT2 analysis, instead the base rotation of the walls from OS and VT2 models were compared.

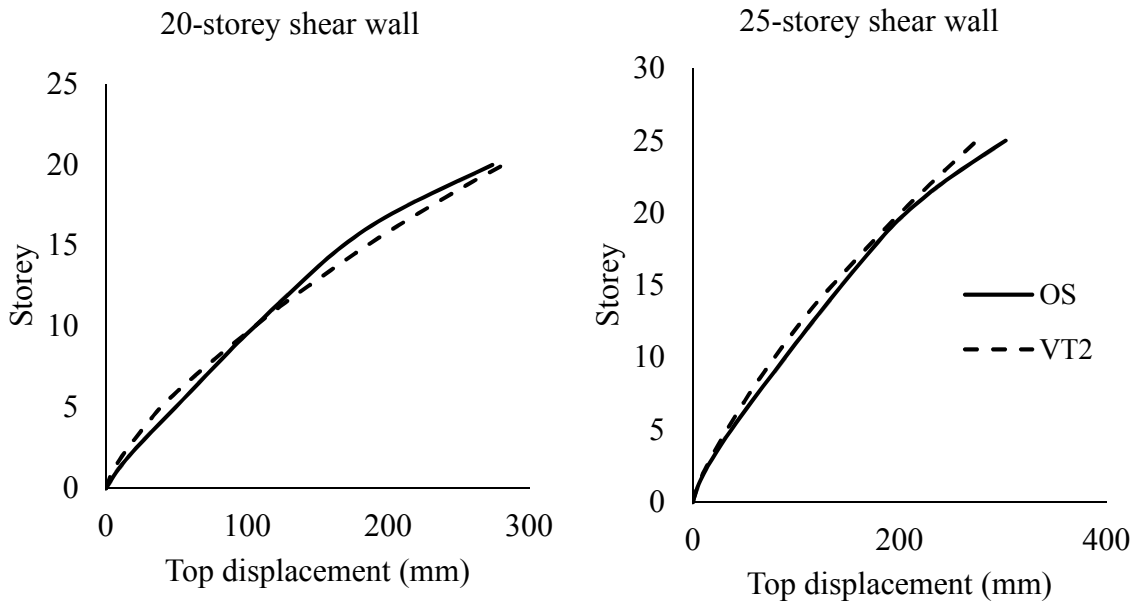

Figure 4-6: Displacement profile from calibrated OpenSees versus the VT2 models.

The base rotation was calculated as the inter-storey drift at the mid-height of the plastic hinge assuming that the length of the plastic hinge is equal to the length of the wall. The outputs of the two models for 20 and 25-sotrey shear wall are shown in Table 4-4.

Table 4-4: Ratio of deformation response from VT2 over OS, average of all records

Ratio	20-storey	25-storey
Top Displacement	0.99946	0.94026
Base rotation	0.75	1.02

While the average base rotation for 25-storey is similar for both models, for 20-storey wall the base rotation from OS model is about 25 percent larger than the VT2 model. Considering the large dispersion of the results obtained for the base rotation and also the fact that OS model provides more conservative estimates it was decided to use OS model for this parametric study.

4.4 Results of nonlinear time history analysis

The nonlinear time history analyses for 100 designed shear walls were performed in OpenSees for minimum 13 simulated ground motions. Some shear walls were analyzed for additional hisotorical records, but as will be explained in section 4.4.1 because the response to historical records were generally less than the simulated records, their outputs were not used. The response of walls was tracked through the deformation response parameters including the displacements, base curvature, inter-storey drifts and curvature and displacement ductility. It was noted that the maximum displacement always occurred at the top of the shear walls whereas the maximum curvature always occurred at the base. To calculate the curvature ductility the yield curvature assumed equal to $2\epsilon_y/l_w$ (NBCC 2015).

According to Tremblay et al. (2015) when two or more earthquake scenario and record groups are being used in time history analysis it is advised to use mean plus standard variation or 84^{th} percentile results obtained for all records or alternatively use the mean or median results of the group of records which cause the largest actions. Since the deformations and specially the base curvature response are very sensitive response parameters for which the higher dispersion of results is anticipated using median and 84^{th} percentile response (in comparison with mean and mean plus standard deviation) is more appropriate for study of the deformation response. Therefore, to estimate the base curvature of a shear wall form its top displacement it makes more sense to develop the relation between the 84^{th} percentile of the base curvature to median of the top displacement response for all records.

4.4.1 Response to simulated ground motion records versus historical records

The deformation response from historical records in comparison with the simulated records is another subject of interest. It was already mentioned that the available historical ground motion records for eastern Canada do not posses enough energy to excite structures with large fundamental periods, and therefore the use of simulated records for time history analysis is quite common. To compare the deformation response under the historical and simulated records, three ground motion records from Nisqually earthquake are applied to a 20-storey shear designed as per CSA A23.2 (FB design, see section 3.1Force-based seismic design of tall shear walls). The selected shear wall has 8m length of the fundamental period of the cracked wall is 3.4 s. Figure 4-7 and

Figure 4-8 show the displacement and curvature profiles under these historical records and five simulated records with predominant low frequency content selected from the set of accelerograms retained for the parametric study. The displacement profile from individual historical records are slightly smaller than those from simulated records. The mean displacement profile from the simulated records overall is about 10 percent larger than the mean displacement profile from the historical records. Although considering the limited number of historical records using mean or median values is not a strong indicative this is only for the sake of relative comparison. As expected, the curvature profiles, illustrated in Figure 4-8 show more significant difference between the simulated and the historical records. The average base curvature induced by the simulated records reaches about three times that caused by the historical records.

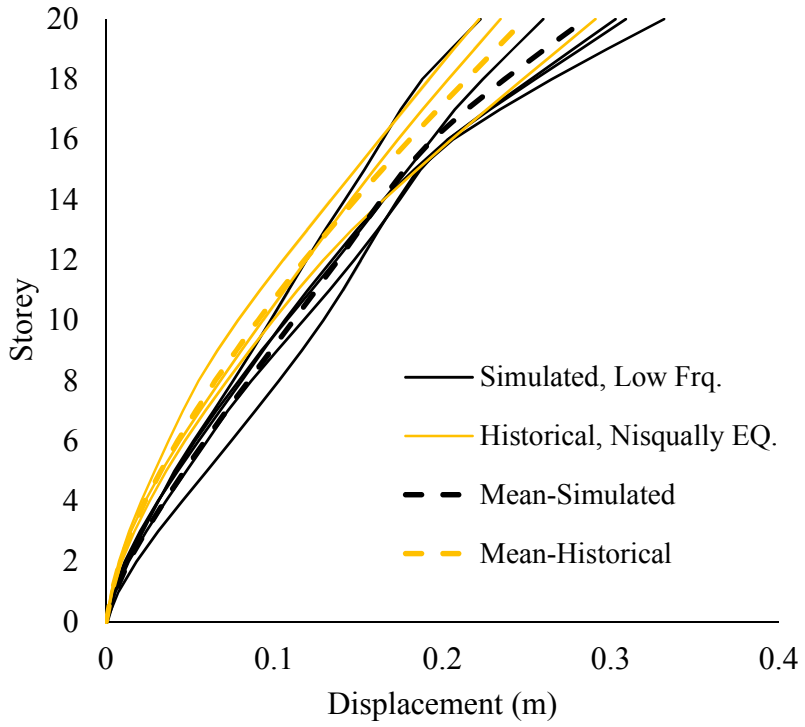

Figure 4-7: Maximum displacement profiles from the simulated and historical ground motion records

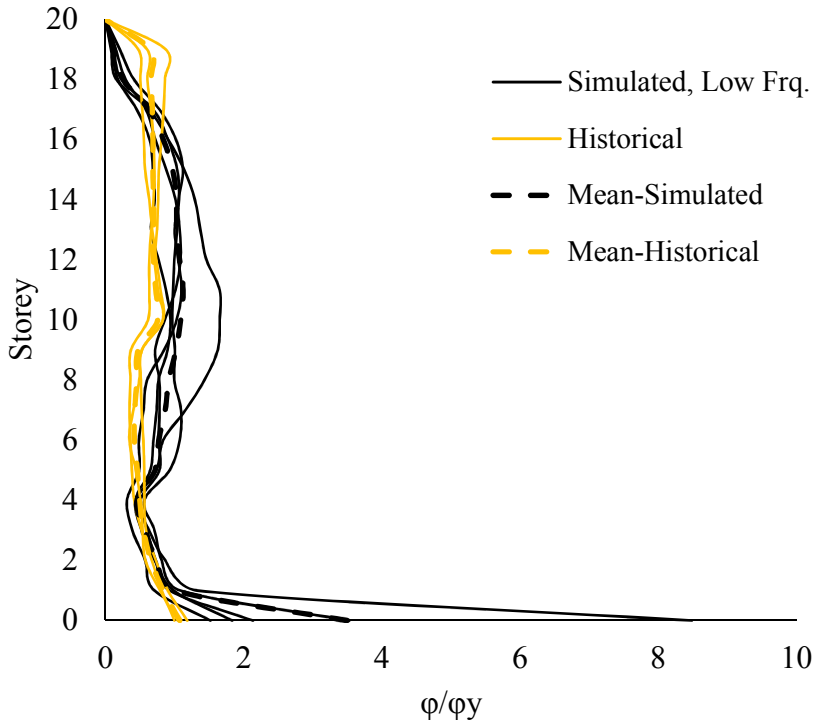

Figure 4-8: Maximum curvature profiles from the simulated and historical ground motion records

From the above comparison it is concluded that the simulated ground motion records impose higher force and deformation demands and thus are more conservative and safer to be used for the parametric study. Therefore, in the followings sections only the response obtained for the simulated records is shown and discussed.

4.4.2 Deformation response of I-shaped wall vs. the rectangular walls

It was previously explained that the I-shaped walls in this study were set to have similar fundamental periods as selected rectangular walls to facilitate the comparison of their response. Figure 4-9 shows the ratios of base curvature and top displacement of I-shaped walls and their rectangular counterparts

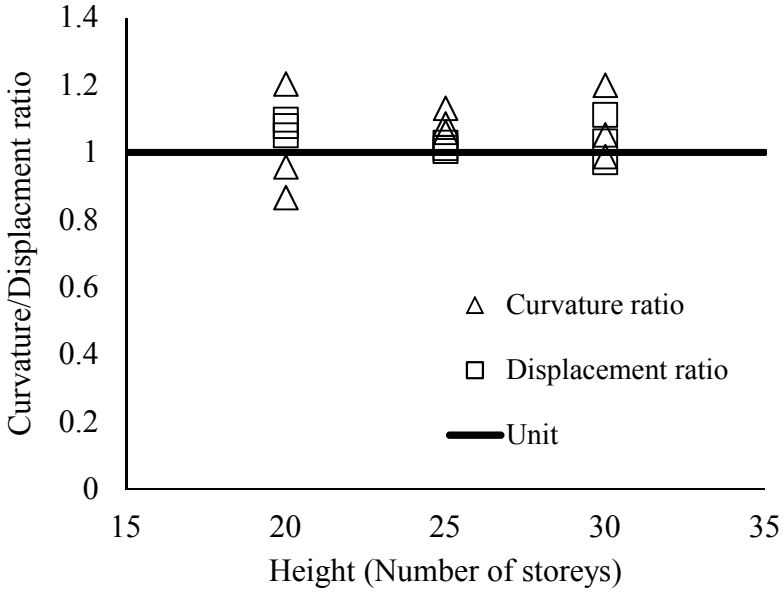

Figure 4-9: The ratio of the displacement and curvature prediction for the I-shaped shear walls to the displacement and curvature of the rectangular walls with similar fundamental periods

For all wall heights, the top displacements of I-shaped walls exceed those of the rectangular walls by up to 10 percent. The difference is more pronounced for 20-sotrey shear walls whereas for 30-storey shear walls the top displacements are almost similar. The base curvatures of I-shaped walls show larger scatter and are up to twenty percent bigger for 20-storey walls. However, for some 20 and 30-storey walls the base curvature for I-shaped walls is smaller up to about fifteen percent (for 20-storey walls). Similar to the top displacement, the scatter of the base curvature for taller walls (25 and 30-storey) is smaller.

For I-shaped cross sections the depth of the neutral axes should be smaller so in turn they have larger rotation capacity at the ultimate limit state compared to rectangular walls. Nevertheless, for the walls under study, with force demands far below their ultimate strength, the curvature demands for I-shaped walls is close to the base curvature demands of the rectangular walls, especially for the taller walls. Therefore, the observations and conclusions regarding the curvature demands in rectangular walls considered in this study could be extended to the I-shaped walls.

4.4.3 Base curvature from NTHA vs design predictions

The design prediction of base curvature for both FB and DDB designed shear walls are compared with the results of NTHA in Figure 4-10. The predicted base curvatures in FBD method are derived by calculating the base rotation (Equation 2-4) and then dividing it by the length of the plastic hinge (Adebar et al, 2005). For DDB designed walls, the predicted design base curvature is derived based on the state of the response. If the response is predicted as inelastic the base curvature is derived from the top displacement based on the same approach as FBD method (Equation 2-4). If the response is elastic the base curvature is derived by multiplying the yield curvature by the ratio of the maximum spectral displacement to the estimated yield displacement of the ESDF system (Equation 3-8).

The black solid line indicates that NLTH result and the design prediction are equal. Through the observation of 84^{th} percentile response, it was noted that the 84^{th} percentile (of all records) base curvatures were very close to the maximum values and in many cases represented by an outlier response. Therefore, it was decided to compare the median response of low frequency records with the design predictions.

It is noted that overall, the NTHA base curvatures exceeds design predictions. This is particularly significant for the DDB designed walls for which almost for all cases the predict base curvature demand is inadequate. For the shorter walls, the curvature demands are larger and under-estimation of the curvature demand is quite significant (minimum 1/25 times the base curvature NTHA).

Overall, the FBD method gives closer predictions compare to the DDBD approach, but with increase of the wall height the design predictions become more and more overestimated. On the other hand, both methods and specially DDBD evidently under-estimate the demands for the shorter walls, specially those with light reinforcement and larger axial gravity stress.

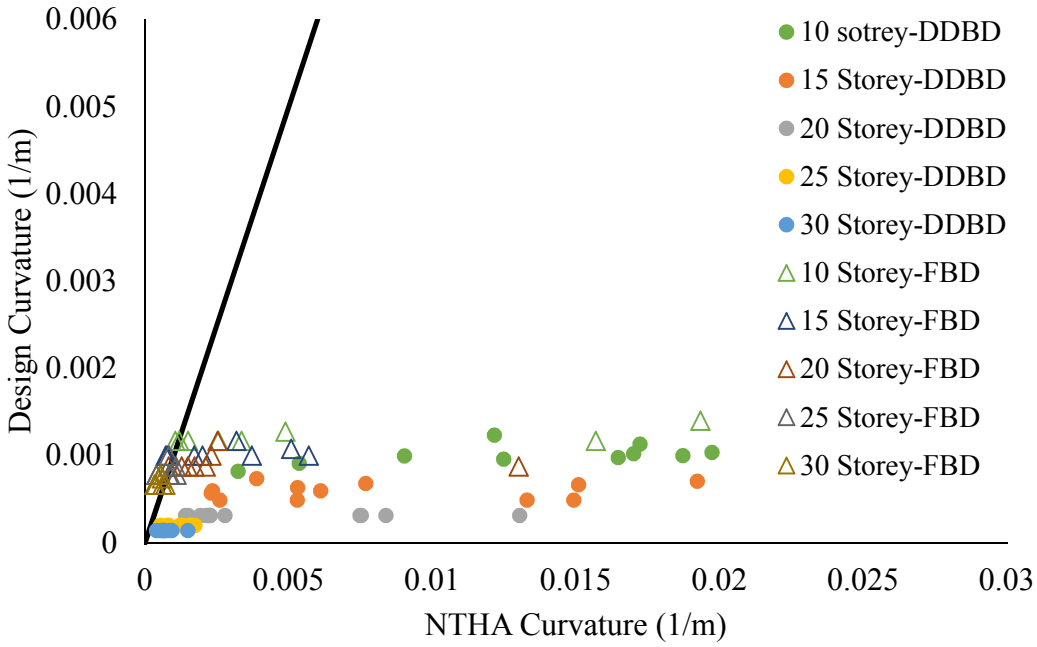

Figure 4-10:Curvature predictions from design versus NTHA

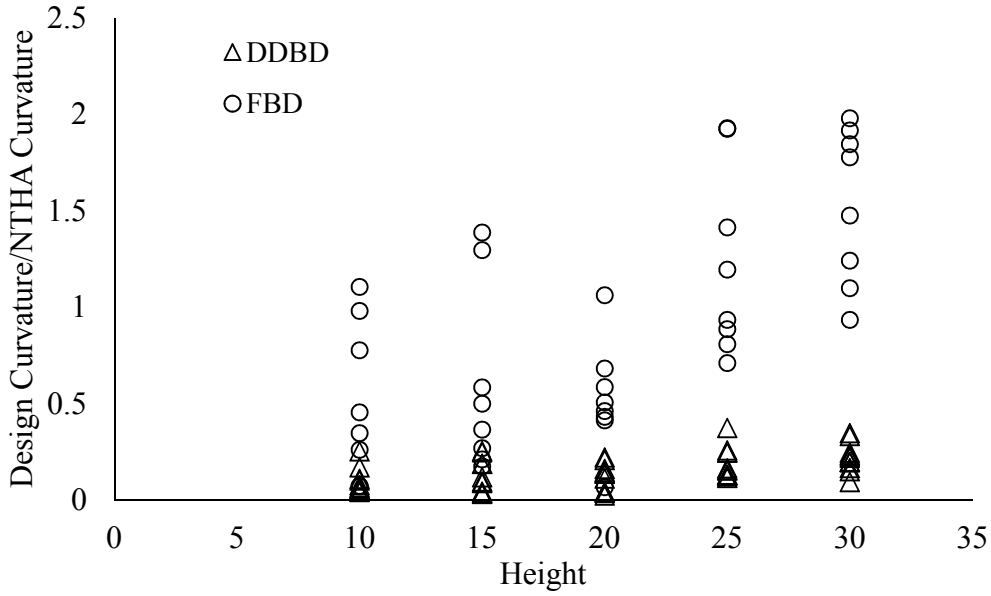

Figure 4-11: The ratios of the curvature from NTHA to the design predictions

In Figure 4-11, the ratios of base curvature design predictions to NTHA values are plotted in function of height of the wall. The largest misfit is recorded for the 10-storey walls for which design prediction is only are only 4% of that recorded in NTHA. This result is obtained for a very slender

DDB designed wall with the minimum cross-sectional reinforcements. A minimal length (l_w=5m) was selected for this wall and its mass was increased to obtain the fundamental period above the corner period. DDBD procedure predicted elastic response of this wall. The stability index of this shear wall was 0.25 which smaller than the limit considered in DDBD (0.4). Even though the design satisfies all the requirements of DDBD method and is the wall should exhibit elastic response, it undergoes very large inelastic rotations during the design earthquake. For less slender walls, DDBD showed closer predictions to the NTHA results. However, the curvature predictions are still much smaller in comparison to those obtained from the NTHA.

On the other hand, although FBD approach gives a better prediction for the walls under twenty storeys, it over-predicts the base curvature for the taller walls.

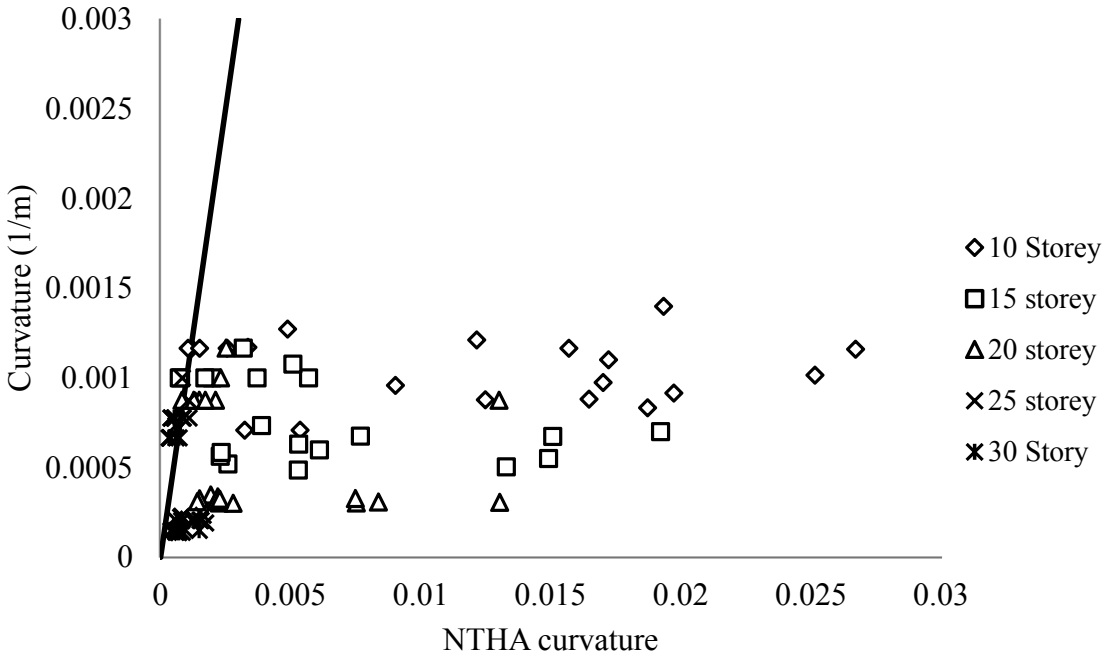

Figure 4-12: Base curvature predictions from design functions based on NTHA displacements versus NTHA base curvature

The underestimation of the base curvature from DDBD approach is a direct consequence of inherent flaws of the DDBD approach. The prediction of elastic response of the slender walls by DDBD approach is based on the assumption that the deformations of the wall are dominating by the first mode. Although the overall inelastic response of these walls is not significant and is less extensive than what is expected by the FBD method, the local response, shows relatively large

inelastic rotations. Therefore, although the prediction of elastic response is applicable if the global response is considered, for local response the approach used in DDBD to estimate the curvature based on the elastic response is not accurate.

To further investigate the applicability of the FBD and DDBD formulations for estimation of the base curvature, for each wall, the median top displacement obtained for complete record set is used to calculate anticipated curvature values. The results are then compared to median of low frequency records from NTHA as shown in Figure 4-12. Similar to what was seen in Figure 4-11, the predictions from design equations for base curvature are much smaller than the NTHA curvatures even when displacement from NTHA are used.

4.4.4 Top displacements from NTHA vs design prediction

In general, the top displacement and overall displacement profile from NTHA are less sensitive to record content and are closer to the design predictions. Figure 4-13 shows the global drift derived from the design versus median top displacement recorded from NTHA for the whole record set normalised by the wall height. The black line in the figure represents the line for which the design prediction is equal to the NTHA results. The FBD top displacement is determined from response spectrum analysis (RSA) and multiplied by ductility factor, R_d=2.0 and a partial over-strength factor (R_o=1.3). The partial over-strength factor considers the over-strength caused by the steel and concrete material over-strength and the over-strength due to strain hardening of the reinforcement steel. The purpose of using partial over-strength factor is to have a comparable value with the results of NTHA. For DDB walls, the top displacement is directly available at the beginning of the design. According to DDBD approach, the 15-storey and taller walls show elastic response. Therefore, the top displacement of the equivalent SDF system for all walls with the same height is limited to maximum spectral displacement. After the transformation for SDF to MDF system is done, the top displacement of the shear walls with the same height would be the same. Note that the walls designed according to FBD approach are generally stiffer and have smaller periods compare to the DDB design walls. While the displacement predictions from FBD approach for shorter walls (10 and 15-storey walls) are close to NTHA results, for taller walls the predicted displacements are overestimated.

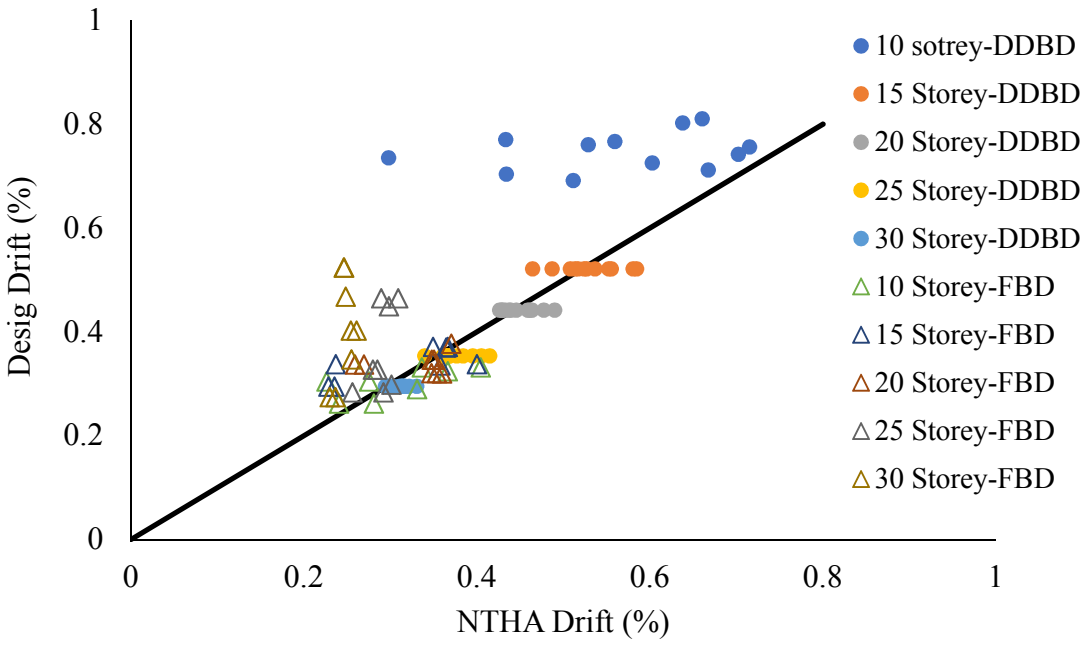

Figure 4-13: Displacement predictions from design (FBD or DDBD) versus median response of all records from NTHA

Figure 4-14 shows the same graph based on the median results of low frequency records. Though the NTHA drifts are slightly larger, similar conclusions as those based on the median response for complete record set can be made. It is also noted that the design predictions for top displacement are closer to median response of all records than the repose of low frequency records.

As the displacements do not appear as sensitive as base curvatures to the frequency content of the records, it is more appropriate discuss the displacement and deformation profile in terms of median results obtained for all records response rather than the median of low-frequency records.

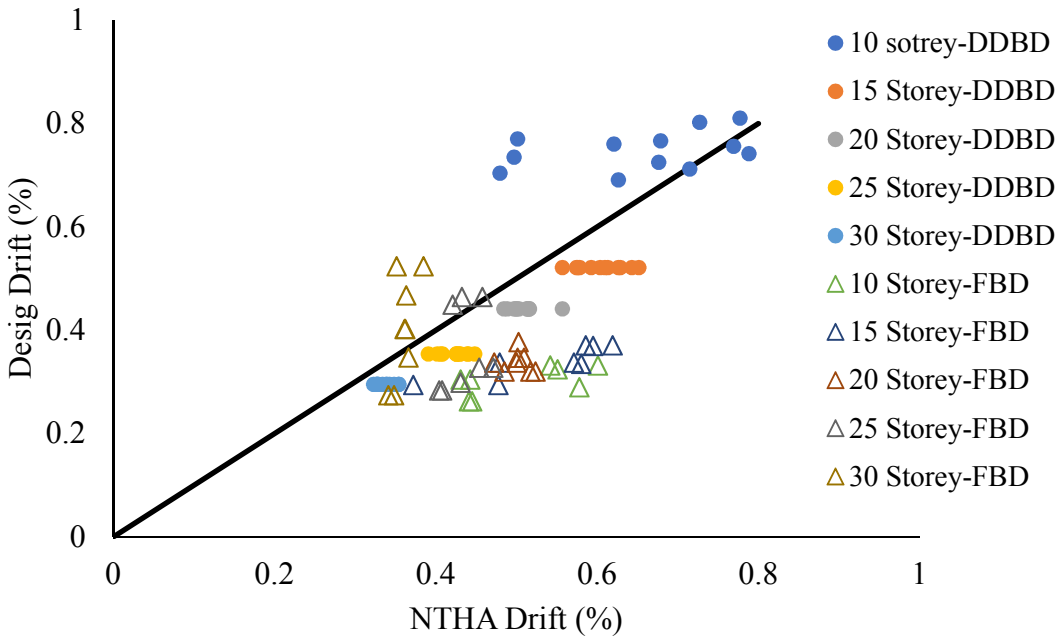

Figure 4-14: Displacement predictions from design (FBD or DDBD) versus median response of low frequency records from NTHA

4.5 Response sensitivity to the studied parameters

4.5.1 Fundamental period and height

From reviewing the results of NTHA, it was noted that among the parameters under study, height, and thereby the fundamental periods of the walls have the most significant impact on the deformation response, for both the base curvature and top displacement. However, this impact is more pronounced for the base curvature demands. As the height and fundamental period increase, the inelastic response of the shear walls reduces, and the base curvature demands significantly reduce. In this study the height is represented through the number of storeys.

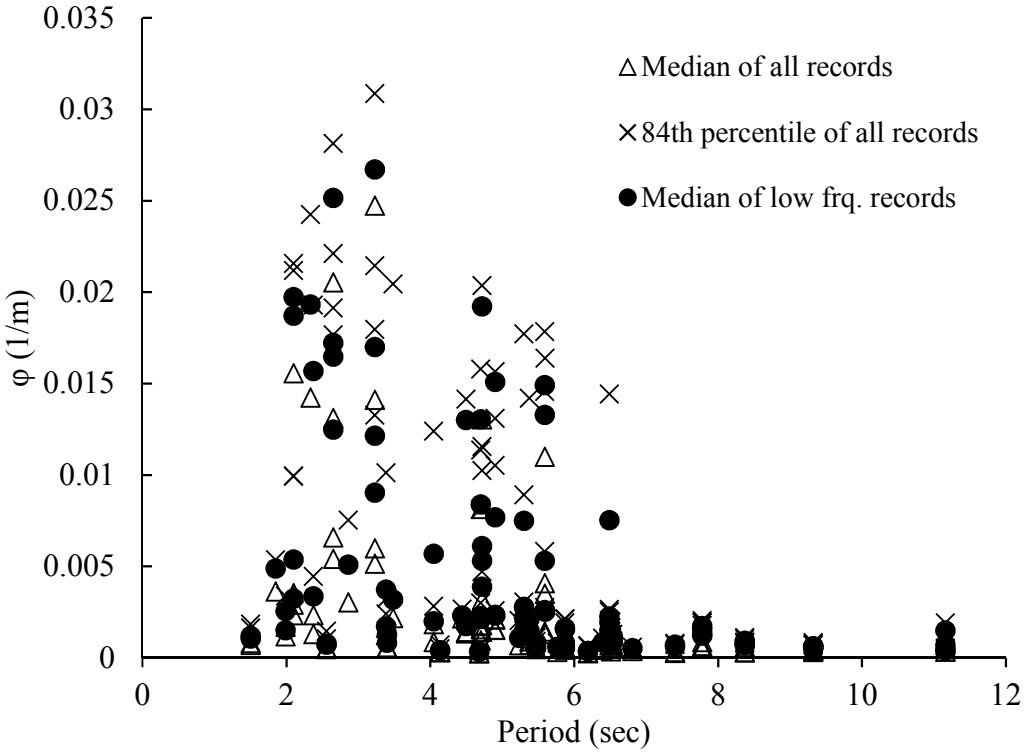

Figure 4-15: Base curvature response of the shear walls versus their analytical periods

Although, the fundamental period can provide a relevant representation of the height of shear walls, it was noted that that by representing the base curvature versus the fundamental period it is more difficult to find the trends of base curvature variation (Figure 4-15). Therefore, it was decided to use the variation of base curvature response in function of height to identify trends in base curvature variations more clearly (Figure 4-16). In Figure 4-16 the curvature variation for taller walls (more than 15-storeys) is much smaller compared to the shorter walls. The base curvature quickly reduces for the taller walls and confirming thereby the trend of the elastic response for the taller shear walls. There is a significant difference between the of the 84th percentile response and the median response which is the indicator of the sensitivity of the base curvature to ground motion input.

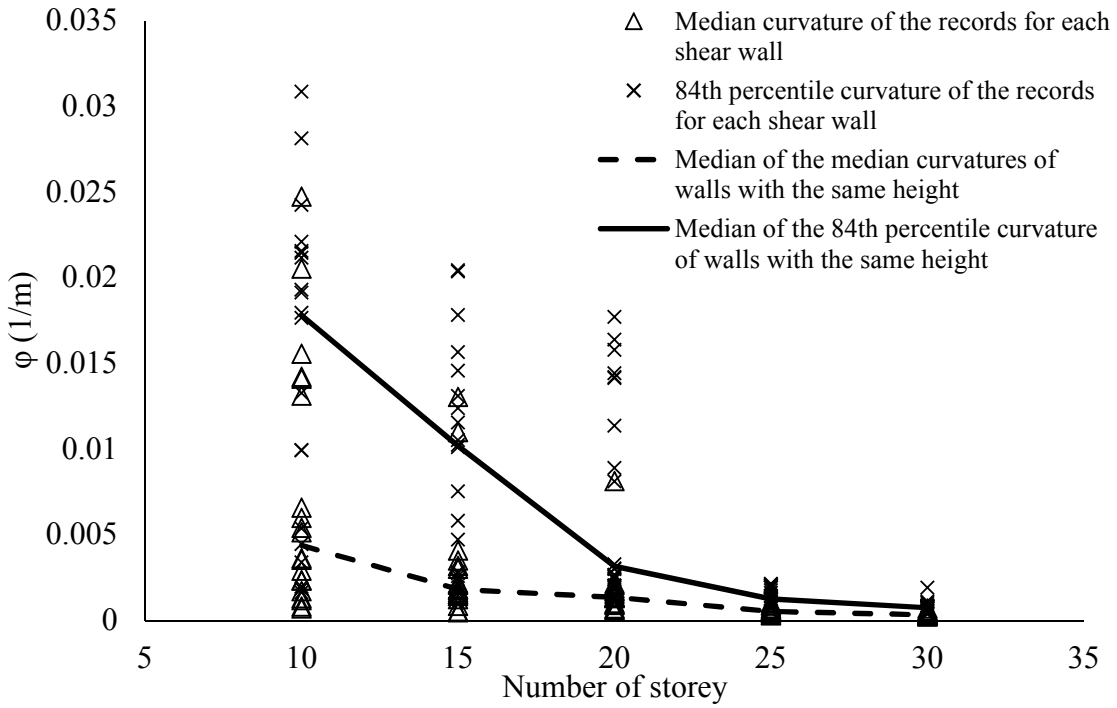

Figure 4-16: Base curvature demands variation with height.

Figure 4-17 shows the variation of the base curvature with the height for the median response for all records, 84th percentile response of all records and the median response of the low-frequency records. At each height, the median of each response is shown (i.e. median of the response of shear walls with the same height). The median response from low frequency records is larger than the median of all records for all heights, especially for shear walls less than 20 storeys. The ratio of the median response to low frequency records to the median response of all records varies between to 1.84 to 2.81 for 30-storey to 10-storey shear walls respectively.

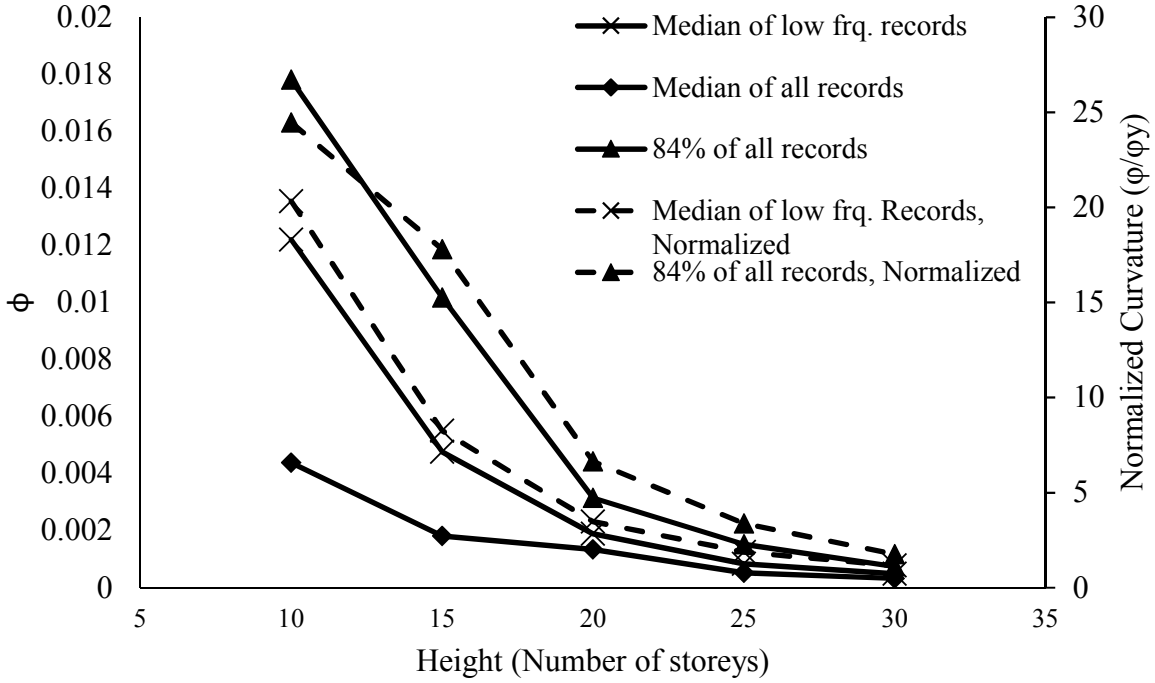

Figure 4-17: Base curvature response comparison; Median response of all records versus 84th percentile response of all records versus median response of the low frequency records. The normalized curvature (i.e. the curvature ductility) is show on right axis.

On the other hand, for all shear walls, especially the ones under twenty storeys the base curvatures from 84th percentile response of all records is even larger (about two times) than the median response of low frequency records. It is noted that, the base curvatures recorded for FB designed walls is smaller than those obtained for the 10 and 15-storey DDB designs. The base curvatures are very large for special cases characterised by a combination of minimum reinforcement, highest axial force stress and largest seismic mass. In the figure above, if these special cases are neglected, the median response of the low frequency record can be conservatively considered as the median indicator for the base curvature.

Figure 4-17 also shows the variation of normalized base curvatures indicative of the curvature ductility at the base. The normalized curvature is the ratio of the base curvature to the yield curvature, the later being defined as $\varphi_y=2\epsilon_y/l_w$. The median curvature ductility from the median response under all records varies between 0.75 to 6.3 while the one from the median response of low frequency records verifies between 1.6 to 20.3. The 84th percentile response gives the largest

base curvature ductility varying from 1.75 to 24.45 for 30-storey to 10-storey shear walls, respectively.

Figure 4-18 shows the variation of the top displacement with the height of the shear walls. In this figure, the median responses of all records are represented. As the height increases, the median top displacement reaches a maximum value equal to 280mm and 300 mm, for all records and low frequency records, respectively.

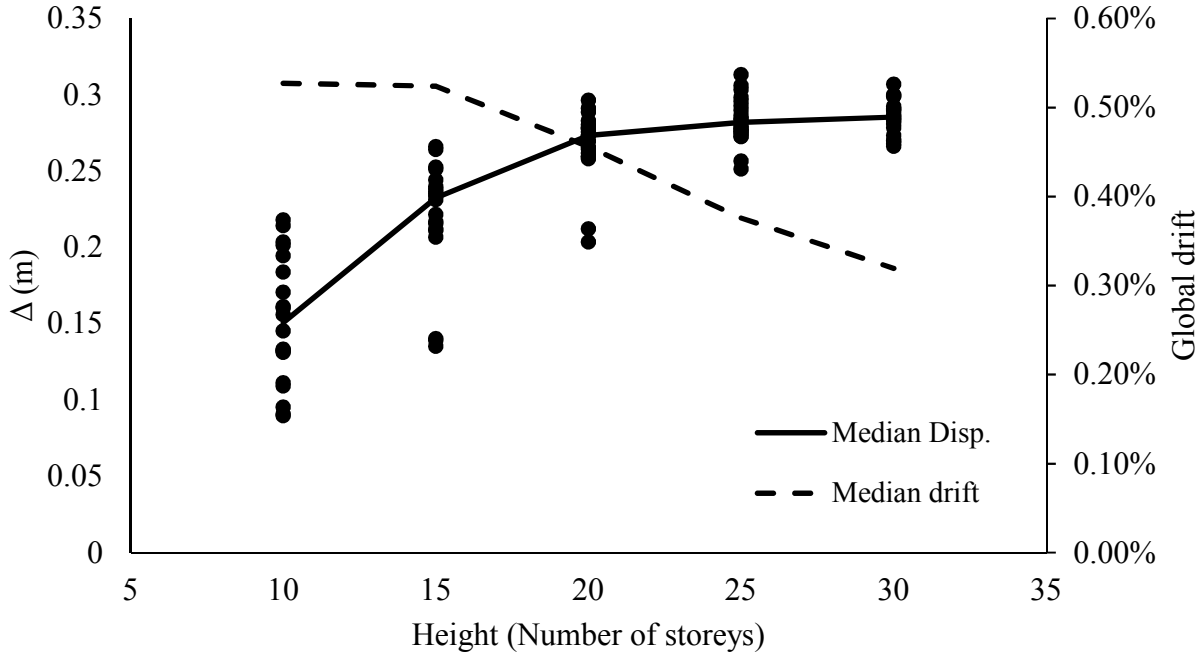

Figure 4-18: Top displacement variation of the shear walls against their height. Since the displacement become relatively constant above 20-storeys, the global drift (shown on the right axis) decrease.

The top displacement reaches this maximum limit starting from the 20-storey wall for both median response of all records and median response of low-frequency records. The maximum top displacement, (median of records, 280mm) is about 50% larger than the maximum spectral displacement (Δ_{max}=185mm for 2% damping) based on the corner period of displacement spectrum for Montreal. The maximum spectral displacement is the maximum deformation of the ESDF (maximum displacement at the first mode) which can be calculated as the deformation of the MDF system at effective height (H_e). Depending on the mass distribution and dynamic properties of the

shear wall the effective height of the wall normally varies between two third to three forth of the height of shear wall. If the concentrated mass displacement at the effective height is limited to Δ_{max}, and a triangular displacement profile is approximated, the displacement at the top of the shear wall would vary between around 1.3 to 1.5 times of Δ_{max}. It is seen that the maximum top displacement of the shear walls (280mm) is about 1.5 times of Δ_{max} and is larger than this range. A combination of different factors can be the reason for this observation. The most important reason is the contribution of the rigid body deformation compatible with the fundamental mode. Considering that the first mode is assumed as the dominate mode for the displacement response, the shear wall can be represented by an effective concentrated mass at an effective height.

Other parameters also could have a minor participation for the observed augmented displacement is the augmenting impact of the higher modes on the displacement response.

The standard deviation of the top displacements for 10-storey walls is larger than that determined for the other walls. The dispersion of the data sharply decreases for 15-storey walls and then gently reduces for the taller walls. Similar to the base curvature, the scatter of top displacements is larger for 10-storey walls, but unlike the base curvature results, it quickly drops for the 15-storey walls and remain constant for the taller walls.

Based on the observations from Figure 4-18, because shear walls above 20-stores have relatively constant median top displacement, the spectral corner period should be around the fundamental period of the 20-storey shear walls. The analytical period of 20-storey walls varies between 4.7 to 6.4 second with average of 5.3s. The assumed corner period for DDBD design (T_c=6s) is slightly larger than this value. As the height of the shear walls increases, the small amplification of the displacement for taller wall would lead to decrease in the global drift response of these walls.

4.5.2 Axial compressive force

To investigate the impact of axial compressive force at the base of the wall on the base curvature and top displacement, 50 studied walls were designed considering the axial base force equal to $0.12f'_cA_c$ and other 50 considering the axial force equal to $0.08f'_cA_c$ where f'_c is the specified concrete compressive strength and A_c is the gross section area of the wall. This range would generally cover the level of realistic axial compressive forces in RC shear wall buildings for interior

and perimeter walls. The variation of the base curvature and top displacement in function of the height for the two level of axial force are shown in Figure 4-19 and Figure 4-20 respectively. For the base curvatures (Figure 4-19) the outputs based on the median response of the low frequency records are shown. For each height, the median of the base curvature is represented. For top displacements (Figure 4-20), the data is based on the median response of all records. Similar to Figure 4-19, for each height, the median of the top displacements is represented.

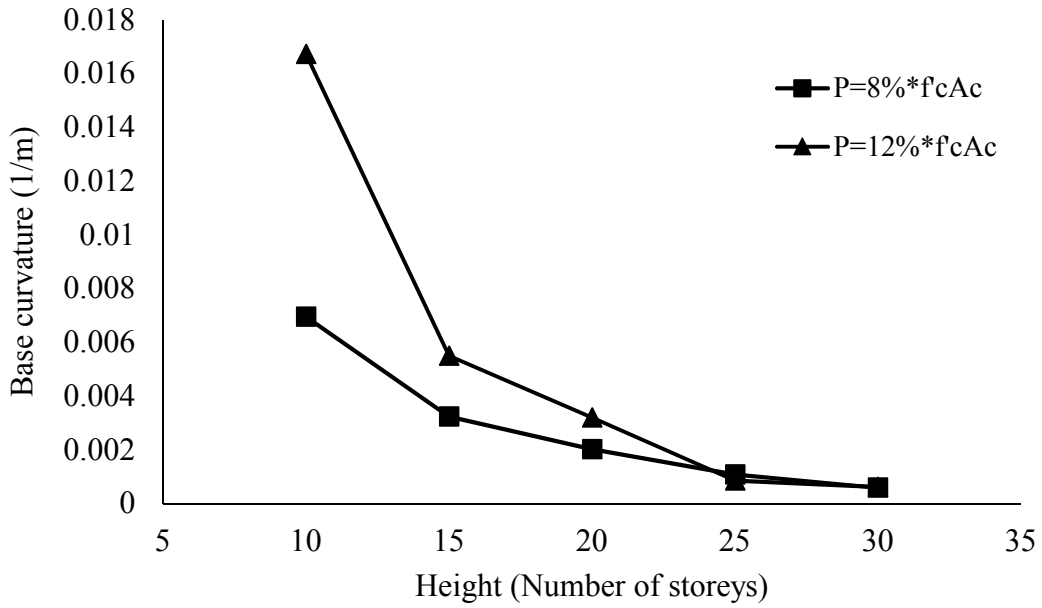

Figure 4-19: Variation of base curvature for the walls with different compressive axial force.

As seen in Figure 4-19, the base curvature of the shorter walls is significantly affected by the amount of the axial compressive force at the base. This is particularly true for 10-storey shear walls, for which the inelastic curvature demand for higher axial force is 1.75 times larger compared to that obtained for lower axial force level when median response of the complete ground motion ensemble is considered. When the median of low frequency records is considered, 2.4 times higher curvature demand is recorded for the wall with higher axial force. Curvature response is impacted by the level of the axial force up to 20-storey walls but to a lesser extent. For taller walls, for which the structural response is principally elastic, the impact of axial compressive force is negligible.

It is noted that as soon the response tends to be elastic the impacts of the gravity load on the response would be negligible. The larger base curvature of 10-storey walls with larger axial indicates that in the inelastic domain larger axial load causes larger compression stress in concrete

and not larger compression depth. Such phenomenon quickly diminishes when the inelastic large response is reducing. Reader should note that the presented information in Figure 4-19 are the curvature demands from NTHA and are different from the maximum curvature capacity of the section. The larger axial load always reduces the ultimate curvature capacity of the section. According to CSA A23.3-14 the ultimate curvature capacity of the section is based on the maximum compressive strain capacity of concrete and compression depth of the section ($\varphi_{max}= \epsilon_{cu}/c$). If maximum compressive strain capacity of the section is assumed as constant, the curvature capacity would reduce by the increase in compression depth. Therefore, increase in axial force would reduce the curvature capacity of the section at the ultimate limit state. Considering the smaller curvature capacity of the RC sections with larger axial force and larger demands for these walls (Figure 4-19) for 10 and 15-storey shear walls, it could be concluded that the axial load plays a critical role in design of the shear walls with inelastic response.

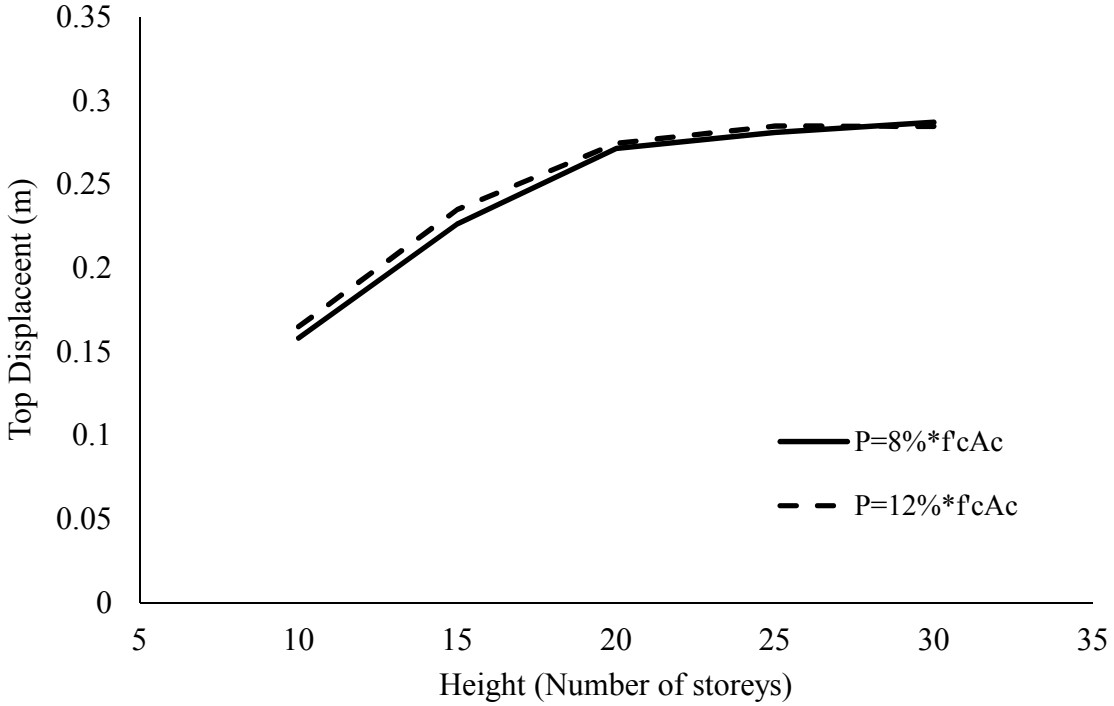

Figure 4-20: Variation of top displacement for the walls with different axial compressive force

On the other hand, the displacement profile, regardless of the height of the structure, shows the negligible sensitivity to the axial compressive load considering the results based on median of all records (Figure 4-20). There is a slight recorded impact when low-frequency records are

considered, but that still remains insignificant. It appears that because the relatively weak demand of the ground motions and overall relatively large stiffness of shear walls, the P-Delta impact on the top displacement is very small. Even the large inelastic response in the shorter walls have very small impact on the top displacement.

4.5.3 Cross-sectional reinforcement ratio at the base

The amount of reinforcement in the RC shear wall cross-section and its impact on demand forces is usually represented by an over-strength factor. In A23.3 the over-strength factor is defined as nominal bending strength-to- demand ratio and is depended on the reinforcement ratio and the axial load in the shear wall cross section. This definition works well in force-based seismic design methodology; however, it is not easily applicable within the scope of DDBD because unique values of the demand bending moment is not available. For this reason, the impact of axial force and the section reinforcement at the base of the wall on the deformation response are studied separately.

In this respect, in this study the shear walls were categorised in three categories based on the percentage of the cross-sectional reinforcement (including the uniform and concentrated flexural rebar) ratio at the base of the wall:

- Light: $\rho < 0.60\%$
- Moderate: $0.60\% < \rho < 1.05\%$
- Heavy: $\rho > 1.05\%$

The minimum and maximum reinforcement ratio of the walls in this parametric study are 0.45% and 1.54%. Figure 4-21 shows the strong influence that the reinforcement ratio at the base section has on base curvature response. The trend is similar to that previously observed for axial compressive force. Base curvature demand increases as the reinforcement ratio decreases. The median curvature demand for 10-sotrey wall with light reinforcement is about two times the median curvature of the heavy reinforced cross sections. The base curvature for the shear wall with moderate and heavy reinforcement are relatively similar. The influence of the reinforcement ratio is much less pronounced for walls with 20 storeys and more.

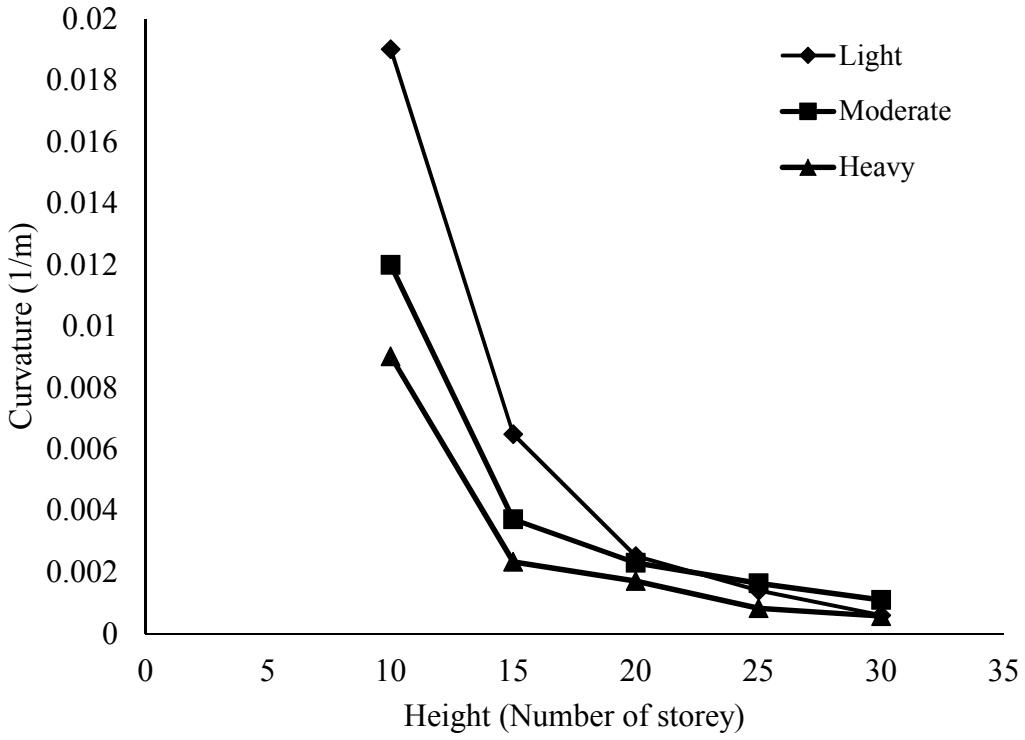

Figure 4-21: Comparison of the impact of the reinforcement ratio at the base on variation of base curvature against height.

As seen in Figure 4-22, the sections with light, moderate and heavy reinforcement show the similar top displacement response for walls exceeding 10-storey. For 10-storey walls, the sections with moderate reinforcement develop slightly smaller top displacement compared to the other walls This is contra intuitive as it would be expected that the shear walls with heavier reinforcement ratio should have smaller top displacement. This may be attributed to the fact that the shear walls with heavy reinforcement have more stiffness at the base and at the mid-height which limits the impact of the higher modes on the rotations and leads to first mode dominant deformation profile. Therefore, the heavy reinforced sections have smaller contribution from the higher modes on the deformation response which tend to slightly reduce the top displacement as they cause the top displacements in the opposite direction. Thus, the shear walls with heavier reinforcement ratio will end up having slightly larger displacement compared to the walls with moderate or low reinforcement ratios.

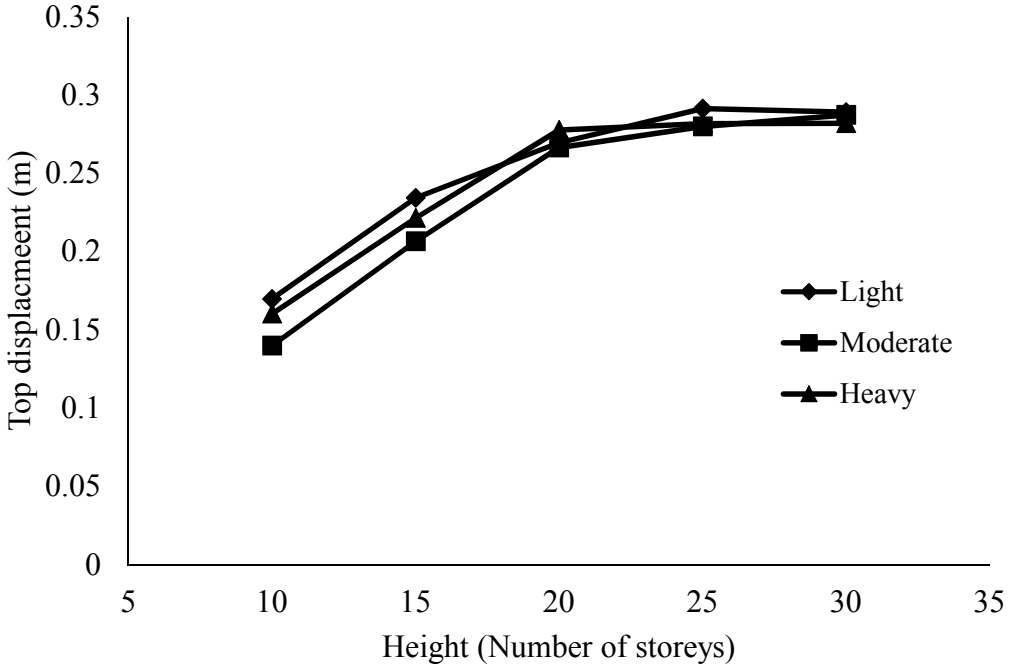

Figure 4-22: Comparison of the impact of the reinforcement ratio at the base on variation of top displacement against height.

4.5.4 Influence of fundamental period and wall aspect ratio

For fifty studied walls, which had the same height and length, three levels of seismic mass were considered to account for the variations in dynamic modal periods. As seismic mass is an essential parameter influencing the period of the shear wall, this is an indirect way to consider the impact of the fundamental period on base curvature and top displacement. It was previously mentioned that base curvatures and top displacements demonstrated more clear trends when they are plotted in function of height (number of storeys) than in function of fundamental periods.

For each wall, the original mass is scaled to 100%, 70% and 40%. In Figure 4-23 and Figure 4-24 the variation of the base curvature and top displacement against height are shown. The studied walls are designed according to FBD approach and have various reinforcement ratios at the base section and as the result various over-strength factors. As anticipated, the impact of the seismic mass on the displacement response is not significant. This is especially true for 25- and 30-storey shear walls. The impact of seismic mass on the base curvature is predictably higher, particularly for the 10- and 15-storey shear walls with large seismic mass (100%) for which the median base

curvature is about 20% larger than the median base curvature for the walls with 40% and 70% seismic mass. For these short shear walls, when the seismic mass increases to 100%, the inelastic base curvature is amplified. However, this amplification is not as significant as the impact of other previously discussed parameters.

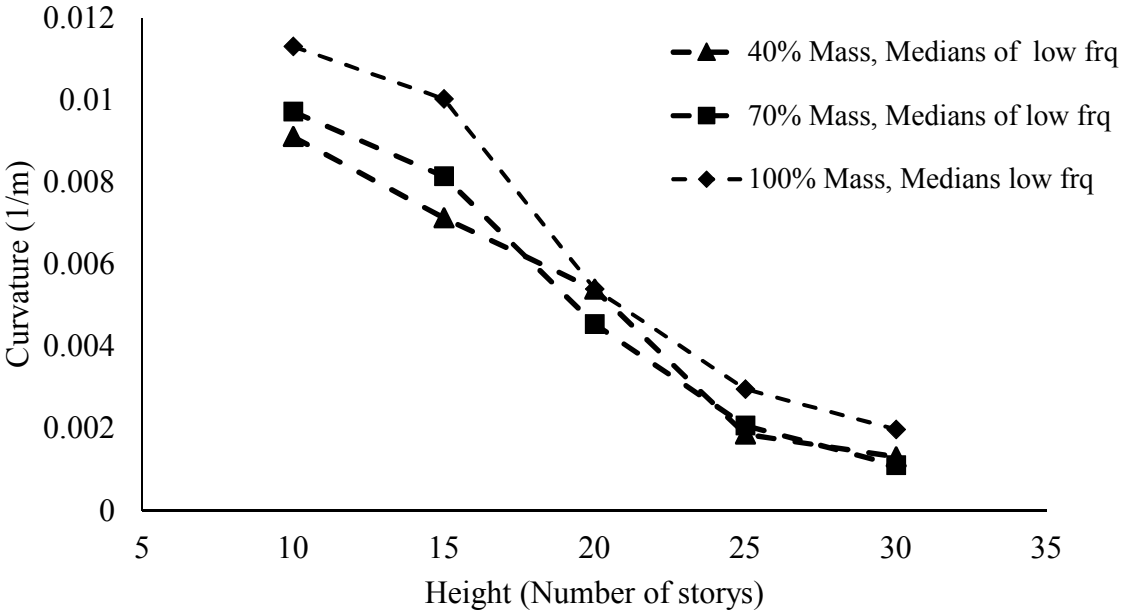

Figure 4-23: The impact of the seismic mass on the variation of base curvatures against height

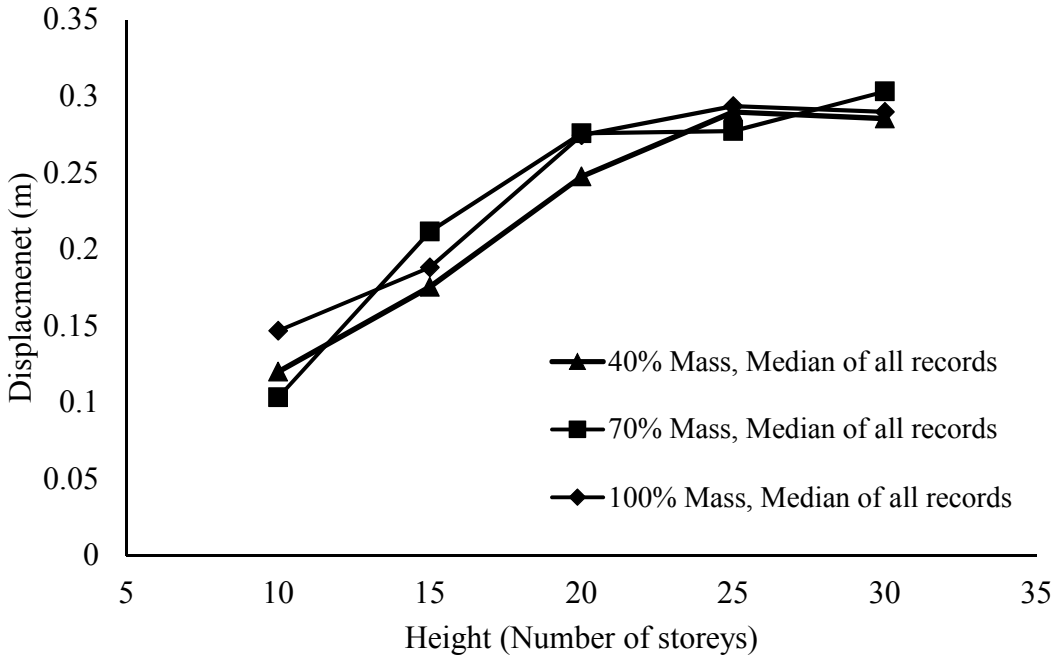

Figure 4-24: The impact of the seismic mass on the variation of top displacements against height

Another parameter which can be considered as potentially influential parameter is the geometrical wall aspect ratio (the ratio of the wall height over its length) which, for a given height, is the representative of the length of the shear walls. Designed walls were classified in three groups: low, moderate and large aspect ratios. Figure 4-25 and Figure 4-26 show the sensitivity of the base curvature and top displacement to the aspect ratios. Although the displacements of the walls with larger aspect ratios are slightly larger than those developed for the walls with smaller aspect ratios, this difference is negligible except for 10-storey walls. For 10-storey walls, the walls with larger aspect ratios show up to about 55% larger top displacement compared to the walls with smaller aspect ratios. In shear walls with smaller aspect ratios, that is larger length, the first mode is predominant in the displacement profile. Therefore, the top displacements are less impacted by the higher modes and are larger than the displacements of the walls with smaller aspect ratios. As anticipated, this effect is more significant for 10- and 15-storey shear walls for which inelastic response is observed. For taller walls with predominate elastic response the difference is very small. For similar reasons, the amplification of the base curvature for walls with larger aspect ratios is more significant compared to the walls with medium and low aspect ratios.

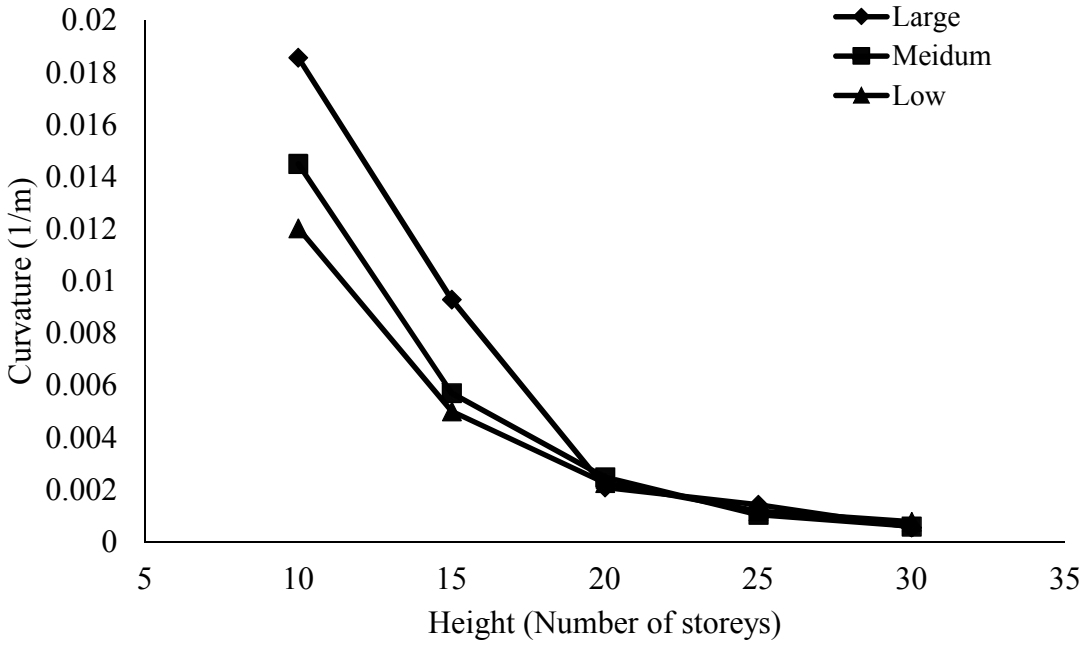

Figure 4-25: Impact of aspect ratio (h_w/l_w) of the shear walls on base curvature variation against height

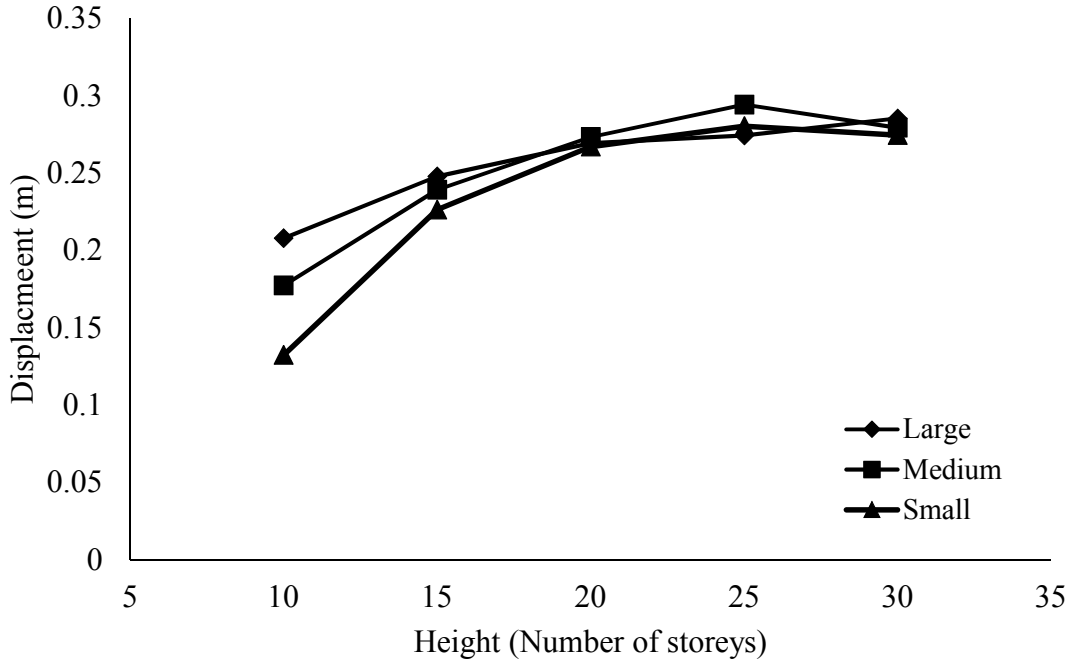

Figure 4-26 Impact of the aspect ratio of the shear walls on top displacement variation against height

4.6 Inter-storey drifts

Unlike the global drift, the maximum inter-storey drift of the walls does not significantly change with the height increase. However, for shorter walls with predominant inelastic response, the maximum inter-storey drift is slightly larger than that of the taller walls with predominant elastic response. The variation of the maximum inter-storey drift for every FB and DDB designed shear walls is shown in Figure 4-27. The maximum inter-storey drift occurred around the top of the shear walls and varied between 0.8% to 1% when the median response of all records is considered. Even when the response to the low frequency records is considered, the maximum inter-storey drift is under 1.05%, thus largely below the limits of 2.5% allowed by NBCC 2015.

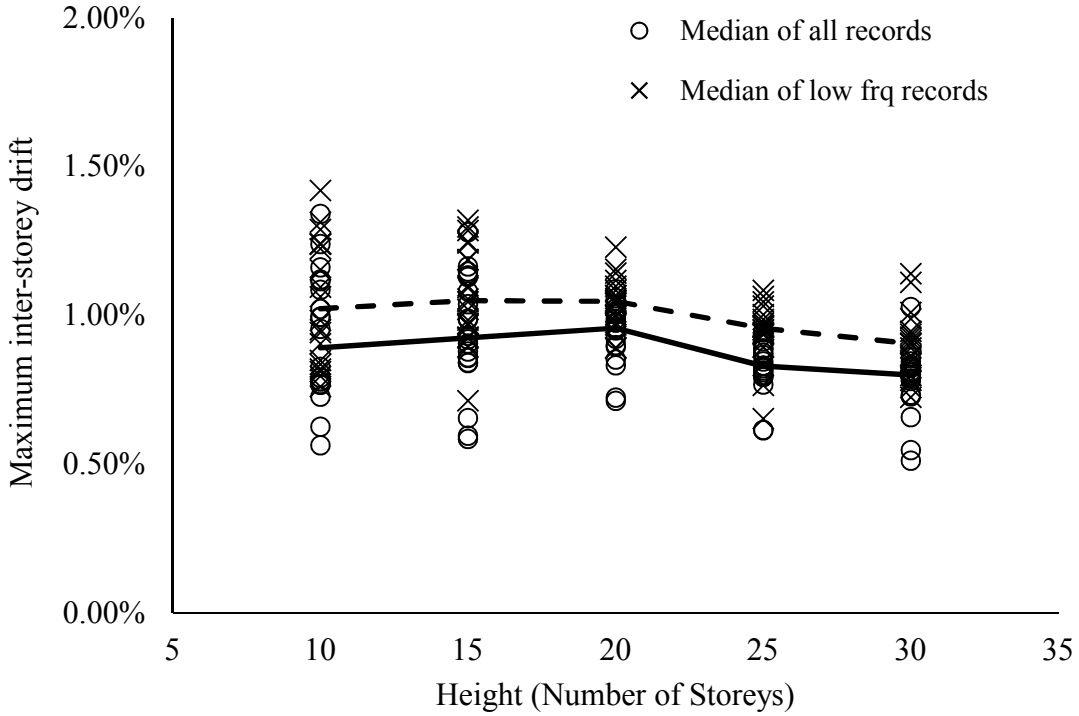

Figure 4-27: Maximum inter-storey drift of the shear walls versus their height. The maximum inter-storey drift normally occurs at the top storey of the shear walls

Figure 4-28 shows the correlation between the global and the inter-storey drift of all FB and DDB designed shear walls. The inter-storey drift from low-frequency record is larger compared to the response from all records by about 10 to 15% which is similar to the result observed for the global drift response. For 10-storey walls and less slender 15-storey walls, the maximum inter-storey drift occurred at the top storey. For slenderer taller walls, however, the maximum drift occurs at the storey just below the top storey.

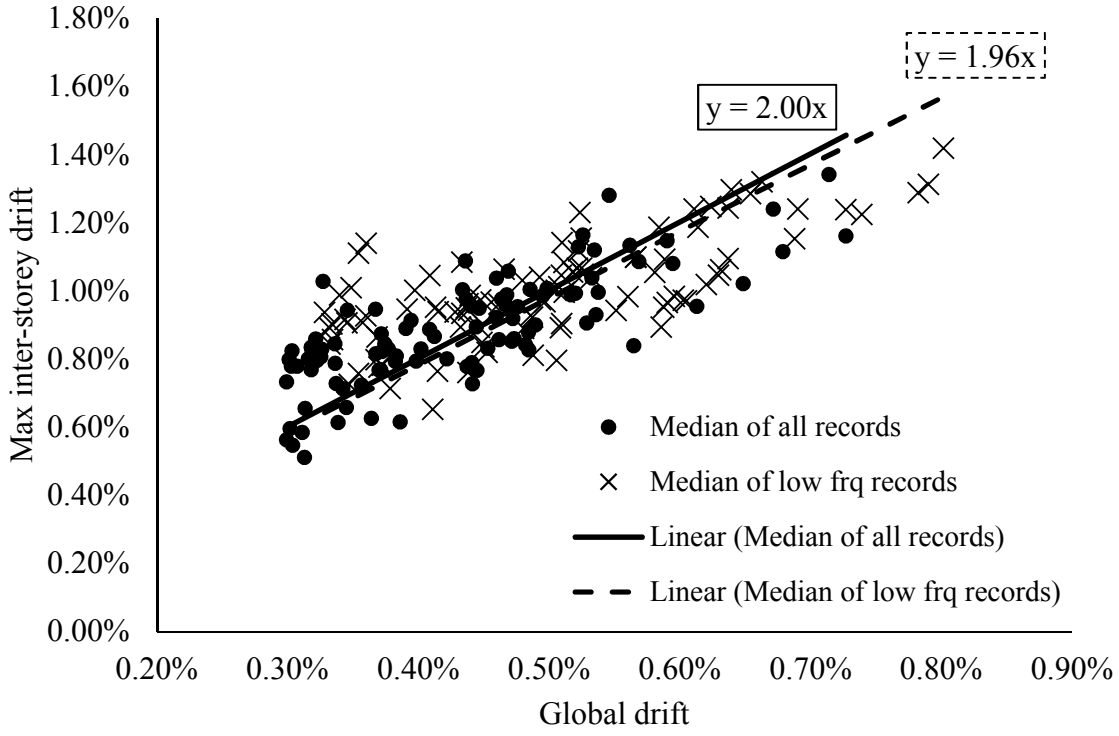

Figure 4-28: Maximum inter-storey drift versus the global drift

The trend of the ratios of maximum inter-storey drift to global drift is very similar regardless of the set of records considered. By passing a linear best fit through the existing data it is estimated that the maximum inter-storey drift is about two times the global drift for the shear walls under study.

4.7 Summary and conclusions

In this chapter, a parametric study on deformation response of shear walls, 10 to 30 storeys high was presented. The most important parameters that could impact the deformation of the shear walls were identified. The difference of response to simulated and historical ground motions records, and the choice of statistical values used to represent the deformation responses obtained for the set of selected ground motions were discussed. For this study, 109 shear walls were designed according to either FBD or DDBD approaches and their deformation response was studied through NTHA. Because of observed sensitivity of base curvature response, it was decided to use 84th percentile response to report the base curvatures and median response for the top displacements.

The deformation responses of the shear walls have a direct relation with the height of the shear wall. Although the fundamental period is a more representative parameter than height, it was noted that plotting the results against the height of the wall, more specifically in function of the number of storeys, makes the trends in base curvature and top displacement responses more clearly identifiable. On the other hand, it was shown that for shear walls with the same height and length, but with different seismic mass (i.e. different fundamental period) the response is not significantly different for the shear walls that exceed fifteen storeys.

Even though it was to use the ground motion records from stronger earthquakes compare to the available ground motions in eastern Canada, the deformation response to historical records was relatively smaller compared with the response to the simulated ground motion. This was more pronounced for the results obtained for the base curvature.

The response of the I-shaped walls and the rectangular shear walls with similar fundamental periods was comparable, with up to 10 percent scatter for the top displacement and up to twenty percent scatter for the base curvature. Although I shaped walls are not the focus of this study, it appears that for I-shaped walls (with fundamental periods around $2*T_a$ or more), the results of the study on rectangular shear walls would be applicable.

Both FBD and DDBD approach were overall unsuccessful in prediction of the base curvatures. This is particularly noticeable for very slender shear walls designed according to DDBD approach. On the other hand, both methods show a better level of accuracy to predict the top displacements. This is because the displacement is a less sensitive seismic responses compared to the base curvature. The FBD method show better predictions of top displacements for shorter shear walls (10-and 15-storey) whereas the DDBD approach gives satisfactory predictions for the taller shear walls (25- and 30-storey walls).

The magnitude of the axial compressive force supported by the shear wall has a considerable impact on the base curvature response for 10 and 15-storey shear walls that underwent highly inelastic response. The higher the axial force the larger base curvature at the base of the shear walls. The influence of the axial compressive force on the base curvature of taller walls (25- and 30-storey) is negligible. Due to relatively high stiffness on the shear systems, the P-Δ effects are very limited and the impact of the axial load on the top displacement is negligible.

Reinforcement ratio at the base section is another important parameter that influences the base curvature. Like the axial compressive loads, the impact of the reinforcement ratio is considerable for the shorter walls which show important inelastic response. Sections with heavier reinforcement tend to have deeper compression zone length and have smaller curvature demands. On the other hand, sections with reinforcement close to minimum required by A23.3 yield more quickly and have higher rotational demands. The impact of the section reinforcement content on the top displacements is minimal.

The results of the study showed that the maximum inter-storey drift of the shear walls have a direct relation with their top displacements. While both global and inter-storey drifts are under 2.5% limit by NBCC 2015, the maximum inter-storey drift for shear walls is approximately two times of the global drift.

CHAPTER 5 CALCULATION OF THE BASE CURVATURE FOR TALLER SHEAR WALLS AND THE APPLICATION TO DDBD

In previous chapter the important parameters which impact the base curvature and top displacement of a shear wall were identified and their influence on the deformation response was discussed. In this chapter, the results of the parametric study are used to estimate the relation between the base curvature and the top displacement of the shear walls located in eastern Canada.

5.1 The important parameters

It was seen in Chapter 4 that as the height of the studied shear walls increased, the top displacement also increased up to about 280mm for 20-storey wall. Further increase in height did not cause the augmentation of top displacement, its value remained constant for taller walls. However, with increase in height, the curvature demands at the base of shear walls reduced. This confirms that, contrary to the commonly used assumptions, the relationship between the top displacement and the base curvature is not linear. It was observed that the base curvature ductility for the 20-storey and taller walls is very small indicating that the global response of the shear wall can be considered as elastic.

The length, the height and the seismic mass of the shear wall are all indicative of its fundamental period. In the previous chapter the influences of the length and the seismic mass on the base curvature was examined as a function of wall height as it was observed that the main trends could be more easily identified. Although it was shown that the base curvature shows a better trend when it is only compared versus height, the fundamental period can still be a good indicator of the length of and mass for the walls with the same height.

For shorter shear walls, especially the 10-storey walls, further parameters such as axial load and reinforcement ratio in the plastic hinge region play important roles. The values of inelastic curvature, for 10- and 15-storey shear walls were significant and specially for 10-storey shear walls a significant scatter of results was observed, particularly because of the response to low frequency ground motion records. Thus, the median curvature response for the low frequency records was retained to permit to define an upper bound estimation for the base curvature.

5.2 The relation between the base curvature and the top displacement

In this study, the base curvature and the top displacement were related through the coefficient β. This coefficient could be used within the scope of FBD and DDBD methods to estimate the base curvature, φ_b, from the calculated top displacements, Δ_t. In general, β can be defined in function of height (N), fundamental period (T_1), axial compressive load (P_f) and reinforcement ratio (ρ) at the base of the wall. Note that the height of the shear wall is represented in terms of the number of stories (N).

Equation 5-1 $$\beta\left(N, T_1, P_f, \rho\right) = \frac{\varphi_b}{\Delta_t}$$

In this equation, φ_b is base curvature and Δ_t is the top displacement of the shear walls. The top displacement, Δ_t, represents the median top displacement obtained from NTHA for the complete record set, which as discussed in Section 4.4.4 has a good match with FBD and DDBD top displacement predictions. On the other hand, to cover for the sensitivity of the curvature response, base curvature, φ_b , is based on median response to the low frequency records.

Equation 5-1 is similar to the proposed equation from Dezhdar (Equation 2-2) if *C* replaced with ($\beta * h_w * l_w$). Although, β and *C* are functions of very different parameters. The study by Dezhdar (2012) focused on the seismic events in western Canada, and because the earthquakes of those regions are much stronger than those in eastern Canada, and the ground motion frequencies content is different, the response of the shear walls in that study is largely inelastic and the governing parameters are different. According to Dezhdar coefficient *C* is a function of height and force reduction factor, has an inverse relation with the force reduction factor and a direct relation with the height of the shear wall. Accordingly, for a shear wall with constant length the increase in height and reduction in the force reduction factor, which normally occurs when the height increases, should lead to larger base curvature. In the previous chapter it was shown that, in eastern Canada, the impact is completely opposite to that argued by Dezhdar; an increase in wall height causes a significant reduction in the base curvature demand.

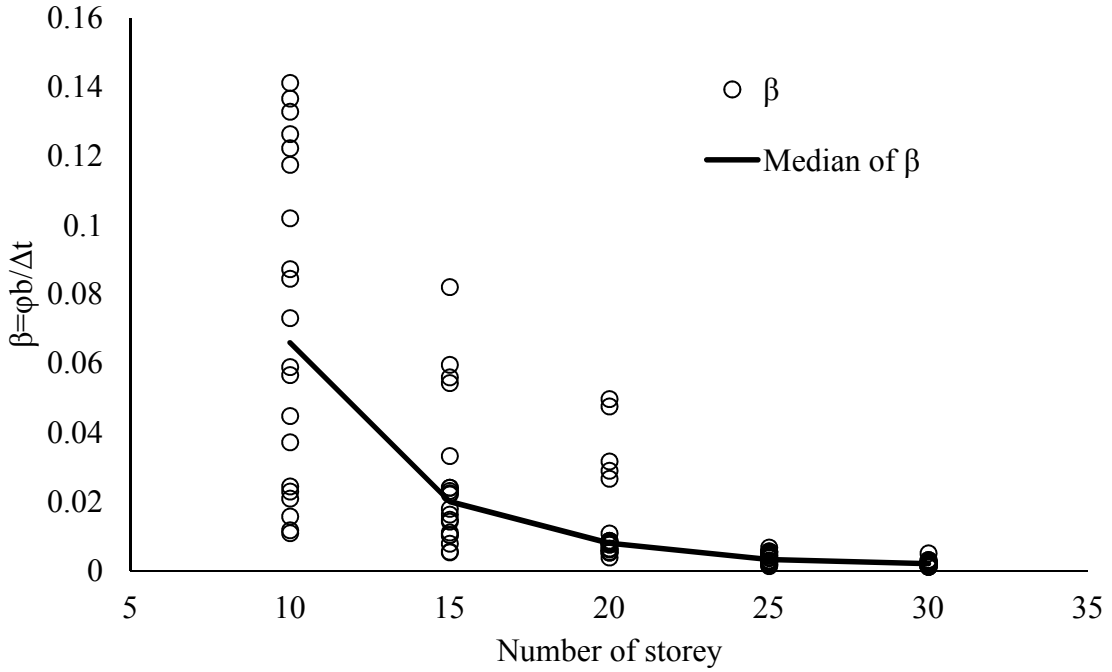

Figure 5-1: Variation of β against height

Figure 5-1 shows the variation of the coefficient, β, with height for each of the rectangular shear walls studied in Chapter 4. A similar trend as the one observed for the base curvature can be seen on this figure. As the height increases, the displacement reaches a constant maximum value, while the base curvature demands reduce and therefore the coefficient β also reduces. The scatter of β for 10-storey walls is significant and clearly indicates that for that wall height additional modification parameters need to be applied to reflect the impact of the axial compressive force and reinforcement ratio.

5.3 Estimation of β to relate the base curvature to the top displacement

It was shown that height is a main parameter with significant impact on the base curvature of shear walls. However, for shorter walls other parameters like the amount of axial stress, fundamental period and reinforcement content of the section are also important. The impact of the seismic mass and wall aspect ratio are both included in fundamental period of the walls.

To develop an equation to estimate β, the impact of each of the important parameter was studied. From the data presented in Chapter 4, it was concluded that the reinforcement ratio and axial load

does not have major influence on β for 20-storey and taller walls. On the other hand, axial load and reinforcement ratio are influential parameters on the base curvature for 15-storey and shorter shear walls. The study presented in Chapter 3 showed that in terms of the global response, the 17-storey shear wall in Montreal was just on the boundary between the elastic and the inelastic domain. Therefore, it appears reasonable to set the 17 storeys height (around 50m) as the point from which the global response of the shear wall becomes predominantly elastic. Accordingly, we can say that the equations to estimate β coefficient should consider the impact of height on fundamental period for all wall heights and additionally include the factors to account for the influence of axial compressive load and reinforcement ratio for shear walls under seventeen storeys.

To develop an equation for β, statistical regressions were done to find the relation of each key parameters and β. In this approach, first the most evident pattern of the variation of β, which is the variation against number of stories, was studied and, by regression, a base equation in function of number of storeys was derived. Then for walls with the same height, axial load ratio and reinforcement ratio, the variation of β against the fundamental period was studied. By averaging the patterns for different cases, an equation was proposed for the period-related modification coefficient (α_1). Since the impact of axial load and reinforcement ratio at the base was only critical for the 10- and 15-storey walls, for these walls the variation of β against the axial load and reinforcement ratio was studied while other parameters (height and fundamental period) were kept constant. Similar to the method used to estimate α_1, two other modification factors, α_2 and α_3, were proposed to consider respectively the impact of axial load and reinforcement ratio on β.

The final equation was derived by combining the base equation and the modification factors. The equations for the modification factors were then calibrated to give the best match with the values of β obtained from the parametric study. The final proposed functions are:

Equation 5-2-a $$\beta = 0.10 * \alpha_1 * \left({}^{1}/_{N}\right)^{0.1} * e^{-0.15N} \geq 0.001$$

For shear walls under 17 storeys the equation above shall be modified as the following:

$$\beta = 0.10 * \alpha_1 * \alpha_2 * \alpha_3 * \left({}^{1}/_{N}\right)^{0.1} * e^{-0.15N} \geq 0.005$$

In equations above α_1, α_2 and α_3 are defined as:

Equation 5 2-b $$\alpha_1 = (0.735 * T_1 - 0.103 * (\frac{10}{N}) \geq \ 1.0$$

$$\alpha_2 = \frac{P_f}{f'_c * A_c} * 20 - 0.6 \geq 1.0$$

$$\alpha_3 = (2.4702 - 146.835 * \rho) \geq 1.0$$

In above equations N is the number of stories, T_1 is the fundamental period of the shear wall, ρ is the reinforcement ratio, P_f is the axial compressive force at the base of the wall, f'_c is the ultimate compressive strength of concrete and A_c is the gross area of the RC section at the base of the wall.

Equation 5-1and Equation 5-2 were applied to the shear walls studied in Chapter 4 to compare prediction of base curvature obtained by current FBD and DBDD design approach and the proposed relationship. The results obtained from the proposed relationship are plotted against NTHA results in (b) the comparison in a smaller range of curvature (0 to 0.005 1/m)

Figure 5-2 (a) and (b). Note that (b) the comparison in a smaller range of curvature (0 to 0.005 1/m)

Figure 5-2 (b) shows the results in a narrower curvature range (0 to 0.005 1/m) which covers the base curvature values for most of the shear walls considered in the parametric study. The comparison of this graph with the graph shown in Figure 4-12 demonstrates the impact of using the proposed equation in comparison with the current FBD and DDBD predictions. The comparison clearly shows an improved prediction of the base curvature, particularly for shear walls with 20-stories and more. For 10- and 20-storey walls, especially the very slender ones designed according to DDBD, the proposed equation still underestimates the base curvature compare to NTHA results. However, it gives much better results compared to current FBD and DDBD predictions. It should be noted that for these shear walls, with high inelastic response, the scatter of curvature is significant, especially for low frequency records. This makes it challenging to establish a sufficiently accurate estimation of the base curvature. Additionally, when we compare the predictions of the proposed equation with NTHA outputs it should be noted that using the median base curvature only from the low frequency records is already a conservative approach for estimation of the curvatures. The under-estimation of the base curvatures should be seen along these assumptions.

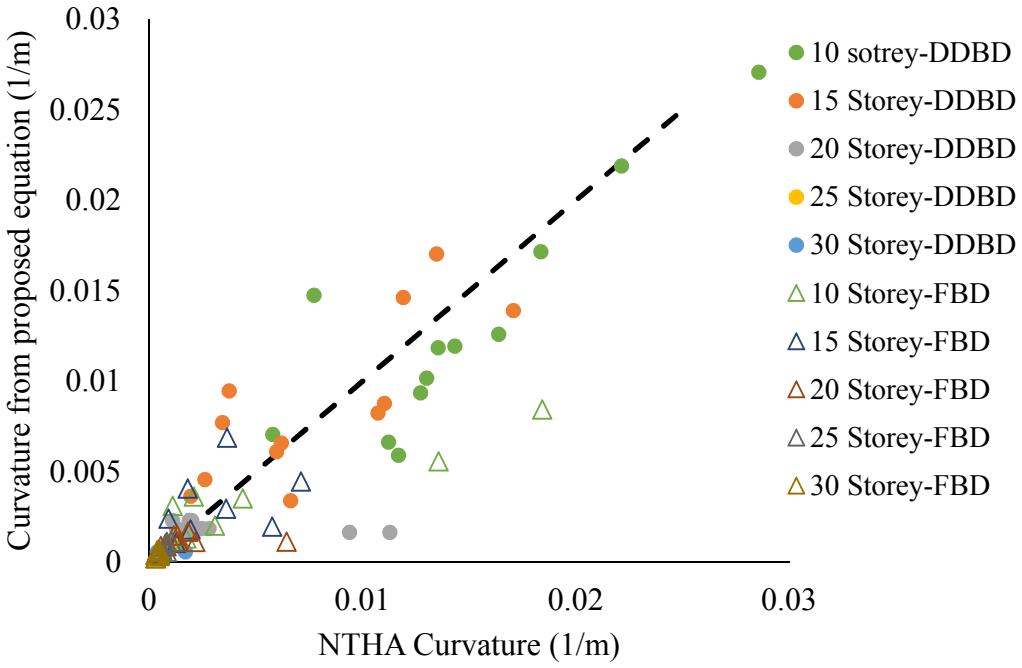

(a) the comparison in larger range of curvature (0 to 0.031/m)

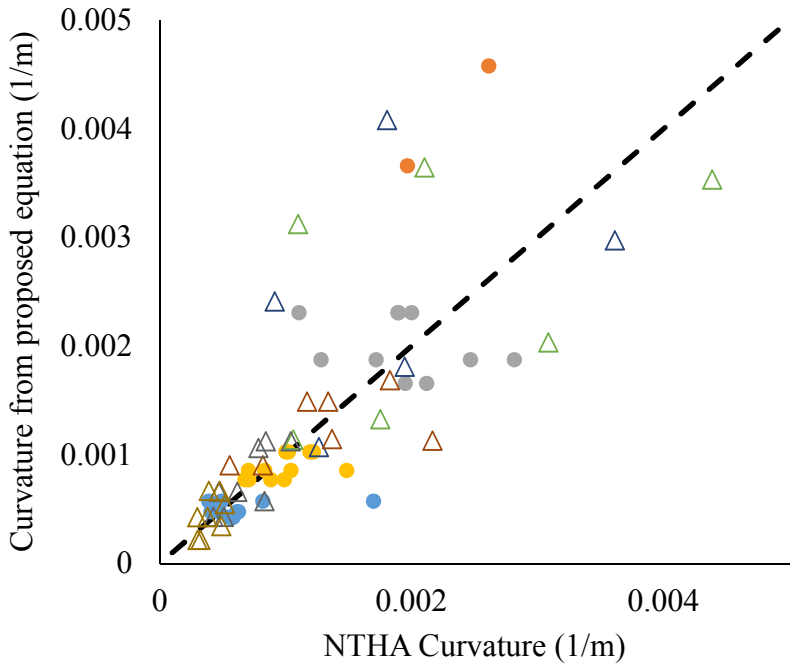

(b) the comparison in a smaller range of curvature (0 to 0.005 1/m)

Figure 5-2: The predicted base curvature from Equation 5-2 versus NTHA

The ratios of the base curvature predictions from NTHA to the proposed equation, and also to those obtained when FBD and DDBD predictions are considered, are shown in Figure 5-3. The ratio

when the FBD and DDBD predictions are used varies between 0.42 for a 30-storey FB designed wall to 24.2 for a 10-storey DDB designed wall. On the other hand when Equation 5-1and Equation 5-2 are used the ratio varies 0.41 for a 15-storey FB designed wall to 2.43 for a 10-storey FB designed wall.

Figure 5-3-a shows the significant improvement when the proposed equation is used, specially for DDB designed walls. Also, as seen in Figure 5-3-b, the proposed equation reduces the over-estimation of the base curvature by FBD approach for the taller 25 and 30-storey shear walls. By using of the proposed equation, the overestimation of the base curvature for FD designed walls reduce from 85% to 33% for 25-storey and from 120% to 40% for 30-storey shear walls. However, overall, the impact of using the proposed equation on improvement the prediction of base curvature DDB designed walls are more significant than FB designed walls.

As previously discussed, the scatter of the results for 10 and 15-sotrey shear walls is much larger compared to the taller walls. For 20-storey and above, however, overall the scatter of ratios is between 0.5 and 1.5 and show a good distribution of the data according to the proposed equation.

According to Figure 5-3, to have an upper bound for the evaluation of the base curvature, the results of Equation 5-2 can be approximately amplified two times. This upper bound would cover the base curvature for almost all the design cases except few 10 and 15-sotrey shear walls with very high demands which is a reasonably acceptable estimation. However, by using the upper bound limit, the base curvature could be over-estimated by up to 3 times. Although the magnitude of error for the proposed equation might sound significant, however, it is much smaller than the error from FBD and DDBD approaches.

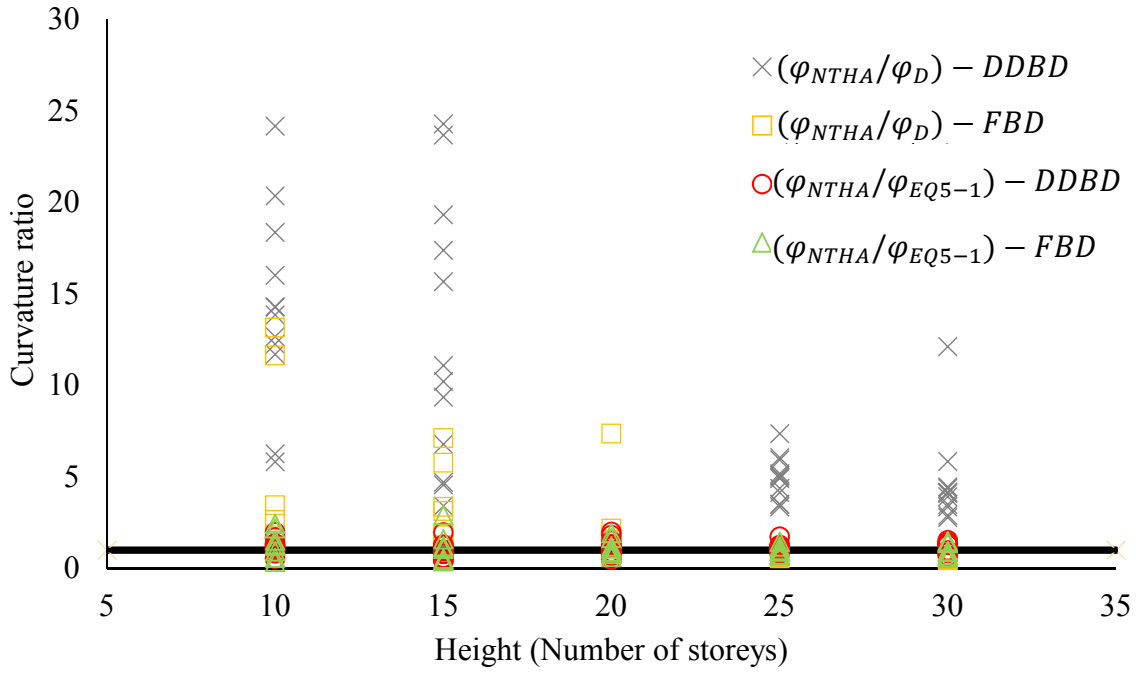

(a) for all walls with the ratios up to 25 and

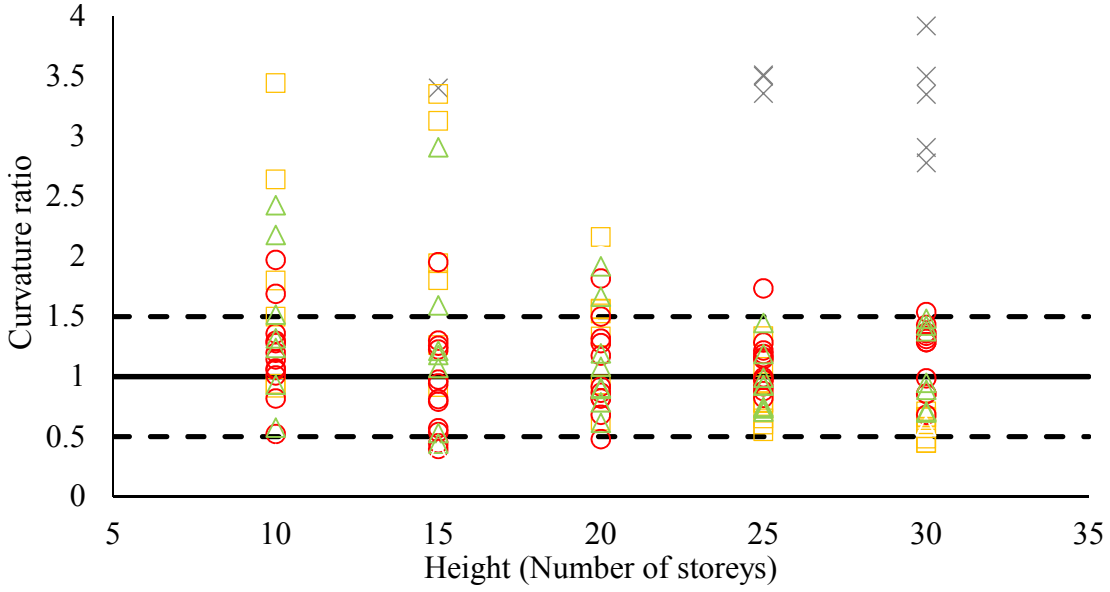

(b) for walls with for ratios under 4

Figure 5-3: Ratio of the base curvature from NTHA to the base curvature from the proposed equation and base predicted base curvature by FBD or DDBD

5.4 Design examples

To further examine the applicability of the developed equation, additional nine shear walls with different geometry and seismic mass were designed and their deformation response was investigated. All shear walls are designed according to NBCC 2015 and CSA A23.3 force-based method. The shear walls were assumed to be the seismic force resisting system of a 30m x 30m office building. In each direction four rectangular shear walls located on the edges of the buildings provide resist seismic loads. The axial compressive force on each shear wall is assumed to be $0.1f'_cA_c$. To investigate the applicability of the proposed equation for the cases of high curvature demand on the wall which was achieved by minimizing the over-strength of the section at the base for each wall height, except for 15-storeys wall, in addition to the calculated seismic mass based on the described geometry, a second shear wall with an amplified seismic mass was designed. Because of the larger seismic mass, these walls have longer fundamental period and their over-strength factors at the base are very close to the minimum value considered in A.23.3 ($\gamma_{w\text{-}min}$=1.3). The shear walls are analyzed using RSA with inclusion of the accidental torsion according to NBCC 2015.For each wall β is calculated and then applied to the predicted displacement obtained by multiplying the result from RSA by R_oR_d. The results are summarised in the Table 5-1.

Depending on the wall considered, the RSA top displacements up to 29% smaller to 40% bigger compared to the NTHA median results. Curiously, the smallest and largest absolute difference between the design predictions and NTHA are both obtained for 30-storey shear walls (-4% and 40%). For other walls, the design displacements are, for most cases, smaller than NTHA and vary between -29% and +6%. On the other hand, FBD approach results in overestimated base curvature ranging from 23% for 20-storey walls up to 327% for 30-storey shear walls. For two 10-storey shear walls, FBD approach yields to underestimated base curvature (-10% and -30% for wall I and II respectively). Compared to NTHA result, the base curvature estimation error largely increases for the taller, 25- and 30-storey shear walls.

Table 5-1: Design information, displacement and curvature predictions for the example shear walls from FBD method, NTHA and the proposed equation

#	10-Storey		15-storey	20-Storey		25-storey		30-storey	
	I	II	III	IV	V	VI	VII	VIII	IX
Height (m)	30	30	44.75	59.5	59.5	74.25	74.25	89	89
Length (m)	6	6	7	8	8	8	8	8	8
Thickness (mm)	300	300	400	350	350	500	400	500	400
Fundamental period (sec)	1.64	2.01	2.44	3.74	4.58	3.95	5.41	4.74	6.49
Over-strength (γw)	1.92	1.47	2.5	1.89	1.47	2.83	1.59	2.82	1.4
$\varphi_y=2\epsilon_y/l_w$	0.00067	0.00067	0.00057	0.00050	0.00050	0.00050	0.00050	0.00050	0.00050
Δ_{FBD} (m)	0.10	0.08	0.13	0.20	0.20	0.22	0.24	0.25	0.39
Δ_{NTHA} (m)	0.11	0.11	0.13	0.24	0.25	0.26	0.23	0.26	0.28
$(\Delta_{FBD}-\Delta_{NTHA})/\Delta_{NTHA}$	-9%	-29%	-0.15%	-17%	-23%	-16%	6%	-4%	40%
φ_{FBD}	0.00233	0.00207	0.00181	0.00176	0.00187	0.00158	0.00158	0.00135	0.00189
$\mu\varphi_{\_FBD}$	3.49	3.11	3.17	3.53	3.74	3.16	3.16	2.70	3.79
φ_{NTHA}	0.00259	0.00294	0.00100	0.00107	0.00152	0.00051	0.00105	0.00032	0.00045
$\mu\varphi_{\_NTHA}$	3.89	4.42	1.75	2.15	3.04	1.03	2.10	0.63	0.89
$(\varphi_{FBD}-\varphi_{NTHA})/\varphi_{NTHA}$	-10%	-30%	65.00%	64%	23%	207%	50%	327%	325%
β	0.0398	0.0497	0.0091	0.0049	0.0060	0.0019	0.0026	0.0013	0.0017
φ_{EQ}	0.00382	0.00404	0.00116	0.00098	0.00121	0.00041	0.00121	0.00031	0.00043
μ_{φ_EQ}	5.73	6.06	2.03	1.96	2.41	0.83	2.41	0.62	0.86
$(\varphi_{EQ5\text{-}1}-\varphi_{NTHA})/\varphi_{NTHA}$	47%	37%	16%	-9%	-21%	-19%	15%	-3%	-3%

*The negative values indicate underestimation compare to NTHA results

When Equation 5-1and Equation 5-2 are used to estimate the base curvature, the results differ between -21% to +47% from NTHA. The largest difference is recorded for 10-storey shear walls (37% and 47% over-estimation) and the smallest difference is for 30-storey shear wall (3% under-estimation). It should be noted that the Equation 5-2 is applied to the displacements estimated obtained from FBD methodology and the difference between the FBD displacements and those from NTHA influences resulting curvature estimates. Therefore, certain level of discrepancy is inevitable in comparison of the base curvatures. Nevertheless, the variance of the results of the proposed equation compared to NTHA is in 50% range, which was previously observed in Figure 5-3-b.

5.5 Application to DDBD approach

5.5.1 General discussion

In Chapter 3 it was mentioned that the DDBD approach predicted elastic response for tall shear walls in eastern Canada. This can be directly concluded by comparing the yield displacement of the ESDF system against the maximum spectral displacement: if the yield displacement of the ESDF system surpasses the maximum spectral displacement a predominantly elastic behaviour is anticipated. According to Equation 3-8, the yield displacement of the ESDF system is only related to length and effective height of the shear wall. If the mass and stiffness are uniformly distributed, the effective height of the system depends only on the height of the shear wall. Therefore, in the context of DDBD approach, the basic parameters necessary to predict whether the response is elastic or not are the length and height of the shear wall. The parametric study presented in Chapter 4 showed that for many of DDB designed shear walls, the base curvature ductility exceeded one, nevertheless the comparison of yield and maximum spectral displacements suggested the elastic wall response. Thus, it is possible that the prediction of the type of response (elastic or inelastic) based on the assumptions adopted in the current DDBD approach could be inaccurate and need to be improved.

In addition to the potential inaccuracy to predict the nature of response, other shortcomings of DDBD method, addressed in Chapter 3, make the use of DDBD to design of tall structural walls impractical. According to DDBD, when an elastic response is predicted for the shear wall, the design forces are not unique. As long as the minimum stiffness is provided to control the global

drift, any design scenario could be acceptable. Such reasoning could be problematic. It was seen in Chapter 3 that, in this way, the design shear forces are likely to be underestimated leading to inadequate shear capacity of the section. Since the concept of DDBD is based on the response in the first dynamic mode, an accurate estimation of the higher mode impact on the shear forces is essential. In the study presented in Chapter 3, the impact of higher modes on the elastic shear amplification was considered by applying the factor M_v defined in NBCC. The comparison with NTHA results showed that using the shear amplification factor (M_v) was not adequate for the wall with elastic response located in Montreal.

One important advantage coming from the use of Equation 5-1and Equation 5-2 for curvature predictions is that it permits the prediction of the response based on the level of local ductility. This is especially useful for tall RC shear wall structures in eastern Canada for which the current FBD and DDBD approaches do not provide accurate predictions and many parameters may impact the response. Since Equation 5-2 is tailored for the response of the shear walls in eastern Canada, it would give less conservative predictions. However, to account more appropriately for higher mode amplification, further investigations are necessary. This subject is discussed in the following section.

5.5.2 Elastic shear amplification due to higher modes for using with DDBD

To investigate the elastic shear amplification due to the higher modes, twenty shear walls are designed according NBCC 2015 FBD approach and analysed using RSA. The elastic shear amplification due to higher mode effect is derived by dividing the base shear obtained considering ten modes (with more than 90% cumulative mass participation) to the base shear obtained considering only the first mode of response. In addition to the elastic shear amplification, the bending moment amplification due to the higher modes is derived using the same procedure.

The design information for the studied walls as well as the values of obtained shear and bending amplification factors are given in Table 5-2. It is noted that similarly to what is suggested by NBCC 2015, as the first fundamental period increases, the higher mode shear amplification also increase. However, as seen in Figure 5-4, there is a significant difference between the values of shear amplification factor obtained from NBCC and those obtained from RSA analysis for the studied walls. For Montreal, the maximum amplification factor by NBCC 2015 ($M_{v\text{-}NBCC}$) is limited to 3.21 at T=5s. On the other hand, the analytical shear amplification factor for the studied walls ($M_{v\text{-}}$

$_{analytical}$) varies between 1.85 to 5.19. The code limits indirectly the higher mode amplification factors by limiting the period of the shear wall structures to two times the empirical value ($2T_a$, $T_a=0.05h_n^{0.75}$). Consequently, as shown in Table 5-2, the shear amplification factor for the 30-sotrey shear walls is to that corresponding to $2T_a$=2.93s, and not their first periods which range between 4.05s to 6.41s. As a result, for 30-storey shear walls $M_{v\text{-}NBCC}$=2.05 while $M_{v\text{-}analytical}$ varies between 3.33 to 5.25. The results also show that the amplification of bending moments differs significantly from that defined for the shear forces. For the studied walls, amplification of the bending moment due to the higher modes $M_{m,}$ varies between 1.09 for a 10-storey to 1.56 for a 30-storey wall, while according to NBCC the increase in bending moments due to higher mode effects would be identical to that defined for the shear forces. The idea of using separate shear (M_v) and bending (M_m) amplification factors was suggested by Filiatrault et al. (1994) and is presently used in New Zealand NZS 1170.5 code. In NBCC 2015, on the other hand, coefficient J is applied that modifies the distribution of the amplified base shear along height to achieve more realistic values of the bending moment along the height of the structure.

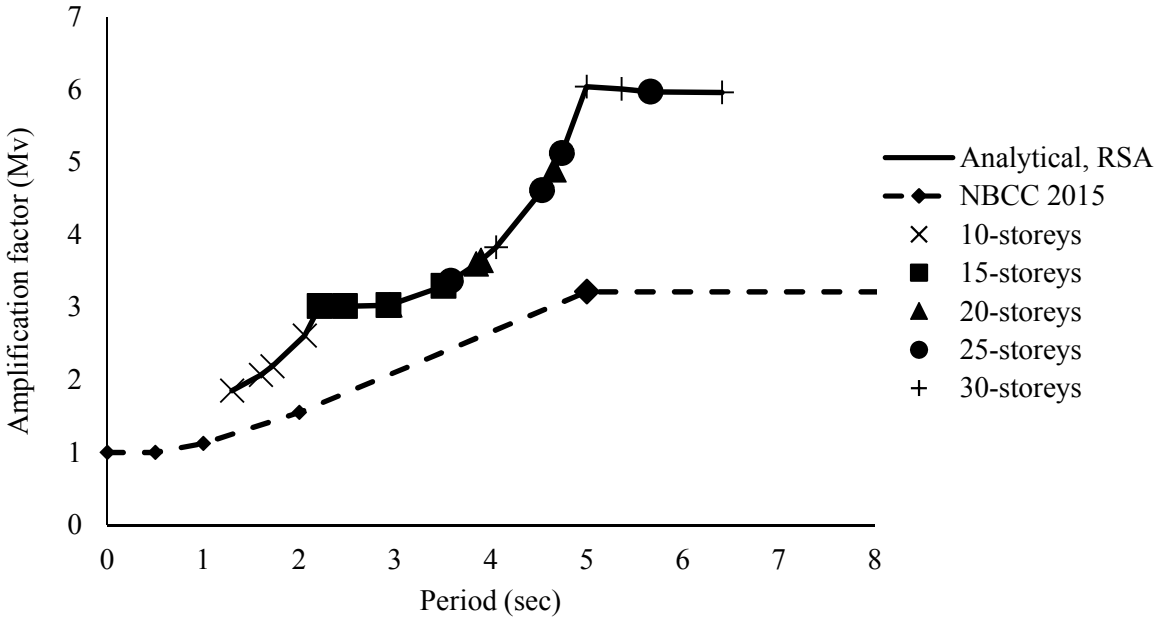

Figure 5-4: Elastic shear amplification variation against the shear wall period

Table 5-2: The design information of the walls used to study the elastic higher mode impact on shear and bending moment

No. of Stories	10				15				20				25				30			
$l_{w\,(m)}$	6	6	6	5.5	7	7	7	6.5	8	8	8	7	9	9	9	8	10.5	10.5	10.5	10.5
$t_{w\,(m)}$	350	350	350	300	350	350	350	350	400	400	400	350	450	450	450	400	450	450	450	450
T_1 (sec)	2.06	1.30	1.72	1.60	3.50	2.22	2.93	2.48	4.66	2.94	3.90	3.85	5.66	3.58	4.74	4.53	6.41	4.05	5.36	5.00
$2*T_a$ (sec)	1.30	1.30	1.30	1.30	1.75	1.75	1.75	1.75	2.17	2.17	2.17	2.17	2.56	2.56	2.56	2.56	2.93	2.93	2.93	2.93
M_f (kNm)	31436	15450	24349	14405	52306	22312	38563	22243	66967	33868	53407	30733	95945	49650	71896	42799	135731	67018	97347	56005
M_c (kNm)	35174	35174	35174	15519	55587	49400	49400	24975	69125	62368	62368	31392	97207	93352	93352	45773	136005	136005	136005	63518
γ_w	1.30	2.65	1.68	1.30	1.30	2.61	1.51	1.30	1.30	2.16	1.37	1.30	1.30	2.19	1.51	1.30	1.30	2.39	1.65	1.30
V_f (kN)	2695	1078	1886	1078	3274	1310	2292	1310	3823	1529	2676	1529	4807	1923	3365	1923	5802	2321	4062	2321
V_d (kN)	5255	2322	4063	1957	6162	2821	4937	2478	6930	3294	5486	2649	8521	4141	7247	3477	10289	4999	8748	4445
Stability Index	0.05	0.05	0.06	0.06	0.08	0.06	0.07	0.06	0.07	0.08	0.07	0.08	0.08	0.07	0.07	0.07	0.10	0.06	0.07	0.06
$M_{v\,(analytical)}$	2.61	1.85	2.19	2.07	2.87	2.62	2.63	2.62	4.26	2.64	3.17	3.13	5.19	2.93	4.45	4.01	5.18	3.33	5.23	5.25
$M_{m\,(analytical)}$	1.19	1.09	1.13	1.11	1.20	1.19	1.18	1.18	1.40	1.18	1.24	1.23	1.52	1.21	1.43	1.36	1.47	1.26	1.54	1.56
$M_m/M_{v\,(analytical)}$	0.46	0.59	0.52	0.54	0.42	0.45	0.45	0.45	0.33	0.45	0.39	0.39	0.29	0.41	0.32	0.34	0.28	0.38	0.29	0.30
$M_{v(@2*Ta)}$ (NBCC-2015)	1.19	1.19	1.19	1.19	1.37	1.37	1.37	1.37	1.62	1.62	1.62	1.62	1.82	1.82	1.82	1.82	2.05	2.05	2.05	2.05
$M_{v(@2*Ta)}$ (NBCC-2010)	1.04	1.04	1.04	1.04	1.30	1.30	1.30	1.30	1.58	1.58	1.58	1.58	1.64	1.64	1.64	1.64	1.71	1.71	1.71	1.71

Study reported in Chapter 3 showed that through the design according to NBCC FBD method, a combination of the conservative minimum limits imposed on the design period and design base shear, the assumption that the ductility foreseen in design fully develops as well as the shear amplification factors accounting for higher mode effects yielded adequate prediction of the shear forces along the height of shear walls both in Vancouver and Montreal. In other words, the M_v factors provided in NBCC are tailored to give reasonably accurate shear forces in combination with other design limits and are not a direct and true representation of the shear amplification caused by the higher mode effects. On the other hand, the study in Chapter 3 showed that for DDB designed shear walls and especially the wall in Montreal, applying uniquely M_v factor did not result in adequate estimation of the shear forces and the design base shear was underestimated. Therefore, using M_v factors determined from RSA ($M_{v\text{-analytical}}$) to account for higher mode impact on shear forces seems more appropriate and justifiable within the scope DDBD method.

5.5.3 Modified DDBD procedure for taller walls in eastern Canada

Following the conclusions made in previous sections, the DDBD approach that was presented in Chapter 3 can be modified to achieve better design predictions for taller shear walls in eastern Canada. As discussed in previous sections, two main objectives should be considered in design of the tall shear walls in this region: (i) the level of inelastic response must be accurately estimated, and the design strategy accordingly adjusted and (ii) Attaining safe design forces for designing the RC shear wall sections.

To achieve these objectives, the steps of DDBD procedure outlined in Chapter 3 can be modified taking into account the observation made in this study. The proposed procedure is adapted for DDBD of mid-height and tall shear walls regardless of the level of seismicity considered in design. However, the procedure is particularly applicable for DDBD of the taller RC shear walls for which elastic or limited inelastic seismic response is likely to occur. Main steps of the proposed procedure are outline below:

1. **Determine the design displacement profile**: To determine the design displacement an assumption shall be made regarding the geometry of the shear wall. The top displacement shall be estimated as minimum of the following variables; the top displacement related to the maximum curvature of the section at the base, Δ_{t1}, the top displacement related to the maximum inter-storey drift, Δ_{t2}. According to the findings of the parametric study in Chapter 4 the

maximum inter-story drift is approximately two times of the global drift. Based on the information in Chapter 4 and this chapter the following equations are proposed to determine the design displacement.

Equation 5-3 $$\Delta_t = \min(\Delta_{t1}, \Delta_{t2})$$

$$\Delta_{t1} = \frac{\varphi_{max}}{\beta}$$

$$\Delta_{t2} = \frac{DRIFT_{max}}{2} * H_n$$

In these equations φ_{max} is the maximum allowable curvature at the section at the base of the wall. β is the relating coefficient as defined in Equation 5-2, $DRIFT_{max}$ represents the maximum allowable inter-storey drift which can be considered equal 2.5% according to NBCC for building with normal importance. Depending the performance level other limits for the maxium drift can be used. And H_n is the height of shear wall.

φ_{max} could be defined according to CSA A23.3 as $\varphi_{max} = \epsilon_{cu}/c$, where ϵ_{cu} is the ultimate compressive strain of concrete and c is an estimated maximum compression depth based on the anticipated the level of inelasticity. This value can be conservatively considered as $0.3l_w$ which is the limit of compression depth for moderate ductile shear walls in CSA A23.3 (Adebar et al, 2005).

If the shear wall is less than 17 storeys tall (about 50 m), assumptions shall be made regarding reinforcement ratio at the base. This assumed value will be confirmed through an iterative procedure. For shear walls taller than 17-storey β is independent of the reinforcement ratio.

2. **Transform the shear wall to a ESDF system and calculate the design displacement:** As described in the Section 3.2(b), the shear wall should be transformed to an ESDF system. The design displacement (Δ_{ed}) of the ESDF system shall be derived from Equation 3-5, but it can not be larger than $\Delta_{max,\xi=5\%}$ which is the maximum spectral displacement with 5% damping. If $\Delta_{ed} > \Delta_{max,\xi=5\%}$ that implies that the wall is likely to be elastic. For such case, the maximum elastic top displacement of the MDF system ($\Delta_{t\text{-}max}$) shall be calculated from first modal shape and the maximum displacement of the ESDF system ($\Delta_{max,\xi=5\%}$). In chapter 4 it was discussed that the effective height of the shear walls with uniform mass distribution is about seventy percent of the height of the shear wall. Thus, by simply assuming a linear deformation profile

the For shear walls with uniform mass distribution along height, alternatively $\Delta_{t\text{-}max}$ can be taken as 1.45 times of $\Delta_{max,\xi=5\%}$.

3. **Predict the state of response**: To predict the level of inelastic response, first the base curvature of the shear walls should be predicted. To do so, the top displacement of the MDF system (Δ_t or $\Delta_{t\text{-}max}$) should be used with Equation 5-2. The calculated base curvature is then divided by the yield curvature (Equation 3-3) and the curvature ductility (μ_φ) is determined. The nature of the response can be predicted by assessing μ_φ. A curvature ductility equal to two can be used as the reference point between the elastic and inelastic domain. This limit has been previously suggested in literature (Boivin and Paultre, 2012).

4. **Determine the global ductility factor:** If the response is elastic, the global ductility of the system is considered equal to one. In case that the inelastic response is predicted, the yield displacement and global ductility factor of the ESDF system can be determined using the methodology described in Section 2.3(b).

5. **Refinement of estimated force-deformation response of the ESDF system**: To facilitate finding a simple and realistic value for the secant stiffness of the system, the bilinear force-deformation response of the ESDF system should be constructed by performing a pushover analysis on a SDF system with M-φ response similar to that assumed for the MDF system. Using an iteration procedure, the estimated values for yield displacement and global ductility is updated based on the results of the pushover analysis.

6. **Construct the modified design spectrum**: Depending on the nature of the response, two scenarios are considered. If the response is predicted as inelastic, the modified design spectrum shall be developed using the procedure presented Section 3.2 (c). If the response is predicted as elastic, the maximum spectral displacement ($\Delta_{max,\xi=5\%}$) is used as the design displacement and there is no need to modify the elastic design displacement spectrum. At the design level, 5% damped spectrum maybe be used as the base spectrum. However, when elastic response is predicted and the level of energy dissipation in the structure is limited, it is recommended (and more conservative) to use lower damping for the design spectrum. Equation 3-11can be used to modify 5% damped elastic spectra for different damping values.

7. **Calculate the design base shear**: If the response is predicted as inelastic, the effective elongated period of the system (T_e) can be derived by applying the design displacement (Δ_{ed}) to the modified design spectrum (Figure 2-2-e). The secant stiffness of the design system is derived from $K_e = 4\pi^2 m_e/T_e^2$. The design base shear is then calculated by multiplying the effective stiffness by the design displacement and shear amplification factor due to elastic and inelastic higher modes impact as specified in the Equation 5-4.

   Equation 5-4 $$V_{bd} = K_e * \Delta_{ed} * M_{v-analytical} * \Omega_v/R_o$$

   In this equation, M_v is the elastic amplification factor and shall be derived from the analytical elastic higher mode amplification as described in Section 5.5.2. According to CSA A23.3, for tall and slender walls in eastern Canada the inelastic higher modes shear amplification factor (Ω_v) when the ductility of the shear is fully mobilized. For shear walls with moderate ductility in eastern Canada, from Equation 2-12 and by conservatively considering the minimum over strength factor (γ_w=1.3) and R_o*R_d=2.8, Ω_v is calculated as 1.3. Conservatively, it can be suggested that when ductility curvature is more than μ_φ=4, an amplification factor equal to Ω_v=1.3 can be used. For curvature ductility between two and four, the inelastic higher mode amplification factor can be determined by linear interpolation whereas for μ_φ=2 the amplification factor can be taken equal to one (Ω_v=1.0).

   For shear walls with elastic response the design base shear is calculated by replacing the equivalent stiffness (K_e) with elastic stiffness of the ESDF system (K_{el}) and assuming Ω_v=1.0.

   The stability index of the ESDF system according to Equation 3-12 shall be limited to 0.4.

   The value of over-strength factor (R_0) suggested by NBCC 2015 for moderate ductile shear walls can be considered (R_0=1.4). However, if the response is predicted as elastic or the inelastic response is limited, it is more advisable to use R_0=1.0.

8. **Distribution of the base shear along the height:** After determining the design base shear, the procedure similar to the one given in NBCC 2015 can be applied to distribute the forces over the height of the structure. The design base shear can be distributed using equivalent static method or based on the profile determined from RSA. In later case, similar to FBD procedure, the base shear from RSA shall be calibrated to the design base shear from DDBD.

5.5.4 Design examples using modified DDBD approach

To validate the proposed design procedure, four shear walls were designed following the steps outlined above and their response was examined using NTHA. The walls are situated on the perimeter of 30 m x30 m building, two in each direction. The building is located in Montreal, on class "C" site. Four buildings heights are considered; 10, 20, 25 and 30 storeys". Design displacement spectrum is characterised by the corner period T_c equal to 6s and the maximum spectral displacement for 5% damping is Δ_{max}=155mm which was previously used for design in chapter 4. The relevant information regarding the dimensions and design for each shear wall are shown in Table 5-3. In this table, the preliminary fundamental periods (T_1) are derived by assuming 70% effective moment inertia for the shear wall sections. The predicted base curvature, as well as M_v and Ω_v factor are determined as proposed in this chapter. Note that the design shear force shown in the table is multiplied by the over-strength factor, R_o to provide the consistent comparison with the results of NTHA.

Similar to what was seen in Chapter 3 and 4, for all shear walls the design displacement of SDF system is governed by the maximum spectral displacement (155mm), and not by the maximum allowed drift nor the maximum allowable curvature. The response for the 10-sotrey shear wall is considered as inelastic because the anticipated curvature ductility is larger than two (μ_φ =4.96). For 20-storey shear wall the predicted response is elastic because μ_φ =1.78 is less than two. However, since the curvature ductility is close to two, some inelastic activity is expected. For 25- and 30-storey shear walls elastic response is anticipated as their predicted curvature ductility are smaller than one (0.88 and 0.72 respectively). According to the type of anticipated response (elastic or inelastic), the appropriate DDBD procedure is applied as explained in Section 3.2.

In Figure 5-5 to Figure 5-8 and Figure 5-10 to Figure 5-21, design demands predicted by DDBD are compared with the results of NTHA. The NTHA analyses have been carried out in OpenSees using the set of thirteen records. Modeling details and information on selected accelerograms are available in Section 4.3.1 and 4.2 respectively. 5% damping was applied for these analyses to maintain consistency with the value used for design. The response to high and low frequency records are distinguished to illustrate the influence of ground motion frequency content on response. For displacement profiles, the median response of all records is examined while for curvature profiles, the comparisons are made for the median results obtained for the low frequency

records. For shear force and bending moment profiles, the mean response of all records is used for comparison because the scatter of the data was not significant.

Table 5-3: Design information and summary of the outputs for the shear walls designed according to the proposed modified DDBD approach

Shear wall height	10_Storey	20_Storey	25_Storey	30_Storey
H_w (m)	30	59.5	74.25	89
l_w (m)	6.5	8	8.5	9
Thickness (mm)	350	450	500	500
T_1 (s)	1.38	3.30	4.36	5.70
$2*T_{NBCC}$ (s)	1.30	2.17	2.56	2.93
M_v	1.76	3.02	3.42	5.23
$M_{v\text{-}NBCC}$	1.19	1.62	1.82	2.05
Δ_{max} (mm)	155	155	155	155
P_{base}	0.0043	0.0036	0.0038	0.0037
$P_f/A_c f'_c$	0.1	0.1	0.1	0.1
β	0.0132	0.0037	0.0017	0.0010
Δ_{de} (mm)	155	155	155	155
$\Delta_{d\text{-}top}$ (mm)	231	241	243	245
φ_{base} (1/m)	0.0031	0.0009	0.0004	0.0003
μ_φ	4.96	1.78	0.88	0.72
Predicted response	Inelastic	Elastic	Elastic	Elastic
Ω_v	1.3	1	1	1
M_e (tons)	1685	3174	3611	4305
H_e (m)	22.59	44.09	56.06	66.97
Δ_{ey} (mm)	81	206	229	424
μ_Δ (global ductility factor)	1.93	1.00	1.00	1.00
K_e (kN/m)	9274	10040	6983	4861
T_e (s)	2.68	3.39	4.52	5.91
R_o*V_{bd} (kN)	3705	4087	3705	3938
Stability index	0.07	0.06	0.09	0.13
$(R_o*V_{b\text{-}DDBD})/V_{b\text{-}NTHA}$	0.99	0.94	0.84	1.00
$(R_o*M_{bDDBD})/M_{bNTHA}$	0.98	1.22	1.13	1.01

For 10-storey shear wall with μ_φ =4.96 and μ =1.93 the response is clearly inelastic. Curvature profile from NTHA is illustrated in Figure 5-5. As expected the curvature demands from the high frequency records are significantly smaller than the response to low-frequency records. The base curvature calculated from Equation 5-1 exceeds the NTHA median base curvature of low frequency

records by about 36%. On the other hand, the global ductility is about 10% smaller than the ductility factor suggested by NBCC 2015 ($\mu=R_D=2.0$). It is noted in Figure 5-6 that the DDBD displacement profile over-estimates by about 3.8 times the displacement obtained for this shear wall from NTHA. However, even though the displacement profile is over-estimated, the predicted drift of the shear wall is not significant and is only about 0.7%. The comparison of the design shear force to NTHA values, (Figure 5-7) shows that the design shear has an excellent match with NTHA mean shear force, with only one percent of difference. As seen in Figure 5-8, the DDBD bending moment at the base is very similar to that obtained from NTHA with only 2% difference. However, from 4th storey above, the DDBD bending moment is smaller than the NTHA. This confirms that for shear walls with inelastic response, capacity design shall be applied to determine bending moment envelope outside of the plastic hinge region.

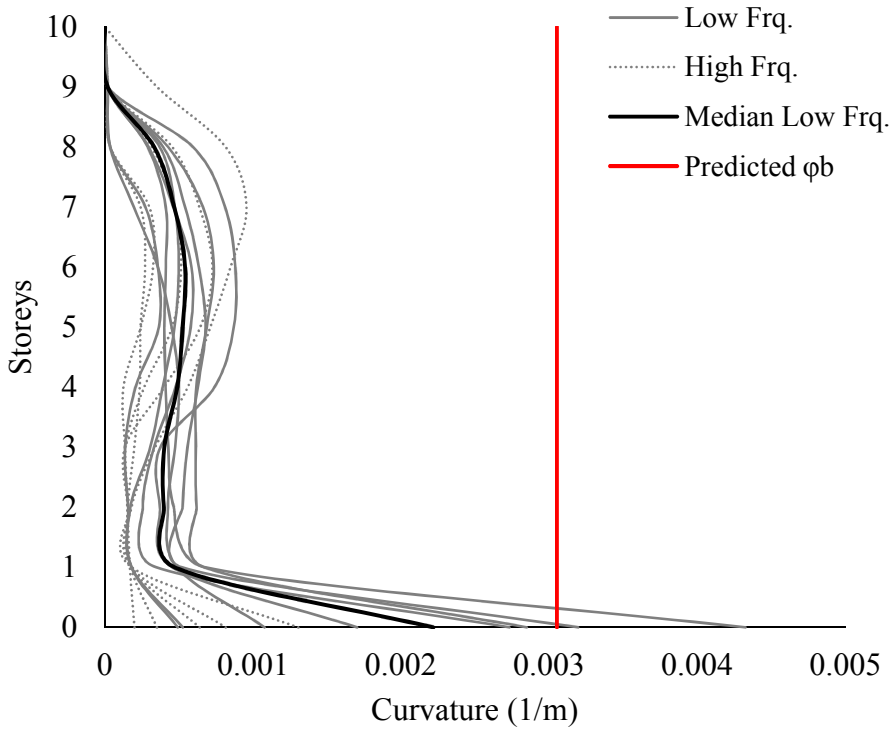

Figure 5-5: Predicted curvature profile of 10-storey shear wall compared to NTHA demands

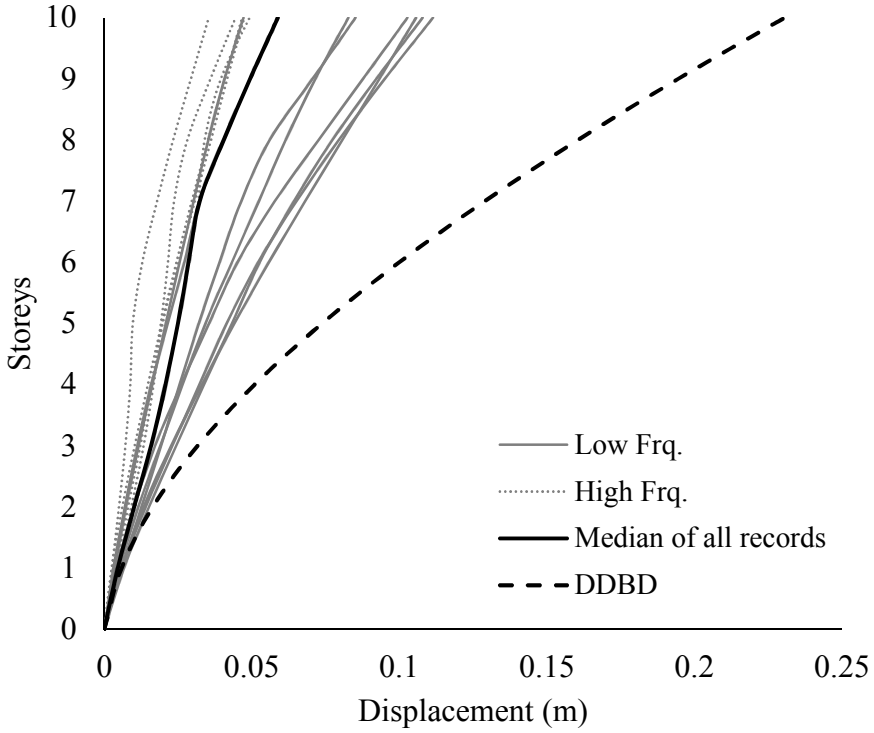

Figure 5-6: Predicted displacement profile of 10-storey shear wall compared to NTHA demands

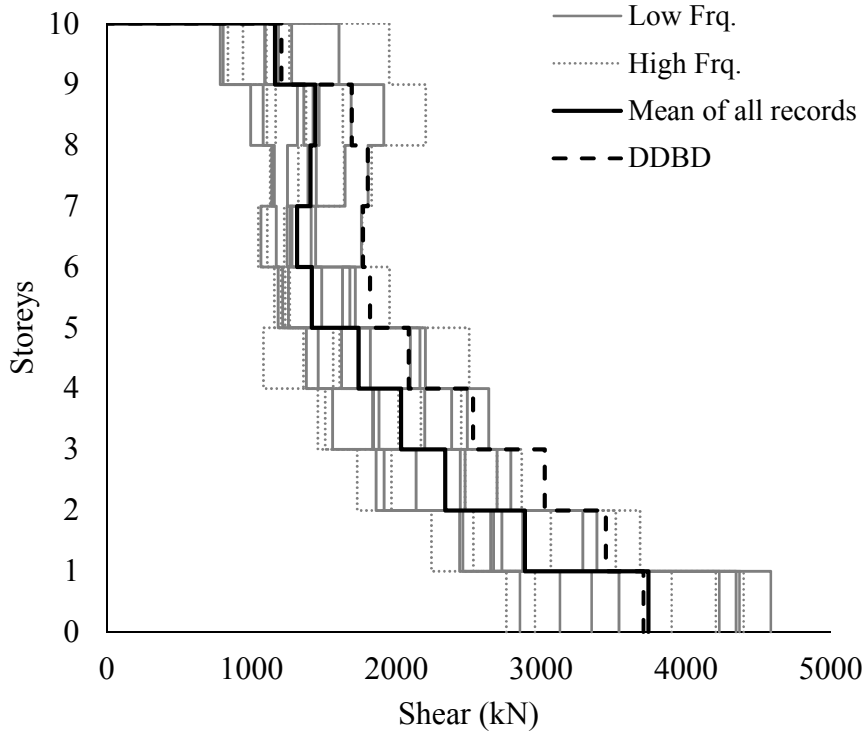

Figure 5-7: Predicted shear force profile of 10-storey shear wall compared to NTHA demands

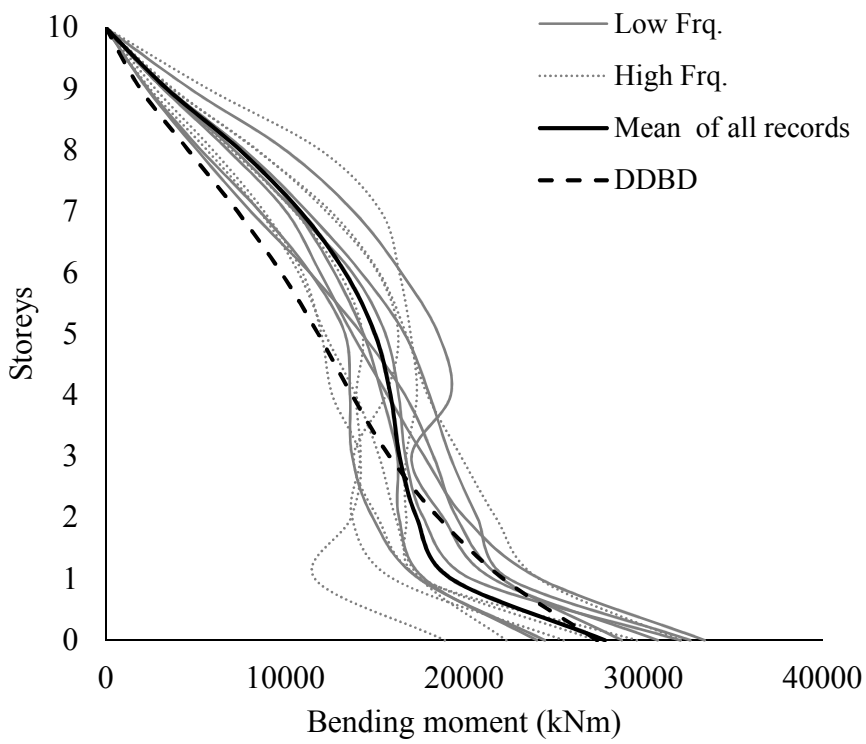

Figure 5-8: Predicted bending moment profile of 10-storey wall compared to NTHA demands

The curvature ductility (calculated from Equation 5-1and Equation 5-2) for 20-storey wall is larger than one but smaller than two, thus, based on the proposed method, the overall response was considered as elastic. The same conclusion is made from pushover analysis of the ESDF system used in DDBD. In Figure 5-9, the yield displacement of the ESDF system is indicated. In this figure, the estimated yield displacement from bi-linear regression (206mm) and the displacement corresponding to the yield curvature ($2\epsilon_y/l_w$,212mm) are both larger than the maximum spectral displacement (155mm). However, since the predicted base curvature ductility (μ_φ =1.78) is more than one, some minor inelastic deformation is expected at the base of the shear wall. The results of NTHA showed that the median demand curvature at the base is even larger than what was preliminary calculated from Equation 5-1and Equation 5-2. The NTHA base curvature is about two times the estimated curvature which is close to the proposed upper bound for calculating the curvature, considering two times β in the Equation 5-2. The curvature ductility at base from NTHA is $\mu_{\varphi\text{-NTHA}}$ =3.40. Thus, for cases that are likely to have limited inelastic response, like this particular case for which the design base curvature was close to two, it is suggested to use the upper bound value of Equation 5-2 (2β) to obtain a conservative estimation of the base curvature.

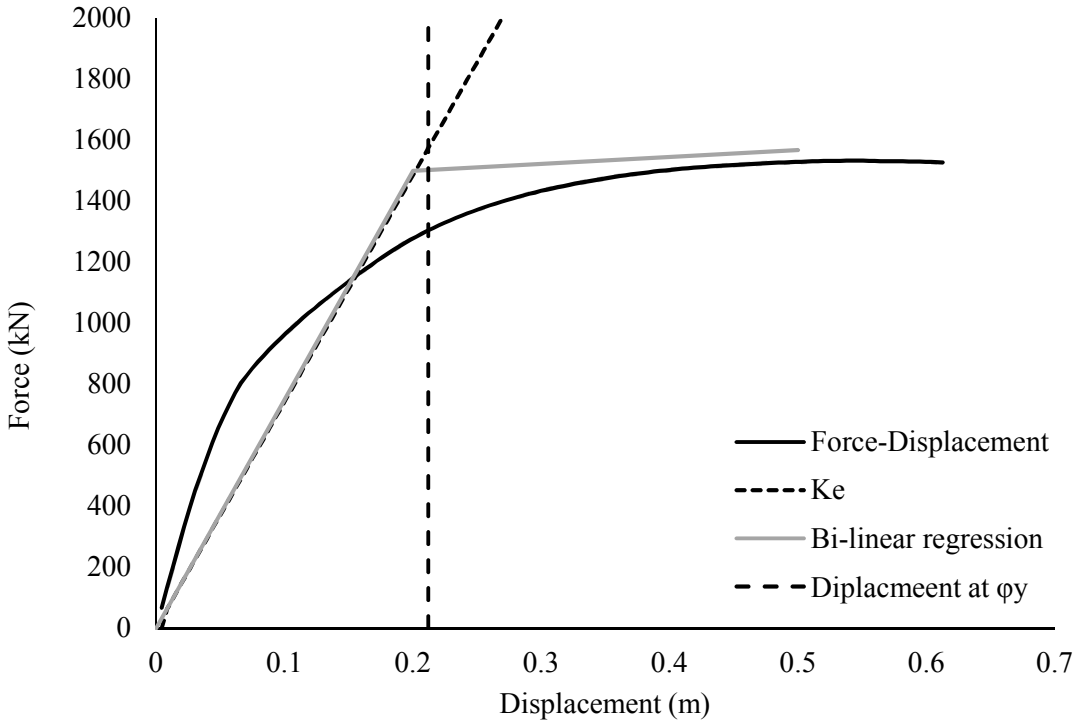

Figure 5-9: Force-displacement relations of SDF system for 20-storey shear wall.

The predicted top displacement from DDBD is about 50% larger than the median of all records and shows a better match with the response of the low frequency records.

The comparison of shear force distribution from DDBD approach to the NTHA results is shown in Figure 5-12. The predicted base shear from DDBD is 94% of the NTHA median base shear. The DDBD shear force profile encompasses the NTHA mean shear force distribution along the height. The DDBD bending moment, however, is about 22% larger than mean bending moment from NTHA (Figure 5-13) at base of the shear wall. By comparing the bending moment profiles form DDBD to NTHA it appears that for this wall, applying the capacity design approach would not be necessary to determine design bending moment outside of the plastic hinge region. However, to insure the adequate capacity in shear walls cross sections, it is advisable to use the capacity design approach for any shear wall for which the inelastic response is anticipated. Although this approach is conservative for the case of shear walls with limited inelastic response, like abovementioned 20-storey wall, overall it ensures a safe design envelope for all walls with inelastic response.

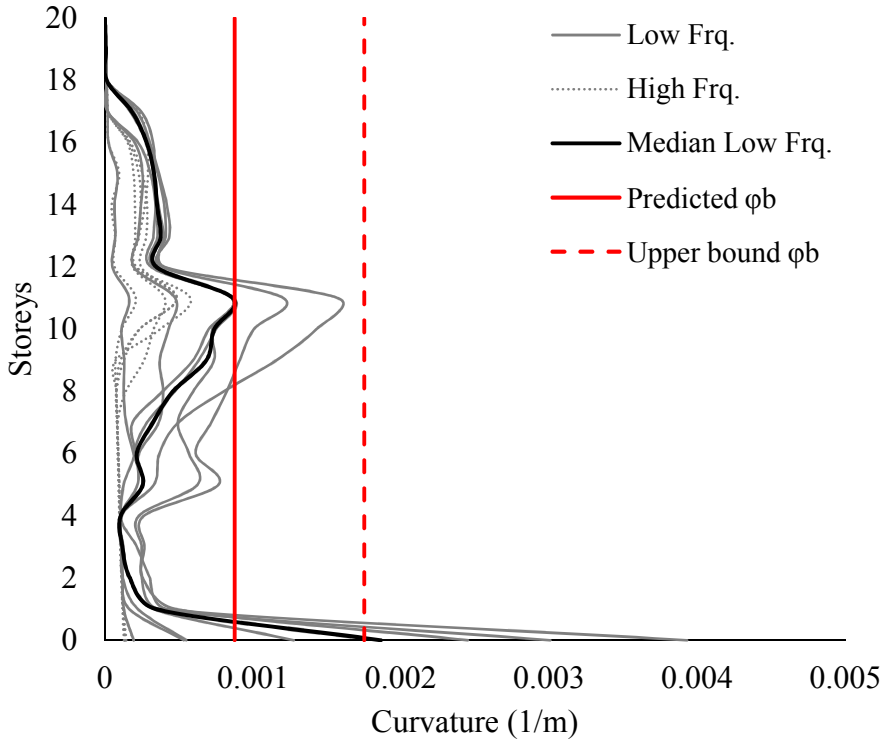

Figure 5-10: Predicted curvature profile of 20-storey shear wall compare to NTHA demands

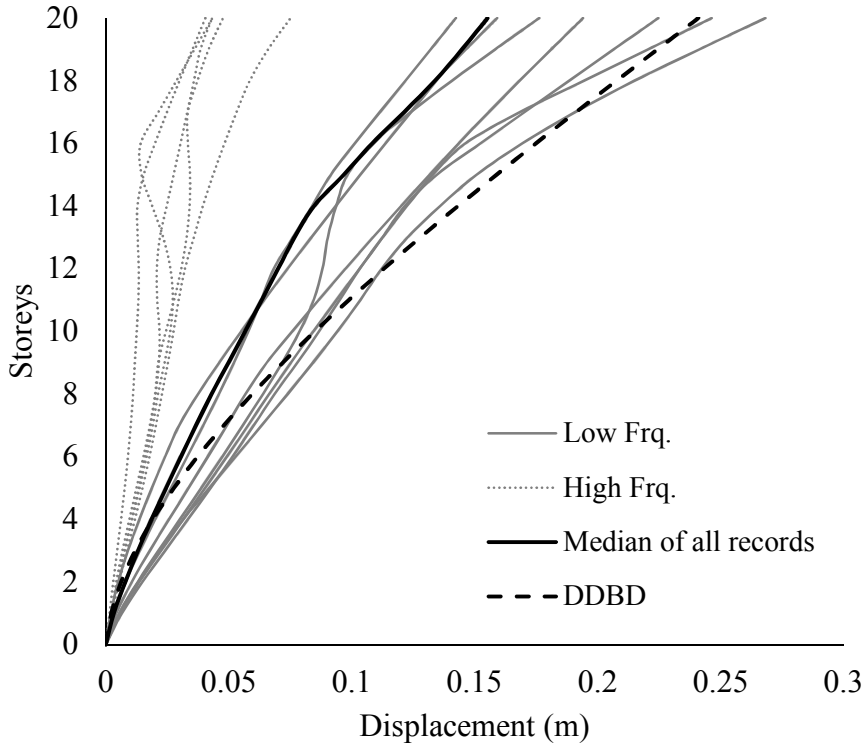

Figure 5-11: Predicted displacement profile of 20-storey shear wall compare to NTHA demands

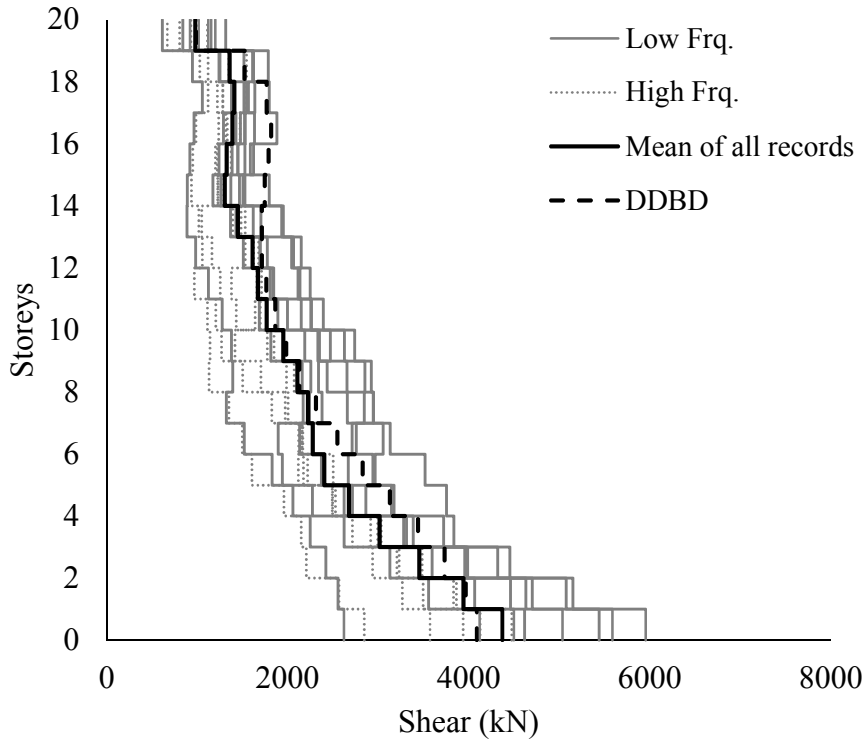

Figure 5-12: Predicted shear force profile of 20-storey shear wall compare to NTHA demands

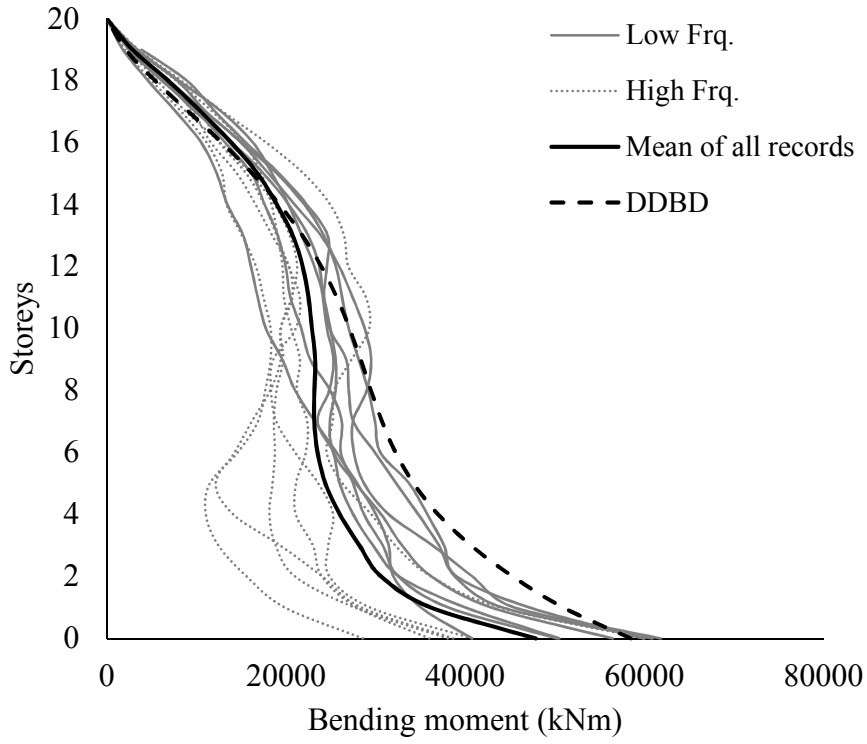

Figure 5-13: Predicted bending moment profile of 20-storey wall compared to NTHA demands

The design predictions for 25 and 30-storey shear walls are more straight forward. For 25-storey wall the elastic is anticipated as it has curvature ductility less than two. In fact, the curvature ductility of these walls is even less than one and from the design perspective the elastic response is obvious. The predicted curvature is 26% smaller compared to NTHA curvature demand at the base which can be considered a good match in view of sensibility of this response parameter to ground motion input. The top displacement from DDBD, on the other hand, is about 20% larger than the NTHA median response and show a better match compared to 10- and 20-storey shear walls. Although the design base shear for 25-storey shear wall is smaller than NTHA mean base shear by about 16%, the bending moments from DDBD approach overestimates the bending moment by about 13%. It should be noted that shear force response is very sensitive to the shear stiffness used in the OpenSees model, and to achieve an accurate estimation of shear force demands more detailed modeling are needed.

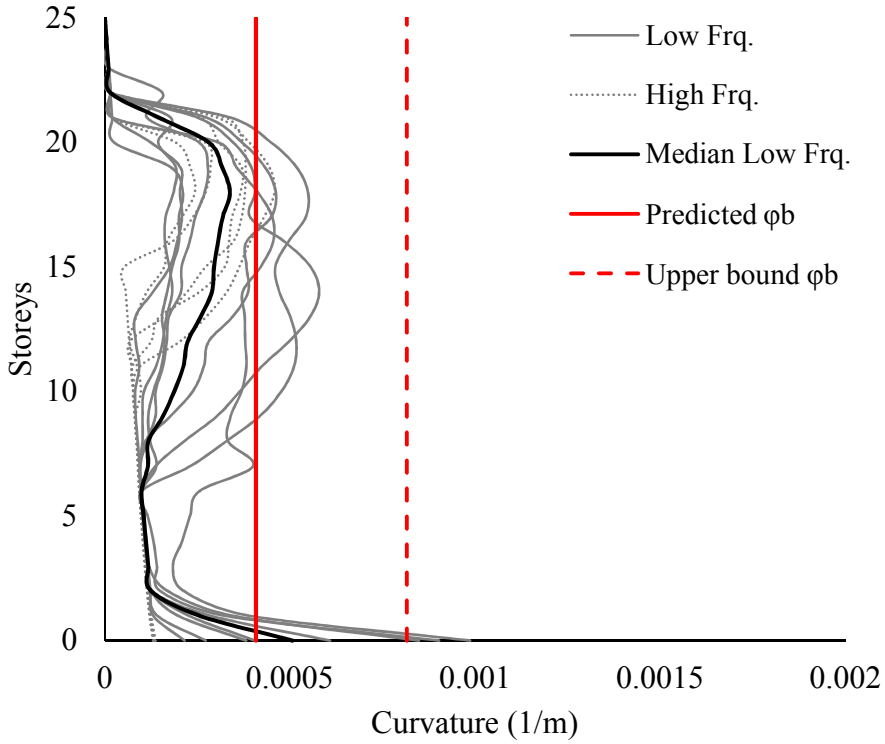

Figure 5-14: Predicted curvature profile of 25-storey shear wall compare to NTHA demands

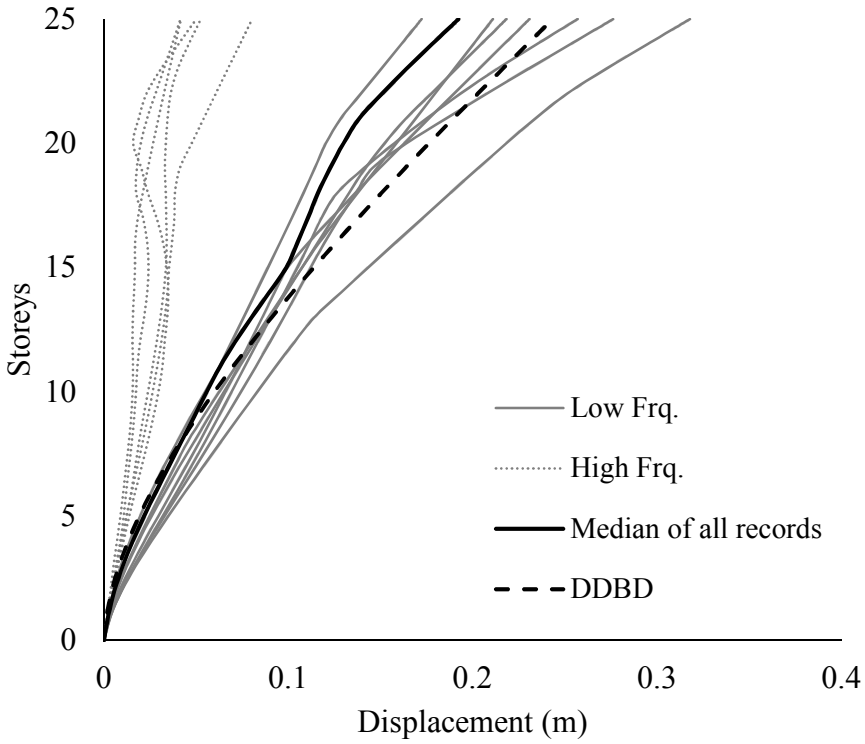

Figure 5-15: Predicted displacement profile of 25-storey shear wall compare to NTHA demands

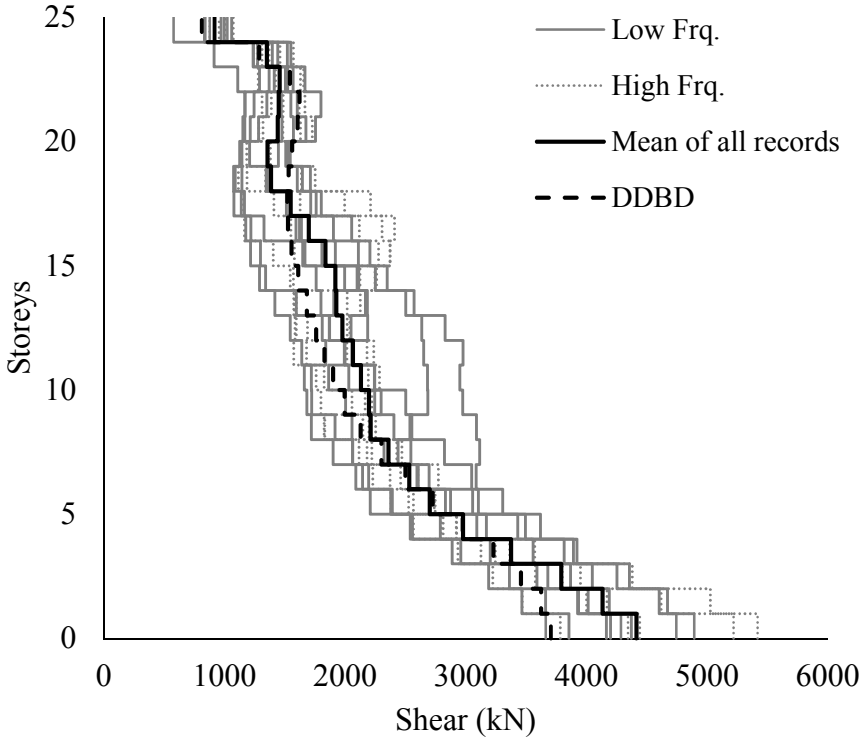

Figure 5-16: Predicted shear force profile of 25-storey shear wall compare to NTHA demands

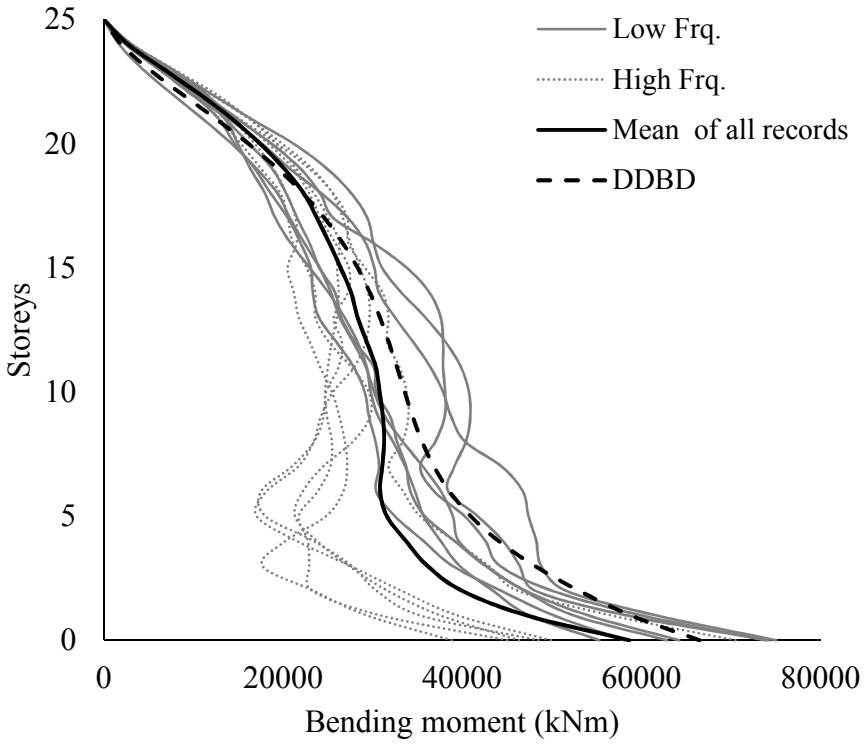

Figure 5-17: Predicted bending moment profile of 25-storey wall compared to NTHA demands

For the 30-storey shear wall the top displacement predictions from DDBD shows about 16% over-estimation over the NTHA median response and are more in line with the displacements from the low-frequency records. The base curvature is about 16% overpredicted which can be considered acceptable. The DDBD base shear and bending moments are almost identical to the NTHA mean response with response ratios equal to 1.0 and 1.01 respectively.

From the curvature profile graphs, it is noted that, similarly to what was observed in Chapter 3 for 20-, 25- and 30-sotrey shear walls in particular, the curvature response to some of the low-frequency records surpasses the yield curvature in upper levels, between the mid-height to 70% of the height of shear walls. This is an indication of potential of the formation of the second plastic hinge in upper levels for some ground motion records. Although the median curvature of low frequency records is smaller than the yield curvature, further study is needed to investigate the possibility of formation of the second plastic hinge for these shear walls. This subject was not the focus of this research and could the addressed in the future studies.

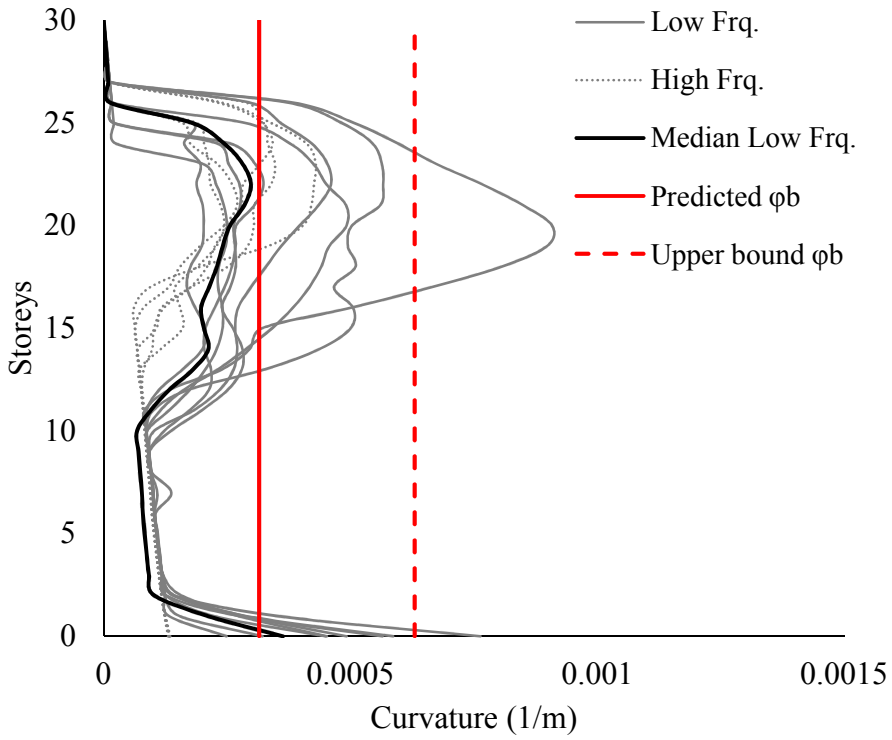

Figure 5-18: Predicted curvature profile of 30-storey shear wall compare to NTHA demands

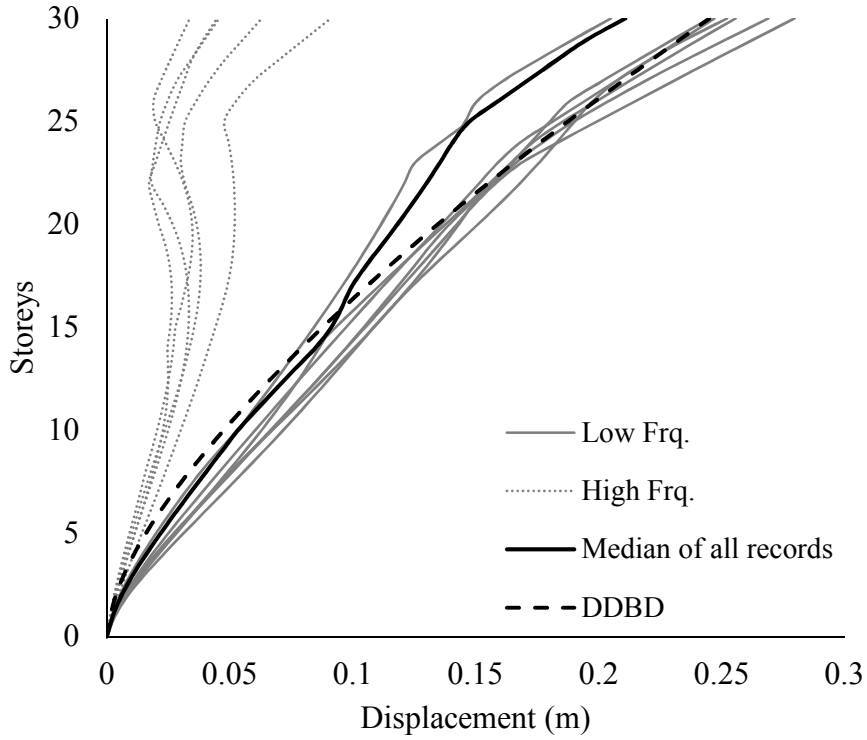

Figure 5-19: Predicted displacement profile of 30-storey shear wall compare to NTHA demands

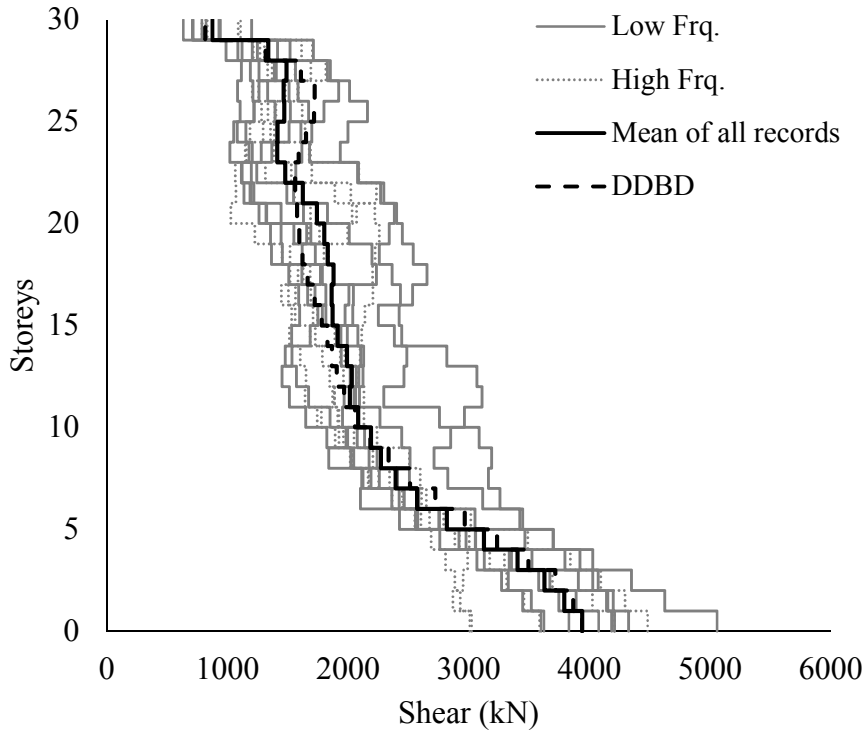

Figure 5-20: Predicted shear force profile of 30-storey shear wall compare to NTHA demands

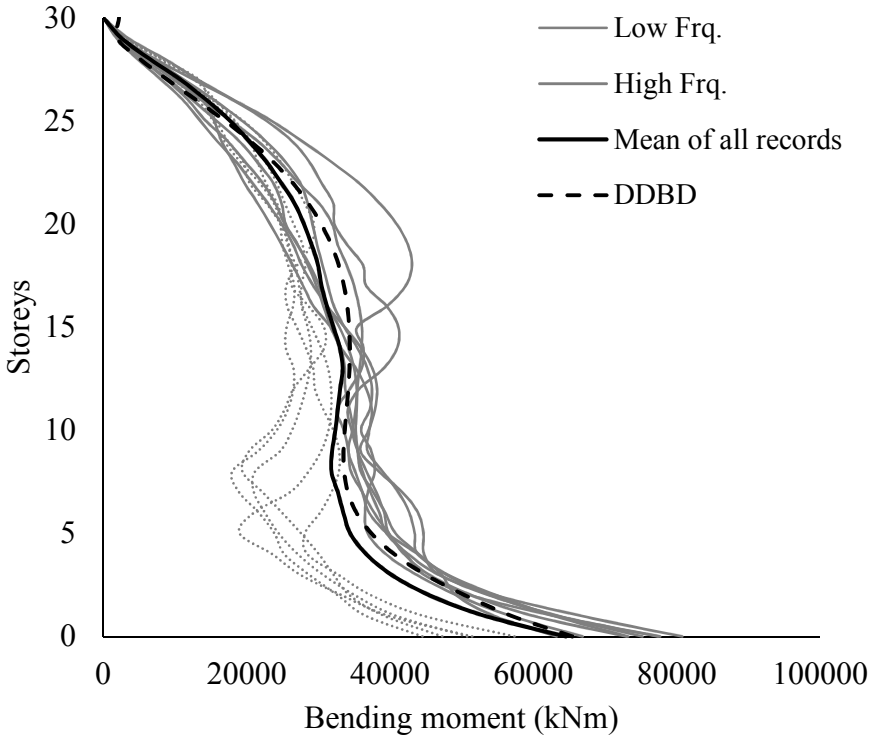

Figure 5-21: Predicted bending moment profile of 30-storey wall compared to NTHA demands

5.6 Summary and conclusions

In this chapter the results of the parametric study presented in Chapter 4 were used to propose an empirical equation based on statistical data which relates the base curvature to the top displacement for the tall shear walls located in eastern Canada. It was established that the parameters that have the most impact on the base curvature were height expressed through the number of storeys, fundamental period, axial force and reinforcement ratio of the section at the base of the wall.

A coefficient (β) was introduced to relate the median base curvature from the low frequency records to the median top displacement from all records. Two equations were introduced to calculate (β) based on the height of the shear walls. It was concluded that walls with 17-storey and above, will demonstrate predominant elastic response. For these walls the proposed equation is only based on the number of storeys and the height. For shear walls with less than 17 storeys, for which the inelastic response is significant, additional variables such as axial stress ratio and the reinforcement ratio at the base of the shear wall are also considered.

The application of the proposed equation to the walls presented in Chapter 4, showed a significant improvement in minimising the cases when the base curvature was underestimated by DDB design or overestimated by FB design. The equation was then applied to nine different shear walls with varying height between 10 to 30-storeys, designed according to FBD. Both the base curvature from FBD approach (CSA A23.3 approach) and from the proposed equation were compared with NTHA results. While the prediction error for FBD approach varied between 10% and 325% with increasing height, the error from the proposed equation varied between 47% and 3% with increasing height.

Because the scatter of results for the base curvature for the shear walls with inelastic response is significant, the proposed equation showed better predictions for taller walls with predominant elastic response and less accuracy for the shorter walls with predominant inelastic response. Nevertheless, compared with FBD (from NBCC 2015) and current DDBD methods, the proposed approach gives a more realistic prediction regarding the level of ductility of taller walls with acceptable accuracy.

The proposed equation was then used to improve the applicability of the current DDBD method for design of taller walls in eastern Canada by suggesting a new approach to predict the elastic or inelastic nature of response.

One main issue that cause the underestimation of the design seismic shear force by DDBD approach identified in Chapter 3 was the use of same M_v factor as proposed by NBCC 2015 to account for the impact of higher modes. The NBCC amplification factor is combined with other design constraints, such as limits imposed on base shear and empirical design period and it is tailored to give appropriate shear force estimates in combination with all these other factors. Therefore, when it is used alone within the scope of the DDBD method, it underestimates the higher mode amplifications. In order to determine more appropriate M_v factors to use in DDBD design, a study was carried out on 20 shear walls with heights varying between 10- to 30-storeys using response spectrum analysis, and the relation between the analytical elastic shear amplification and the fundamental period was established used the analytical results. This amplification factor was significantly higher than what is given by NBCC 2015. The analytical amplification factor is then used in the modified DDBD approach.

In the proposed approach the base curvature and the curvature ductility are first calculated from the design displacement at the top of the shear wall. If the curvature ductility is smaller than two, the response is assumed to be overall elastic, otherwise, the predicted response is inelastic. This information is then used to determine the appropriate shear force amplification due to the higher modes, elastic or inelastic.

The proposed DDBD approach was applied to four shear walls with 10, 20, 25 and 30-storeys height. The design predictions of displacement, curvature, shear force and bending moment were compared with the outputs of the NTHA. The comparison showed a good agreement of the design forces with NTHA results and confirmed that the proposed procedure leads to safe design.

CHAPTER 6 CONCLUSION AND RECOMMENDATIONS

This chapter provides the summary of the research project and discusses the major findings and the conclusions drawn from the study. The recommendations for further studies are presented along the original contributions made in this study.

6.1 Summary

The main objectives of this research project were to study the deformation response of the taller RC walls in eastern Canada and establish a relationship between global and local ductility indicators that could be used to improve seismic design procedures for this system. The current seismic provisions prescribed in Canadian design norms (NBCC 2015 and CSA A23.3) for design of RC shear walls have been developed focusing on the response of the short to mid-height shear walls and such are not always adapted for design of taller walls. Similar observation can be made for displacement-based design approaches which are newer design methods. On the other hand, studies on seismic response of the RC shear walls in eastern north America is limited and mostly focused on the aspects of force demands.

To achieve these objectives, a preliminary study was carried out first to investigate and compare the response of the tall shear walls in eastern and western Canada. Two shear wall buildings, one located in Montreal and another in Vancouver, were designed according to the current Canadian design provisions (FBD approach) and direct displacement-based design (DDBD) approach. The design predictions for each design method were compared against the results of nonlinear time history analysis (NTHA). It was noted that the response of the tall shear walls in eastern Canada does not necessarily match the prediction regardless of design method used, especially regarding the level of mobilized ductility. For this preliminary study, the FB designed shear walls were designed according NBCC 2010 and CSA 23.3-14 and to construct the displacement design spectrum for DDBD, the maximum spectral displacement was derived from the UHS of NBCC 2010 (Δ_{max}=201mm). During the course of the research project, the 2015 edition of NBCC became available and displacement design spectrum were updated with the maximum spectral displacement (Δ_{max}=155mm). The next steps of the research were carried out according to NBCC 2015 and the new value for the maximum spectral displacement.

A more detailed study was carried next to determine the important parameters that affect the deformation response of taller RC walls in eastern Canada. The finding of the preliminary study brought to light the need to propose a more accurate approach to estimate the level of mobilized ductility in the tall shear walls. To do so, the prediction of the base curvature, which is a measure of local ductility for RC shear walls, was a key objective. A parametric study was carried out on more than hundred shear walls which were designed according to FB and DDB design approaches. The designed walls were analysed using NTHA and the accuracy of both design approaches in predicting the deformation response was investigated.

The findings of the parametric study were used to develop an empirical relationship between the base curvature and top displacement. This equation is then used to propose a modified version of DDBD methodology for shear wall design and provide more accurate estimations of shear wall seismic behaviour in regions with moderate seismicity like eastern Canada.

6.2 Original contributions of the research

Several original contributions have been made through this research project.

A practical and clear, step-by-step application of the DDBD method to perform seismic design for shear walls with predicted elastic response represents an original contribution, highly relevant to regions in eastern Canada as well as other regions with moderate seismicity and similar seismic context. Another originality of this research is that it is the first study that investigate the impact and importance of the frequency content of the selected records on either force or displacement seismic response of the shear walls located in eastern north America. To authors knowledge this is the first study that investigate directly the nature of the response of the tall shear walls in eastern Canada and the mobilised global ductility. The only other existing study addressing the displacement-based design approach for designing the shear walls in eastern Canada (Alexieva, 2007) did not consider any limit on maximum design spectral displacement. This assumption may lead to very conservative design and over-may estimate the level of ductility demands. The present research tried to tackle the seismic response of tall RC shear walls in terms of the deformation response and to investigate the level of mobilized ductility contrary to the force-oriented studies which focus on force reduction factors or higher modes amplifications. In this respect, to the best

of our knowledge, this is the first study in eastern Canada and, more generally, in eastern north America.

In the past, the studies from Canadian researchers addressing the estimation of the base rotation and section curvature for the RC shear walls have been performed for western Canada. However, the response of the shear walls in eastern Canada is significantly different and does not follow trends established for western locations. One of the main contribution of this research is the study and formulation of the relation between the top displacement and the base curvatures in eastern Canada region. The findings could be applied in FBD method in NBCC 2015/CSA A23.3 or any displacement-based approach which is used to design shear walls in eastern Canada.

Another original contribution of this research is the proposal of a modified DDBD approach which can be used for design of tall RC shear walls in eastern Canada. The proposed concept can be used for any other regions with moderate or low seismicity.

6.3 Conclusions

Following conclusions have been made from the findings of this research:

6.3.1 General observations on the design predictions and response of tall shear walls in eastern and western Canada

1. For tall shear walls with high axial stress, ensuring an adequate rotational capacity is an important design constraint when the NBCC force-based design procedure is applied. To fulfill this requirement, the length of the rectangular wall has to be increased to provide the required rotational ductility capacity at the base; nevertheless, the results of the NTHA for a sample shear wall located in Montreal showed that the response of the wall is nearly elastic. On the other hand, study of a sample RC shear wall in west (Vancouver) showed that the ductility anticipated in the design is fully mobilised under intermediate- to high-frequency records, and significantly surpassed for low-frequency records. For both FB and DDB designs of sample shear wall in Montreal, the observed levels of base curvature ductility indicated very limited inelastic response, significantly smaller than the one predicted by NBCC. Accordingly, the underestimation of the shear forces can be attributed to the combination of elastic higher mode amplification and over-estimation of the level of inelastic response.

2. The seismic response of the walls is very sensitive to the frequency content of ground motions. For both eastern and western locations (Montreal and Vancouver) and DDBD and FBD design methods, low frequency records induced inelastic response at the base of the structure, although to a much lesser extent in Montreal walls. Displacement response showed the same trend. High frequency records, on the other hand, induced more significant demand in the upper levels, confirming the potential to develop second plastic hinge at this location. Although this tendency is more pronounced for Montreal structures, it is also observed for Vancouver walls particularly at the levels where the transition in reinforcement curtailing is present.

3. Even though the study of the force demands was not the main object of this research, it was observed in several occasions that the amplification factors provided by NBCC for use in seismic design procedure (force-based design) underestimate the higher modes amplification of the base shear for both location, but especially for the shear wall in Montreal. It was noted that the NBCC elastic amplification factors should not be applied in conjunction with DDBD approach, because their use lead to significantly under-estimated shear forces.

4. The use of DDBD method to design walls in high seismicity region like Vancouver, for which the significant inelastic seismic response is anticipated, is straight forward. However, when the elastic structural response is anticipated, current DDBD method does not provide the unique solution because the yield displacement of the system exceeds the maximum spectral displacement. Other design criteria, specific for tall wall design are not discussed in detail in literature. In this study, the stability index was selected as a criterion to provide a minimum limit for the stiffness of the shear wall and control the P-Δ effects. The maximum limit for the stability index was selected based on the requirements in NBCC (2010, 2015) as 1.4. For walls, located in low-to-moderate seismic zones like Montreal, elastic seismic response is quite likely.

5. The application of DDBD method requires the use of displacement design spectra. Such spectra are not readily available in NBCC (2010, 2015) so it was necessary to construct one based on the results available in the literature and the study realised in the scope of this project. For this study, displacement spectra are derived from pseudo-acceleration design spectra by considering corner periods equal to 6 s and 16 s for Montreal and Vancouver, respectively.

6. The results of NTHA confirmed that for the shear walls under study, the top displacement and maximum base curvature do not occur simultaneously for the taller shear walls. The current

DDBD is more successful to predict the nature of seismic response (i.e. elastic vs. inelastic) and gives a possibility to estimate seismic demand that better reflect the level of mobilised system ductility. However, the final design forces are largely under-estimated because of the under-estimation of the higher mode impact on the elastic shear. Thus, it is necessary to define complementary design criteria to estimate the appropriate value of design seismic base shear. For the structures located in severe seismic zone (Vancouver) DDBD design may lead to slightly smaller seismic design forces compared to FBD, however, its impact on the final design is negligible.

6.3.2 Deformation response of the tall shear walls located in eastern Canada

1. The deformation response of the shear walls and specifically the values of the base curvature are in direct relation with their height. Although the fundamental period is a more general parameter than height that is used to quantify dynamic signature of a given system, it was noted that height, or more specifically in this study the number of storeys, could provide more clear trends of the base curvature response. On the other hand, it was shown that for shear walls with the same height and length, but with different seismic mass (i.e. different fundamental period) the base curvatures are not significantly different for the shear walls more than fifteen storeys.
2. Compared to the response to simulated records for eastern Canada, the deformation response to historical records, characterised by dominant high-frequency dominated content, were relatively smaller. This was more pronounced for the base curvature.
3. Although I-shaped walls were not the focus of this study, the response of the I-shaped walls which with the same fundamental period as the studied rectangular walls, was reasonably close to that of the rectangular shear walls, with up to 10 percent scatter for the top displacement and up to twenty percent scatter for the base curvature.
4. Both current FBD and DDBD approach are overall unsuccessful in prediction of the base curvatures. This was particularly noticeable for very slender shear walls designed according to DDBD approach. On the other hand, both methods show an acceptable level of accuracy to predict the top displacements. This is because the displacement is significantly less sensitive to ground motion characteristics compared to the base curvature. The FBD method show better

predictions of top displacements for shorter (10 and 15-sotrey) shear walls whereas the DDBD approach gives better predictions for the taller shear walls (25 and 30-sotrey walls).

5. The magnitude of the axial load supported by the shear wall had a considerable impact on the base curvature response for 10- and 15-storey shear walls which have highly inelastic response; the higher the axial force, the larger base curvature at the base. The influence of the axial loads on the base curvature for taller walls (25- and 30-storey) is negligible. Due to relatively high stiffness of the shear wall systems, the P-Δ effects are very limited and the impact of the axial load on the top displacement is negligible.
6. Reinforcement ratio at the base section is another important parameter that influences the base curvature of the shear wall. Similar to the axial loads, the impact of the reinforcement ratio is considerable for the shorter walls for which extensive inelastic response develops. Sections with heavier reinforcement tend to have larger compression zone length and have smaller curvature demands. On the other hand, sections with close to minimum reinforcements yield more quickly and have higher rotational demands. The impact of the section reinforcement content on the top displacements is minimal.
7. The inter-storey drift of the shear walls shows a direct relation to the top displacements. While both global and inter-storey drifts are under 2.5% limit by NBCC 2-15, by a linear regression it was shown that the maximum inter-storey drift for shear walls is approximately two time of the global drift.

6.3.3 Base curvature-top displacement relationship for the tall shear walls located in eastern Canada

1. A coefficient β was introduced to relate the median base curvature from the low frequency records to the median top displacement from all records. Two functions were introduced to calculate β based on the height of the shear walls. For walls with 17-storey and above, the response is generally elastic and inelastic activity is very limited. For these walls, β is only dependent on the number of storeys and fundamental period. For shear walls less than 17 storeys high, for which the inelastic response is significant, the axial stress ratio and the reinforcement ratio at the base of the shear wall need to be included in the proposed equation.

2. The application of the proposed equation to the designed walls in Chapter 4, showed a significant improvement in predicting the base curvature specially for DDB designed shear walls. For case of the taller walls, the proposed method helped to reduce the over-estimation of the base curvature by the current design method. Applying of the proposed equation to nine different FB designed shear walls indicated that it is possible to reduce the error in prediction of the base curvatures. For these walls the error was reduced from 10% to 325% related to FBD method predictions to 47% to 3% for the proposed equation. FB predictions were particularly inaccurate for taller walls.
3. Because the scatter of the values for base curvature for the shear walls with inelastic response is significant, the proposed equation showed better predictions for taller walls with predominant elastic response and less accuracy for the for the shorter walls with predominant inelastic response. Nevertheless, the proposed equation always leads to more accurate prediction when it was used for DDBD approach. If NBCC/A23.3 FBD approach is used, it is suggested to use the CSA A.23.3 methodology to calculate the base rotations for shorter walls (under 17-storeys) and to use the proposed equation for the shear walls over 17 storeys.

6.3.4 Modified DDBD approach for design of tall shear walls in eastern Canada

1. The proposed equation to predict the base curvature can be used to put forward a modified version of DDBD method for design of tall RC walls in eastern Canada. The equation is used to predict the inelastic or elastic response of the wall based on its curvature ductility. The curvature can be derived by calculating the base curvature from the proposed empirical equation.
2. Because of the under-estimation of the shear forces when NBCC elastic shear amplification factors are used, it was necessary to perform a study to determine the elastic shear amplification factors appropriate for use with DDBD in eastern Canada. Based on RSA on 20 different shear walls with heights varying between 10 to 30-storeys, a graph was derived which showed the relation between the analytical elastic shear amplification and the fundamental period. These amplification factors were significantly higher than what is given by NBCC 2015. These analytical amplification factors were used in the modified DDBD approach.

3. The application of the proposed DDBD approach to four shear walls with 10, 20, 25 and 30 storeys showed a good match between the design forces and the results of NTHA and indicated that the proposed method could lead to an overall safe design. Compare with the existing DDBD approach. the performance of the proposed method is noticeably better for the case of the taller shear walls.

6.4 Recommendations for future work

This study has addressed several issues regarding the estimation of the deformations and ductility demands of tall RC shear walls in eastern Canada. The findings were used to improve the current design procedures. However, the scopes of this research were limited to specific assumptions and objectives. Also, during the study different questions were raised which require further investigation. Needs and recommendations for future studies are discussed below.

6.4.1 The impact of soil class

All designs in this study were carried out assuming NBCC 2015 class C site, thus firm soil with average shear wave velocity V_{s30} between 360 m/s and 760 m/s. All ground motion records used for NTHA have been selected and scaled for this site class. However, the type of soil has a direct impact on the seismic demand on structures. For periods longer than 2 seconds the spectral accelerations/displacements of the soft soil (i.e. soil class E or F) can be amplified more than two times compared to the spectral acceleration/displacement determined for class C site. This amplification would augment the ductility demands on the shear walls. With corner period remaining constant, the increased maximum spectral displacement could surpass the yield displacement to the system, indicating possible inelastic response for the walls that responds elastically when site class C is considered. On the other hand, when the site classes related to stiffer soil are considered (i.e. class A and B), the acceleration and displacement demands may be significantly smaller than those for class C. Thus, that shear walls that have demonstrated inelastic response in site class C could show elastic response on stiff soil or rock. Therefore, further study is needed to confirm the applicability of the proposed equation to the softer or stiffer soil classes in eastern Canada and make appropriate modifications. This would be particularly needed for softer soils, as it can be assumed that for more competent, stiffer soils the proposed equation would yield conservative results.

6.4.2 Design for other performance levels

The study presented in dissertation focused on design for the collapse prevention performance level which is usually critical for design of the structural elements of a building. However, for design of non-structural components of the building, other performance levels could be critical. For other performance levels, the return periods of the design earthquakes are different, which leads to different governing earthquake scenarios. The research can be extended to other performance level criteria. It is recommended to investigate the important parameters for other performance levels for the tall shear walls buildings using available performance-based design methods such as displacement-based design.

6.4.3 Equivalent viscous damping and damping modification factor for eastern Canada

In this research, because of the elastic response of the majority of shear walls, the equivalent damping (ξ_e) and the damping reduction factor (R_ξ) were not critical to the design outputs. However, for shorter walls with more significant inelastic response, the equivalent damping and the modification factor are critical to the design. In the literature, the proposed equations for calculating the equivalent damping and the modification factor are derived based on the studies that used ground motion records from western North American or European earthquake events. However, there is a lack of specific studies about proposing the appropriate equations to determine these parameters in eastern Canada. Studies on this topic are recommended for future research.

6.4.4 The applicability of the proposed equation to other shapes of RC shear walls

The study presented in this thesis focused on the response of simple RC shear walls. As for the taller walls I-shapes may be a more efficient option, an exploratory study was conducted to compare deformation response of I-shaped and rectangular walls. It was shown in Chapter 4 that the top displacement and base curvature of the rectangular shear walls and I-shaped shear walls with the same height and similar fundamental periods is be comparable. These results suggest that the proposed empirical equation could be used for I -shaped shear walls. However, as only few I-shaped walls were analysed, further work is needed to confirm the applicability of the proposed

equation for this type of walls. The base curvature and ductility for other commonly used shapes for RC walls such as C-shaped and core walls should also be addressed.

In addition, the present study could be extended to coupled shear walls. Although ductility demands of the coupled shear walls has been addressed in the literature, they were all done for western Canadian seismic context. To author's best knowledge, no investigation has been carried out the ductility demands on coupled shear walls in eastern Canada. Accordingly, further study on this topic are needed.

6.4.5 The impact of mass-stiffness eccentricity

The eccentricity between the mass and stiffness in the plan of shear wall building structures at each level causes torsion moments due to seismic accelerations. In turn, torsion moments induce shear forces in simple shear walls and increase or diminish seismic shear force in function on the wall position. In development of the proposed equation, the possible impact of accidental torsion was considered, the impact of intrinsic torsion on the ductility demand requires further investigations.

BIBLIOGRAPHY

ACI. (2017). Building Code Requirements for Structural Concrete and Commentary (Vol. 318M): American Concrete Institue.

Adebar, P., Mutrie, J., & DeVall, R. (2005). Ductility of concrete walls: The Canadian seismic design provisions 1984 to 2004. *Canadian Journal of Civil Engineering, 32*(6), 1124-1137. doi: 10.1139/l05-070

Alexieva, K. (2007). Displacement-based Performance Assessment of RC Shear Walls Designed According to Canadian Seismic Standards, Mémoire de maîtrise, École Polytechnique de Montréal, 289 p.

Amaris, A. D. (2002). *Dynamic amplification of seismic moments and shear forces in cantilever walls.* Master degree, Università degli studi di Pavia, Pavia.

ASCE. (2015). ASCE7-10: Minimum Design Loads for Buildings and Other Structures: American Society of Civil Engineers.

Aschheim, M. (2002). Seismic design based on the yield displacement. [Article]. *Earthquake Spectra, 18*(4), 581-600. doi: 10.1193/1.1516754

ATC72-1. (2010). Modeling and Acceptance Criteria for Seismic Design and Analisys of Tall Buildings: ATC/PEER

Atkinson, G. M. (2009). Earthquake time histories compatible with the 2005 National building code of Canada uniform hazard spectrum. *Canadian Journal of Civil Engineering, 36*(6), 991-1000. doi: 10.1139/l09-044

Boivin, Y., & Paultre, P. (2012). Seismic force demand on ductile reinforced concrete shear walls subjected to western North American ground motions: Part 1 - parametric study. *Canadian Journal of Civil Engineering, 39*(7), 723-737.

Carr, A. (1996). *RUAUMOKO Users Manual*.

CEN. (2001). Eurocode 2: Design of Concrete Structures: European Committee for Standardization.

CEN. (2004). Eurocode 8: design of Structures for Earthquake Resistance: European Committee for Standardization.

Chopra, A. K., & Goel, R. K. (2001a). Direct Displacement-Based Design: Use of Inelastic vs. Elastic Design Spectra. *Earthquake Spectra, 17*(1), 47-64.

Chopra, A. K., & Goel, R. K. (2001b). Direct Displacement-Based Design: Use of Inelastic vs. Elastic Design Spectra. *Earthquake Spectra, 17*(1), 47-64. doi: 10.1193/1.1586166

Crouse, C. B., Leyendecker, E. V., Somerville, P. G., M.Power, & Silva, W. J. (2006, April 18-22 2006). *Development of Seismic Ground-Motion Criteria for the ASCE 7 Standard.* Paper presented at the 8th U.S. National Conference on Earthquake Engineering, San Fransisco, California, USA.

CSA. (2014). CSA-A23.3:Design of Concrete Structures. Mississauga, Ontario: Canadian Standard Association.

Dezhdar, E. (2012). *Seismic response of cantilever shear wall buildings* . PhD, UBC, Vancouver.

Escolano-Margarit, D., Pujol, A. K., & Benavent-Climent, A. (2012). Failure Mechanism of Reinforced Concrete Structural Walls with and without Confinement.

Fox, M. J., Sullivan, T. J., & Beyer, K. (2015). Evaluation of seismic assessment procedures for determining deformation demands in RC wall buildings. *Earthquakes and Structures, 9*(4), 911-936.

Ghorbanirenani, I. (2010). *Experimental and numerical investigations of higher mode effects on seismic inelastic response of reinforced concrete shear walls,* Mémoire de PhD, École polytechnique de Montréal, Montréal.

Goel, R. K., & Chopra, A. K. (2004). *Improved direct displacement-based design procedure for performance-based seismic design of structures.* Paper presented at the 2001 Structures Congress and Exposition, Structures 2001, May 21, 2001 - May 23, 2001, Washington, DC, United states.

Humar, J., Fazileh, F., Ghorbanie-Asl, M., & Pina, F. E. (2011). Displacement-based seismic design of regular reinforced concrete shear wall buildings. *Canadian Journal of Civil Engineering, 38*(6), 616-626. doi: 10.1139/l11-033

Humar, J. L., & Rahgozar, M. A. (2000). Application of uniform hazard spectra in seismic design of multistorey buildings. *Canadian Journal of Civil Engineering, 27*(3), 563-580. doi: 10.1139/l99-045

Ibrahim, A. M. M., & Adebar, P. (2004). Effective flexural stiffness for linear seismic analysis of concrete walls. *Canadian Journal of Civil Engineering, 31*(4), 597-607. doi: 10.1139/l04-014

Kreslin, M., & Fajfar, P. (2011). The extended N2 method taking into account higher mode effects in elevation. *Earthquake Engineering & Structural Dynamics, 40*(14), 1571-1589. doi: doi:10.1002/eqe.1104

Luu, H., Ghorbanirenani, I., Léger, P., & Tremblay, R. (2013). Numerical Modeling of Slender Reinforced Concrete Shear Wall Shaking Table Tests Under High-Frequency Ground Motions. *Journal of Earthquake Engineering, 17*(4), 517-542. doi: 10.1080/13632469.2013.767759

Luu, H., Léger, P., & Tremblay, R. (2013). Seismic demand of moderately ductile reinforced concrete shear walls subjected to high-frequency ground motions. *Canadian Journal of Civil Engineering, 41*(2), 125-135. doi: 10.1139/cjce-2013-0073

Newmark, N., & Hall, W. (1982). *Earthquake Spectra and Design*: Earthquake Engineering Research Institute.

NRC. (2015). Division B, Part4, Sructural Design *National Building Code of Canada*: National Research Council.

NZS. (2005). Structural Design Actions *1170.5: Erthquake Actions-New Zealand*: New Zealand Standards Council.

NZS. (2006). 3101:The Design of Concrete Structures *Concrete Structures Standard*: New Zealand Standards Council.

Panagiotou, M., & Restrepo, J. I. (2011). Displacement-Based Method of Analysis for Regular Reinforced-Concrete Wall Buildings: Application to a Full-Scale 7-Story Building Slice Tested at UC–San Diego. *Journal of Structural Engineering, 137*(6), 677-690. doi: doi:10.1061/(ASCE)ST.1943-541X.0000333

Park, R., Priestley, M. J. N., & D. Gill, W. (1982). *Ductility of Square-Confined Concrete Columns* (Vol. 108).

Priestley, J. N., Calvi, G. M., & Kowalsky, M. J. (2007). *Displacement-based seismic design of structures*: IUSS Press.

Priestley M. J, N., & Kowalsky M, J. (1998). Aspects of drift and ductility capacity of rectangular cantilever structural walls. *Bulletin of the New Zealand National Society for Earthquake Engineering, 31*(2), 73-85.

Priestley, M. J. N., & Kowalsky, M. J. (2000). Direct displacement-based seismic design of concrete buildings. *Bulletin of the New Zealand National Society for Earthquake Engineering, 33*(4), 421-444.

Sadeghian, A., & Koboevic, S. (20142014). *The influence of design displacement spectra on seismic design of taller reinforced concrete shear walls using direct displacement-based approach*. Paper presented at the Second European conferece on earthquake egineering and seismology, Istanbul, Turkey.

Smerzini, C., Paolucci, R., Galasso, C., & Iervolino, I. (2012, August 2012). *Engineering ground motion selection based on displacement-spectrum compatibility.* Paper presented at the 15th World conference on Earthquake Engineering, Lisbon, Portugal.

Sullivan, T., & Fox, M. (2015). *Development of a simplified displacement-based procedure for the seismic assessment of RC wall buildings*.

Tremblay, R., Atkinson, G. M., Bouaanani, N., Daneshvar, P., Léger, P., & Koboevic, S. (2015). *SELECTION AND SCALING OF GROUND MOTION TIME HISTORIES FOR SEISMIC ANALYSIS USING NBCC 2015.* Paper presented at the 11th Canadian Conference on Earthquake Engineering, Victoria, BC, Canada.

White, T., & Adebar, P. (2004, August 1-6). *Estimating rotational demands in high-rise concrete shear wall buildings.* Paper presented at the 13th World Conference on Earthquake Enginnering, Vancouver, Canada.

Wong, P. S., Vecchio, F. J., & Trommels, H. (2013). VecTor2. Toronto: University of Toronto. Retrieved from http://www.civ.utoronto.ca/vector/